A Brief History of Experimental Gravitational-Wave Research

Wei-Tou Ni 倪维斗

Refs: Chen, Nester, and WTN, CJP (2016)

LSC and VC PRL **116** (2016) 061102;

K Kuroda, WTN, WP Pan, IJMPD 24 (2015) 1530031;

WTN, GW detection in space IJMPD 25 (2016) 1530002

Outline

- INTRODUCTION – a brief history
- SCOPE of GW ASTRONOMY
- PRECISION REQUIREMENTS
- INNOVATIVE MANUFACTURING

Observation-Tech Gap 100 years ago

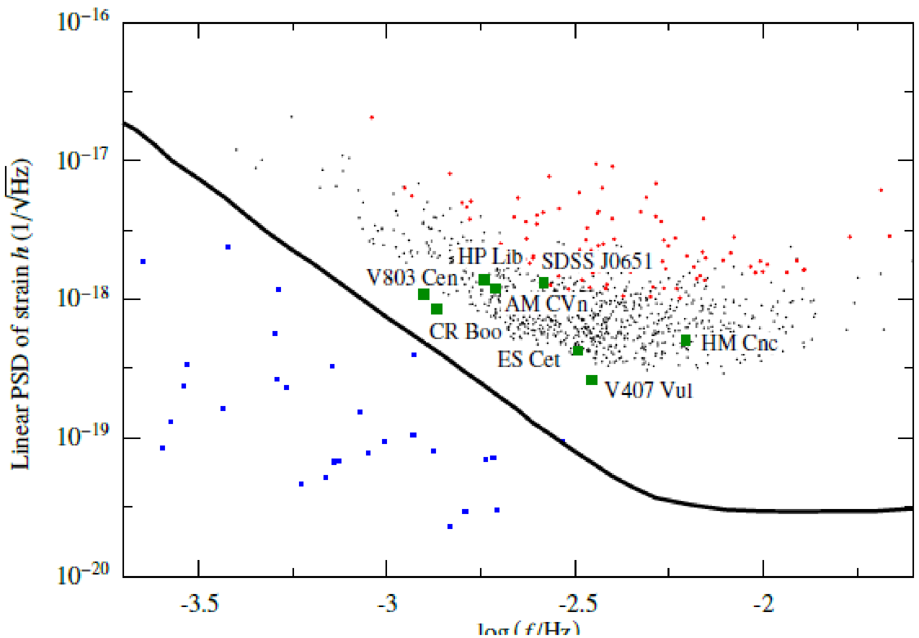

- 1916, 1918 Einstein predicted GW and derived the quadrupole radiation formula
- White dwarf discovered in 1910 with its density soon estimated; GWs from white dwarf binaries in our Galaxy form a stochastic GW background (confusion limit for space GW detection: strain, 10^(-20) in 0.1-1mHz band). [Periods: 5.4 minutes (HM Cancri) to hours](3 mHz)
- One hundred year ago, the sensitivity of astrometric observation through the atmosphere around this band is about 1 arcsec. This means the strain sensitivity to GW detection is about 10^{-5}; 15 orders away from the required sensitivity.
- Observation-Tech Gap 100 years ago

Gravitational Waves – Ripples in Spacetime

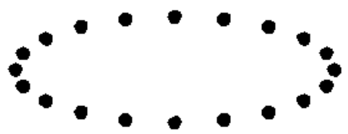

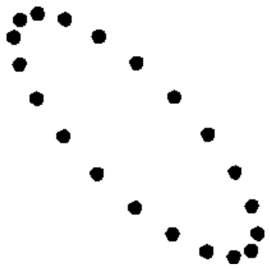

$$[\epsilon^{(1)}]_{ij} = \begin{pmatrix} 0 & 0 & 0 \\ 0 & 0 & 0 \\ 0 & 0 & 1 \end{pmatrix} \qquad [\epsilon^{(2)}]_{ij} = \begin{pmatrix} 0 & 0 & 1 \\ 0 & 0 & 0 \\ 1 & 0 & 0 \end{pmatrix}$$

$$[\epsilon^{(3)}]_{ij} = \begin{pmatrix} 0 & 0 & 0 \\ 0 & 0 & 1 \\ 0 & 1 & 0 \end{pmatrix} \qquad [\epsilon^{(4)}]_{ij} \overset{\text{GR}}{=} \begin{pmatrix} 1 & 0 & 0 \\ 0 & -1 & 0 \\ 0 & 0 & 0 \end{pmatrix}$$

$$[\epsilon^{(5)}]_{ij} \overset{\text{GR}}{=} \begin{pmatrix} 0 & 1 & 0 \\ 1 & 0 & 0 \\ 0 & 0 & 0 \end{pmatrix} \qquad [\epsilon^{(6)}]_{ij} = \begin{pmatrix} 1 & 0 & 0 \\ 0 & 1 & 0 \\ 0 & 0 & 0 \end{pmatrix}.$$

GW propagation direction: z

- Monochromatic

  A single frequency plane GW

- Wave form in time t,

  Spectral form in frequency f

- Noise power amplitude

$$\langle n^2(t)\rangle = \int_0^\infty (df)\, S_n(f),\ h_n(f) \equiv [f\, S_n(f)]^{1/2}$$

- Characteristic amplitude

$$G_{\mu\nu} = \kappa\, T_{\mu\nu},\ R_{\mu\nu} = 8\pi G_N\, [T_{\mu\nu} - (1/2)(g_{\mu\nu}T)]$$

$$A_{\mu,\beta}{}^{\beta} = 4\pi J_\mu,$$

with gauge condition

$$A_{\alpha,}{}^{\alpha} = 0.$$

$$h_{\mu\nu,\beta}{}^{\beta} = -16\pi G_N[T_{\mu\nu} - (1/2)(\eta_{\mu\nu}T)] + O(h^2)$$

$$h_{\mu\nu} = -[(4G_N)/(c^4)] \int \{[T_{\mu\nu} - (1/2)\, g_{\mu\nu}T]/r\}_{\text{retarded}}\, (d^3x') + O(h^2)$$

In harmonic gauge

The retarded solution of equation (12) is

$$A_\mu = \int (J_\mu/r)_{\text{retarded}}\, (d^3x').$$

plane GW $h_{\mu\nu}(n_x x + n_y y + n_z z - ct) = h_{\mu\nu}(U)$

$$h_{\mu\nu}(u, t) \equiv h_{\mu\nu}(U) = \int_{-\infty}^{\infty} {}^{(f)}h_{\mu\nu}(f) \exp(2\pi i f U/c)\, (df) = \int_0^\infty 2f\, |{}^{(f)}h_{\mu\nu}(f)| \cos(2\pi f U/c)\, d(\ln f)$$

$$h_{\mu\nu}(U) = \int_0^\infty 2|{}^{(f)}h_{\mu\nu}(f)| \cos(2\pi f U/c)\, (df)$$
$$= \int_0^\infty 2f\, |{}^{(f)}h_{\mu\nu}(f)| \cos(2\pi f U/c)\, d(\ln f).$$

$$h_{\mu\nu}(x, y, z, t) = (c/2\pi)^3 \int {}^{(k)}h_{\mu\nu}(k_x, k_y, k_z) \exp(ik_x x + ik_y y + ik_z z - 2\pi i f t)\, (dk_x dk_y dk_z)$$

$$h_c(f) \equiv 2f\, [(|{}^{(f)}h_+(f)|^2 + |{}^{(f)}h_\times(f)|^2)]^{1/2};\ h_{cA}(f) \equiv 2f\, |{}^{(f)}h_A(f)|$$

Gap largely bridged

92 days
1440 orbits
83.60 kg mass

- First artificial satellite Sputnik launched in 1957.
- First GW space mission proposed in public in 1981 by Faller & Bender
- LISA proposed as a joint ESA-NASA mission; LISA Pathfinder successfully performed.
- The drag-free tech is fully demonstrated paving the road for GW space missions.

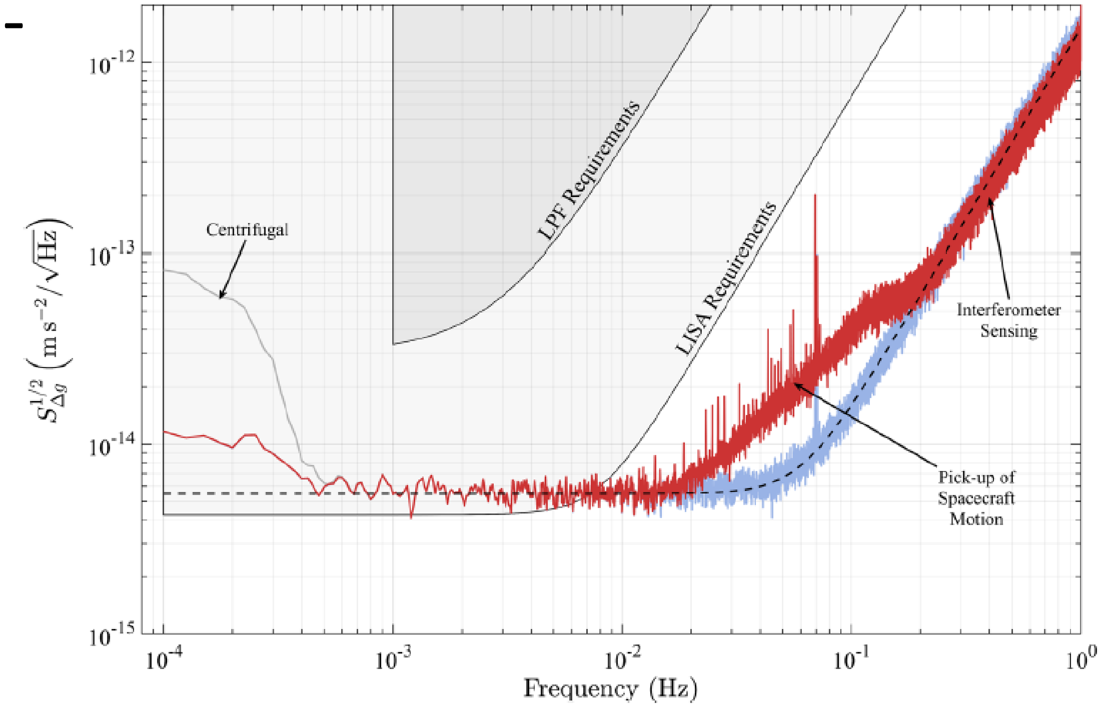

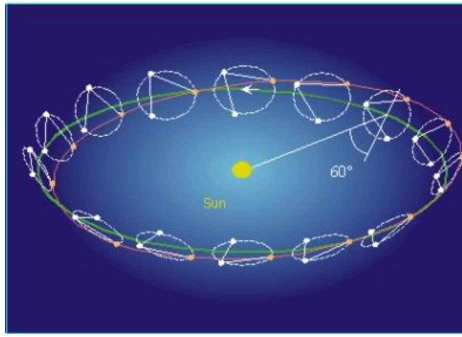

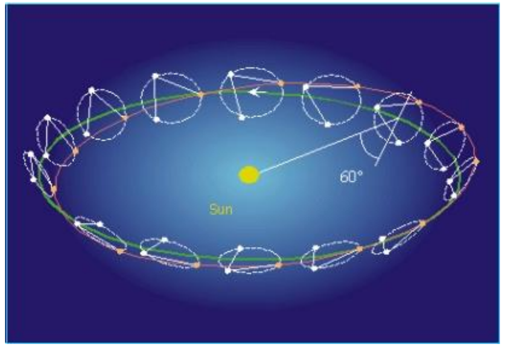

空间引力波探测
A Compilation of GW Mission Proposals LISA Pathfinder Launched on December 3, 2015

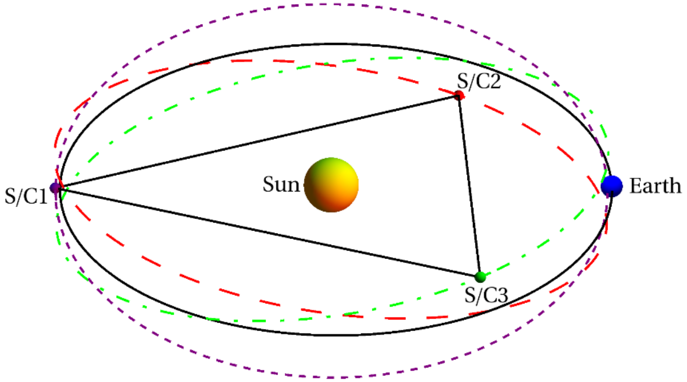

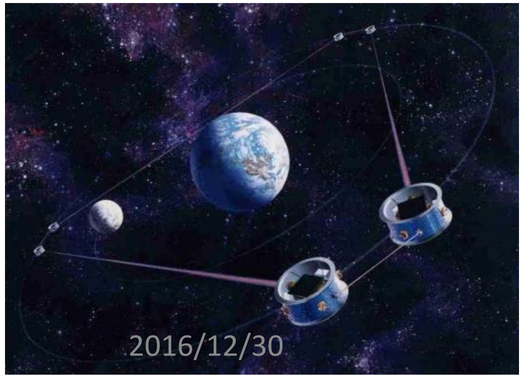

Mission Concept	S/C Configuration	Arm length	Orbit Period	S/C #
Solar-Orbit GW Mission Proposals				
LISA[65]	Earth-like solar orbits with 20° lag	5 Gm	1 year	3
eLISA[64]	Earth-like solar orbits with 10° lag	1 Gm	1 year	3
ASTROD-GW[68]	Near Sun-Earth L3, L4, L5 points	260 Gm	1 year	3
Big Bang Observer[73]	Earth-like solar orbits	0.05 Gm	1 year	12
DECIGO[72]	Earth-like solar orbits	0.001 Gm	1 year	12
ALIA[74]	Earth-like solar orbits	0.5 Gm	1 year	3
ALIA-descope[75] 太极	Earth-like solar orbits	3 Gm	1 year	3
Super-ASTROD[71]	Near Sun-Jupiter L3, L4, L5 points (3 S/C), Jupiter-like solar orbit(s)(1-2 S/C)	1300 Gm	11 year	4 or 5
Earth-Orbit GW Mission Proposals				
OMEGA[81]	0.6 Gm height orbit	1 Gm	53.2 days	6
gLISA/GEOGRAWI[76-78]	Geostationary orbit	0.073 Gm	24 hours	3
GADFLI[79]	Geostationary orbit	0.073 Gm	24 hours	3
TIANQIN[82] 天琴	0.057 Gm height orbit	0.11 Gm	44 hours	3
ASTROD-EM[69,70]	Near Earth-Moon L3, L4, L5 points	0.66 Gm	27.3 days	3
LAGRANGE[80]	Near Earth-Moon L3, L4, L5 points	0.66 Gm	27.3 days	3

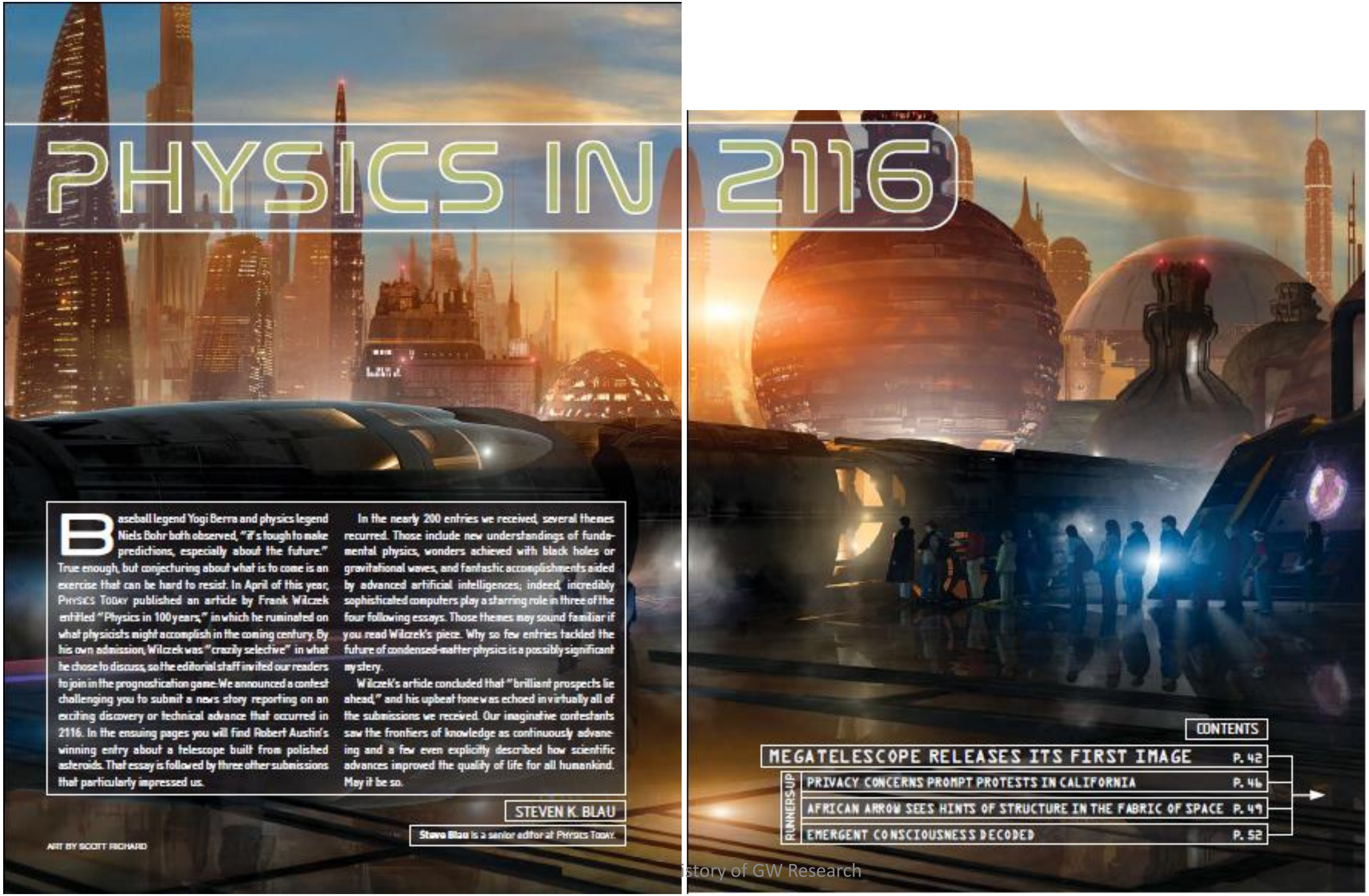

PHYSICS IN 2116

Baseball legend Yogi Berra and physics legend Niels Bohr both observed, "It's tough to make predictions, especially about the future." True enough, but conjecturing about what is to come is an exercise that can be hard to resist. In April of this year, Physics Today published an article by Frank Wilczek entitled "Physics in 100 years," in which he ruminated on what physicists might accomplish in the coming century. By his own admission, Wilczek was "crazily selective" in what he chose to discuss, so the editorial staff invited our readers to join in the prognostication game. We announced a contest challenging you to submit a news story reporting on an exciting discovery or technical advance that occurred in 2116. In the ensuing pages you will find Robert Austin's winning entry about a telescope built from polished asteroids. That essay is followed by three other submissions that particularly impressed us.

In the nearly 200 entries we received, several themes recurred. Those include new understandings of fundamental physics, wonders achieved with black holes or gravitational waves, and fantastic accomplishments aided by advanced artificial intelligences; indeed, incredibly sophisticated computers play a starring role in three of the four following essays. Those themes may sound familiar if you read Wilczek's piece. Why so few entries tackled the future of condensed-matter physics is a possibly significant mystery.

Wilczek's article concluded that "brilliant prospects lie ahead," and his upbeat tone was echoed in virtually all of the submissions we received. Our imaginative contestants saw the frontiers of knowledge as continuously advancing and a few even explicitly described how scientific advances improved the quality of life for all humankind. May it be so.

STEVEN K. BLAU

Steve Blau is a senior editor at Physics Today.

ART BY SCOTT RICHARD

CONTENTS

releases its first image

Megatelescope

Super-ASTROD
1996, 2009

Robert Austin is a visiting assistant professor of physics at Florida Polytechnic University in Lakeland and an online instructor of astronomy for the University of Phoenix.

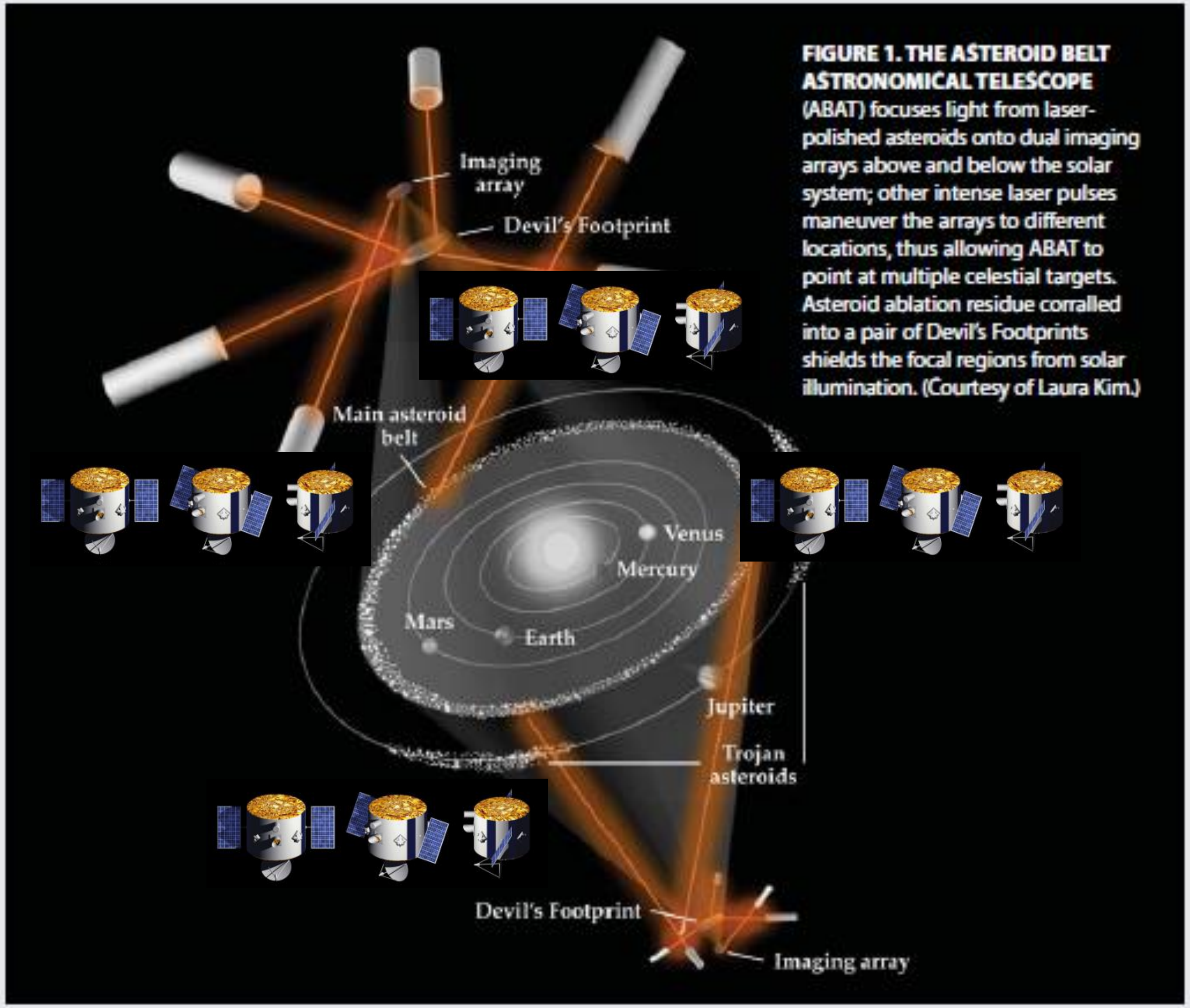

FIGURE 1. THE ASTEROID BELT ASTRONOMICAL TELESCOPE (ABAT) focuses light from laser-polished asteroids onto dual imaging arrays above and below the solar system; other intense laser pulses maneuver the arrays to different locations, thus allowing ABAT to point at multiple celestial targets. Asteroid ablation residue corralled into a pair of Devil's Footprints shields the focal regions from solar illumination. (Courtesy of Laura Kim.)

引力波谱分类 The Gravitation-Wave (GW) Spectrum Classification

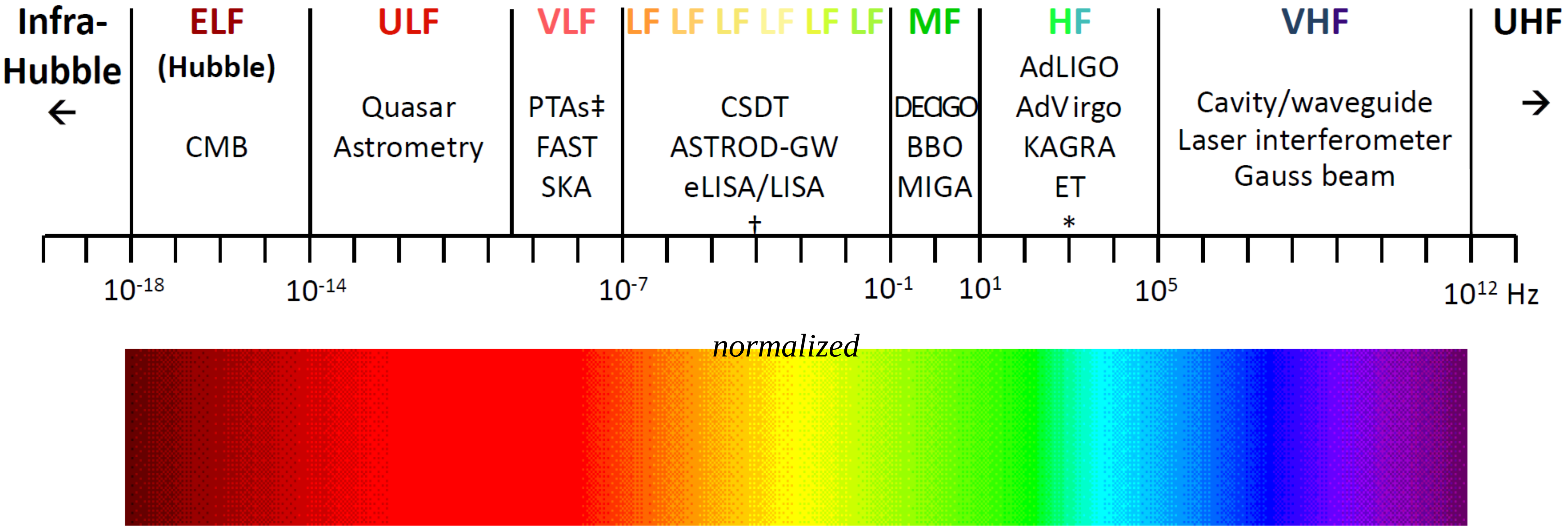

* AIGO, AURIGA, EXPLORER, GEO, NAUTILUS, MiniGRAIL, Schenberg.

† OMEGA, gLISA/GEOGRAWI, GADFLI, TIANQIN, ASTROD-EM, LAGRANGE, ALIA, ALIA-descope.

‡ EPTA, NANOGrav, PPTA, IPTA.

The observation and technology gap 100 years ago in the 10 Hz – 1 kHz band

- In the LIGO discovery of 2 GW events and 1 probable GW candidate, the maximum peak strain intensity is 10^{-21}; the frequency range is 30-450 Hz.
- Strain gauge in this frequency region could reach 10^{-5} with a fast recorder about 100 years ago;
- thus, the technology gap would be 16 orders of magnitudes.
- Michelson interferometer for Michelson-Morley experiment[10] has a strain ($\Delta l/l$) sensitivity of 5×10^{-10} with 0.01 fringe detectability and 11 m path length;
- however, the appropriate test mass suspension system with fast (30-450 Hz in the high-frequency GW band) white-light observing system is lacking.

Weber Bar (50 Years ago)
10 orders of gap abridged

- OBSERVATION OF THE THERMAL FLUCTUATIONNS OF A GRAVITATIONAL-WAVE DETECTOR* J. Weber

  PRL 1966 (Received 3 October 1966)

  Strains as small as a few parts in 10^{16} are observable for a compressional mode of a large cylinder.

- GRAVITATIONAL RADIATION* J. Weber

  PRL 1967 (Received 8 February 1967)

- The results of two years of operation of a 1660-cps gravitational-wave detector are reviewed. The possibility that some gravitational signals may have been observed cannot completely be ruled out. New gravimeter-noise data enable us to place low limits on gravitational radiation in the vicinity of the earth's normal modes near one cycle per hour, implying an energy-density limit over a given detection mode smaller than that needed to provide a closed universe.

Sinsky's Calibration in Weber's Lab

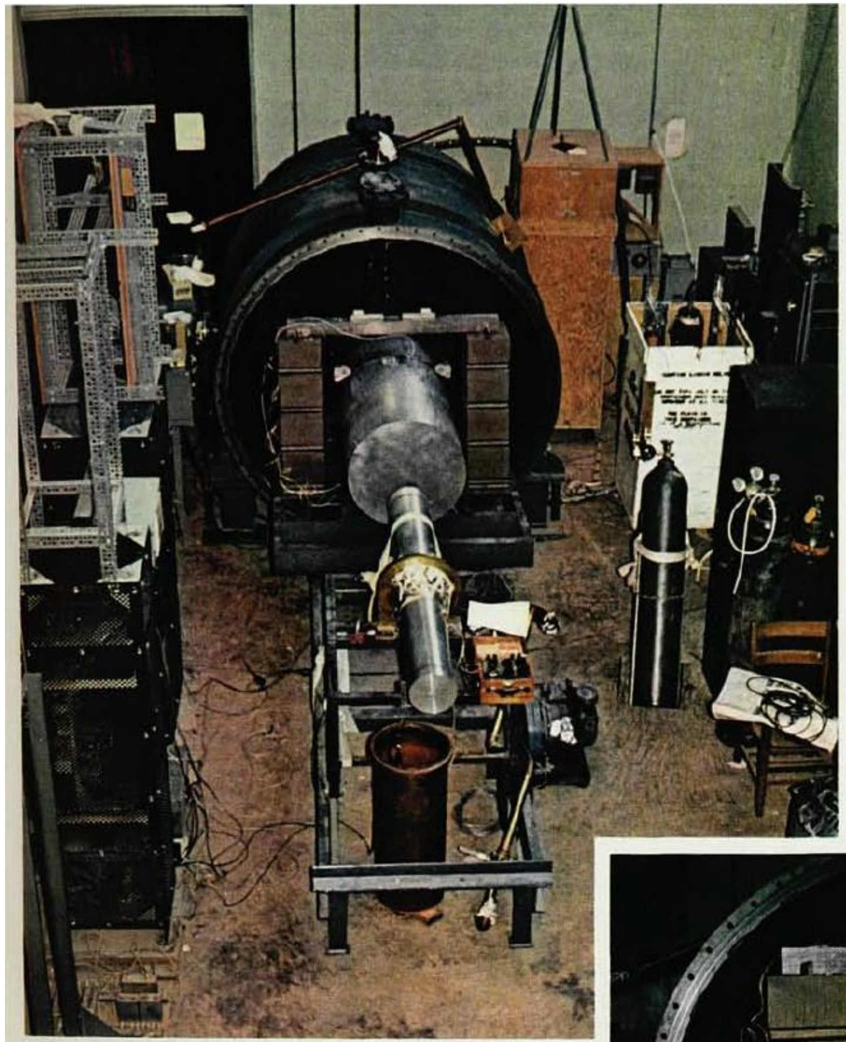

ALUMINUM CYLINDER of 1400-kg mass is suspended by a wire on acoustic filters. Piezoelectric transducers are bonded to the top surface, as shown in the closeup.

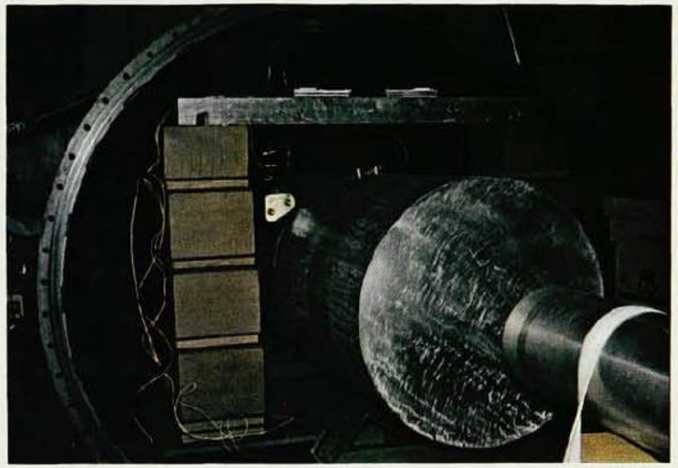

DETECTOR and dynamic gravitational field generator are shown removed from their common vacuum chamber.

The start of precision laser interferometry for GW detection

(left) Interferometer system noise measurement at 5 kHz of Moss, Miller and Forward (1971); (right) Schematic of Malibu Laser Interferometer GW Antenna of Forward (1978)

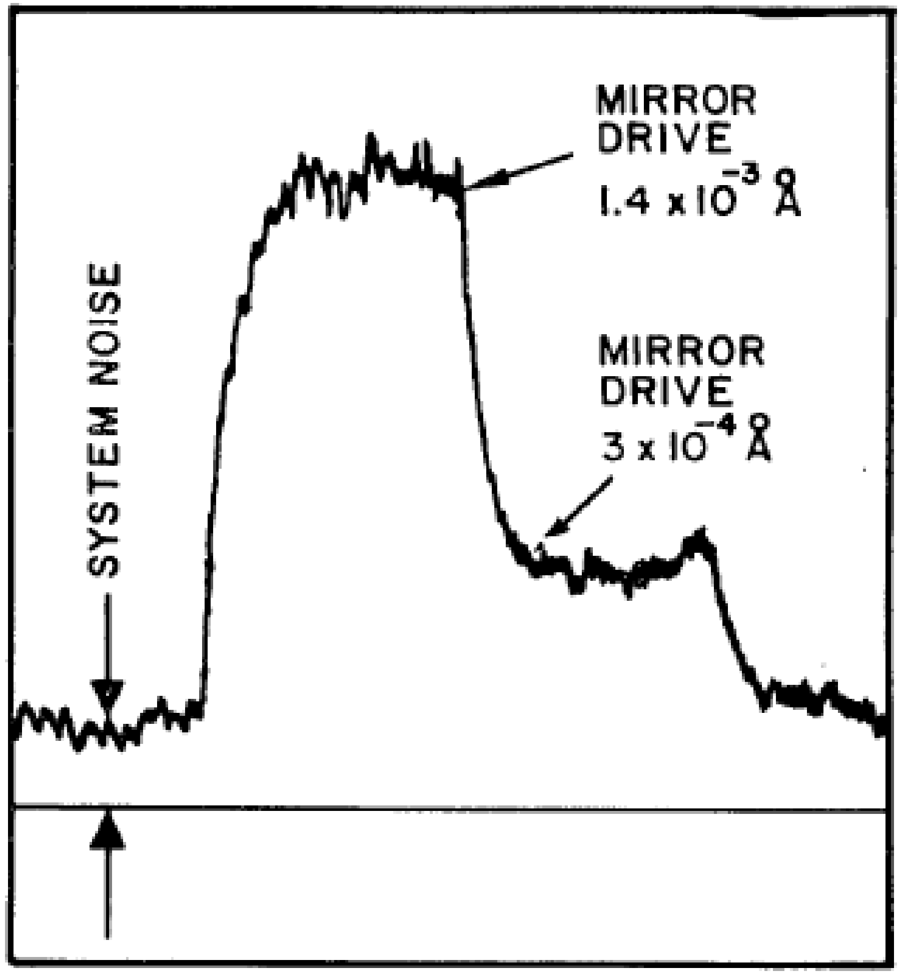

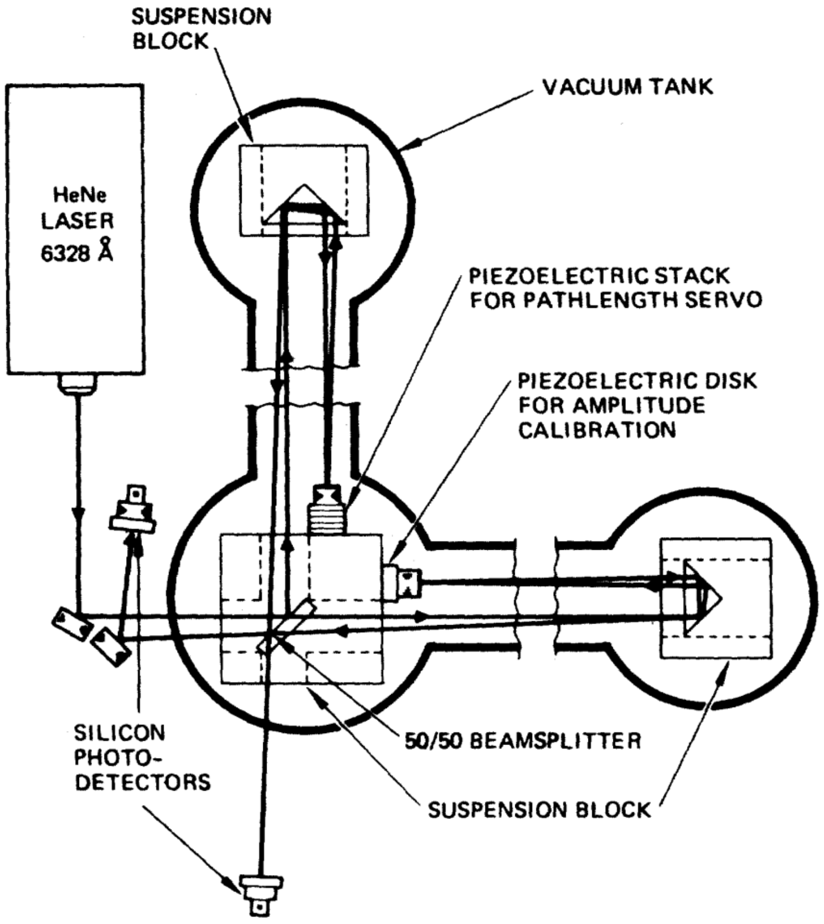

The fundamental noise sources of Weiss 1972

- km-sized interferometer proposed

- a. Amplitude noise in the laser output power;
- b. Laser phase noise or frequency instability;
- c. Mechanical thermal noise in the antenna;
- d. Radiation-pressure noise from laser light;
- e. Seismic noise;
- f. Thermal-gradient noise;
- g. Cosmic-ray noise;
- h. Gravitational-gradient noise;
- i. Electric field and magnetic field noise.

探测引力波的原型光学干涉仪盛行时期
Flourish of Prototype Optical Interferometers for GW Detection

- Hughes Research Lab (HRL) 0.75 m
- MIT prototype interferometer 1.5 m
- Glasgow prototype interferometer 10 m
- Garching prototype interferometer 30 m
- Tokyo prototype interferometer 3 m
- Paris prototype interferometer 7 m
- ISAS prototype interferometer 10 m
- NAOJ prototype interferometer 20 m
- ISAS prototype interferometer 100 m

TAMA 300 m

GEO 600 m

Laser interferometers with independently suspended mirrors. In third column, in the parenthesis either the number N of paths is given or Fabry-Perot Finesse F is given.

Interferometer	Arm length [m]	Effective optical path length [km]	Year Construction Started
Hughes Research Lab (HRL) [87,137,142]	2	0.0085 (N = 4)	1966
MIT prototype [202]	1.5	0.075 (N = 50)	1971
Garching 3 m prototype	3	0.012 (N = 4)	1975
Glasgow 1 m prototype [210]	1	0.036 (N = 36; in static test reached N = 280)	1976
Glasgow 10 m prototype [210]	10	25.5 (F-P: F = 4000)	1980
Caltech 40 m prototype	40	75	1980
Garching 30 m prototype	30	2.7 (N = 90)	1983
ISAS Tenko 10 m prototype [112]	10	1 (N= 100)	1986
U. Tokyo prototype [14,111]	3	0.42 (F-P: F = 220)	1987
ISAS Tenko 100 m prototype [114,139–141]	100	10 (N = 100)	1991
NAOJ 20 m prototype [16]	20	4.5 (F-P: F = 350)	1991
Q&A 3.5 m prototype [55]	3.5	67 (F-P: F = 30000)	1993
TAMA 300 m [184]	300	96 (F-P: F = 500)	1995
GEO 600 m [91,209]	600	1.2 (N = 2)	1995
LIGO Hanford (2 km) [1,124]	2000	143 (F-P: F = 112)	1994
LIGO Hanford (4 km) [124,130]	4000	1150 (F-P: F = 450)	1994
LIGO Livingston (4 km) [124,130]	4000	1150 (F-P: F = 450)	1995
VIRGO [5,191]	3000	850 (F-P: F = 440)	1996
AIGO prototype [205,206]	80	760/66 (F-P: east arm F= 15000; south arm F = 1300)	1997
LISM [168]	20	320 (F-P: F = 25000)	1999
CLIO 100 m cryogenic [7]	100	190 (F-P: F = 3000)	2000
Q&A 7 m [134]	7	450 (F-P: F = 100000)	2008
LCGT/KAGRA [21,109]	3000	2850 (F-P: F = 1500)	2010
Q&A 9 m [208]	9	570 (F-P: F = 100000)	2016
LIGO India [102]	4000	1150 (F-P: F = 450)	2016
ET [99]	10000	3200 (F-P: F~ 500)	Proposal under study

Ground-based GW detectors

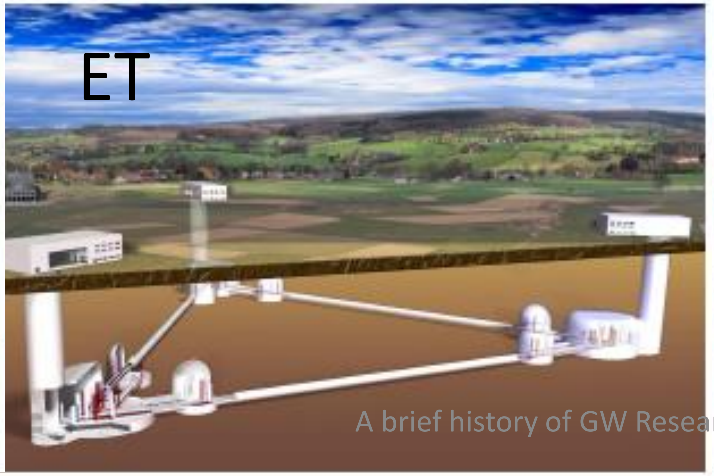

LLR – measurement

- telescope, diameter 0.7 m – 3.5 m
- pulsed laser, pulse length 0.07 ns – 0.2 ns
- footprint at the Moon ~20 km² (reflector ¼ - ½ m²)
- 10^{19} photons/pulse sent, ~1 - 50 photons received
- filtering
  - spatial
  - spectral
  - temporal
- LLR data

  1- 15 min → 1 normal point

  17,700 normal points in 43 years

重力波雷射干涉探測器
基本原理

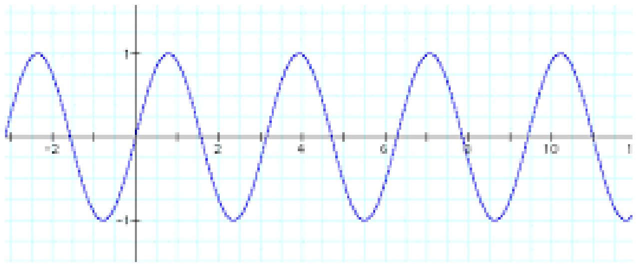

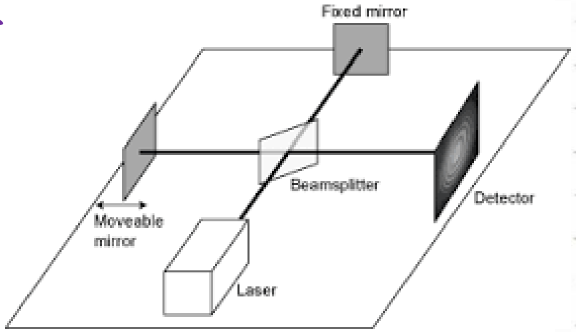

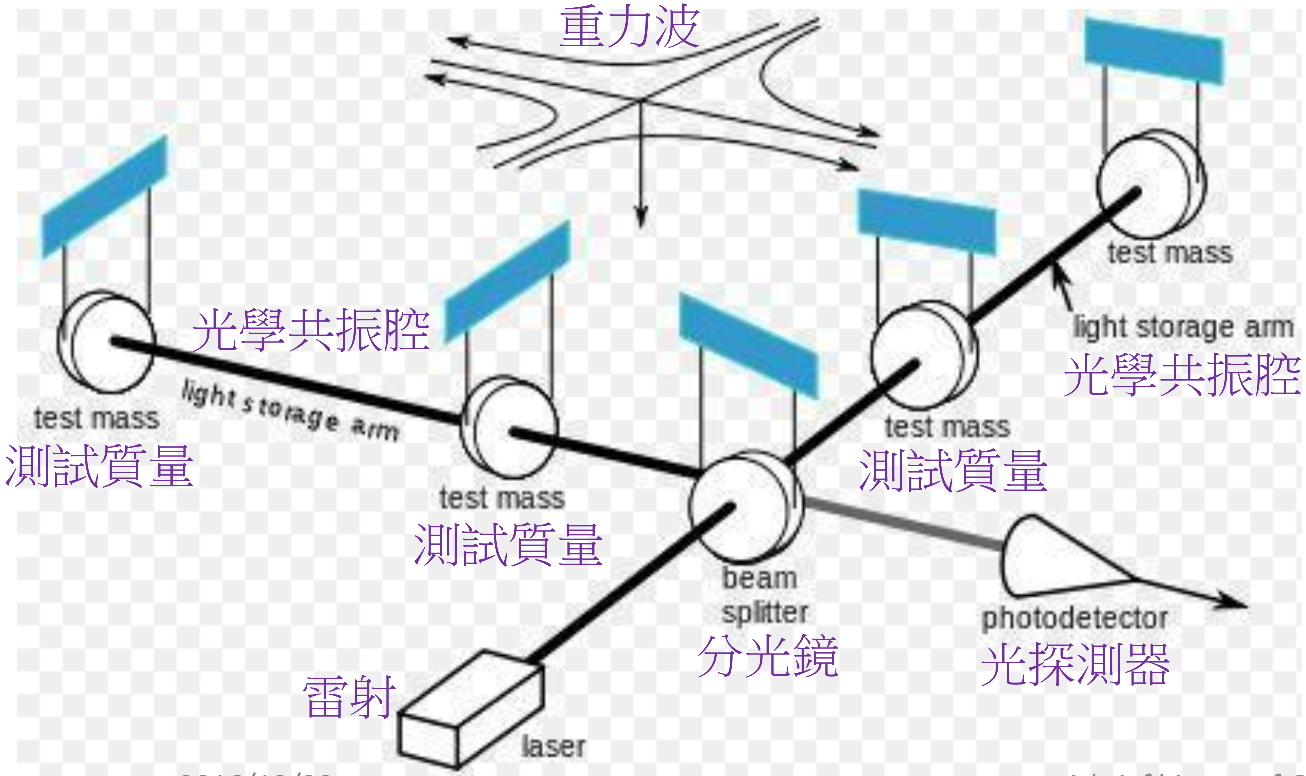

高精細度 Fabry-Perot 空腔與雷射穩頻實驗

High Finesse Fabry-Perot Cavity and Laser Stabilization

光学实验(四)

倪維斗

目的：(i) 瞭解 Fabry-Perot 干涉儀(空腔)之精細度.

(ii) 精細度之測量.

(iii) 用 Fabry-Perot 腔共振基模鎖定 He-Ne 雷射穩頻之.

原理：(i) Fabry-Perot 干涉儀之精細度

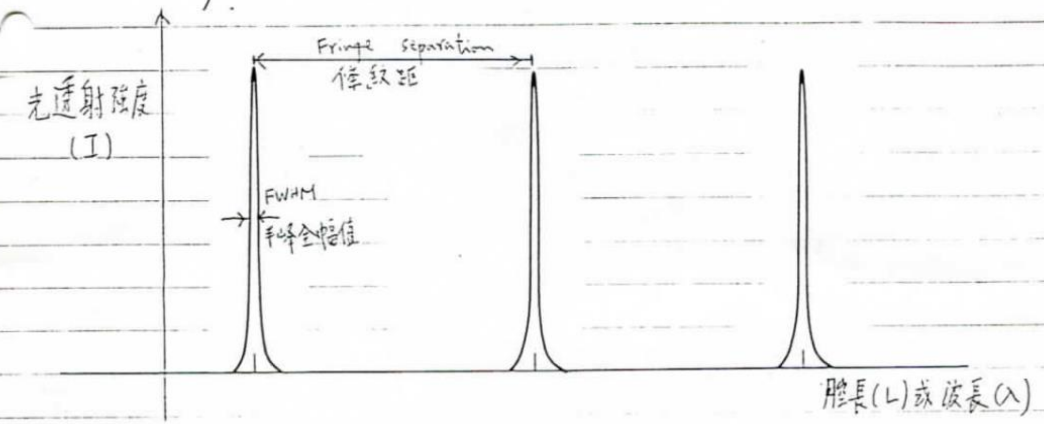

$$\text{精細度} = \frac{\text{半峰全幅值}}{\text{條紋距}} = \frac{\pi\sqrt[4]{R_1R_2}}{(1-\sqrt{R_1R_2})} \simeq \pi\frac{1}{1-\sqrt{R_1R_2}} \quad \text{for } R_1\simeq 1,\ R_2\simeq 1$$

其中 R_1 為第一面鏡之反射率

R_2 為第二面 " " " "

本实驗中之精細度約為 200，若假設 $R_1=R_2$ 則

$R_1 \simeq R_2 \simeq 0.984$

(a) 相對於條紋距之腔長改变 ΔL 為 $\frac{\lambda}{2} = \frac{633}{2}\ \text{nm} = 316\ \text{nm}$

(b) 相對於 FWHM (半峰全幅值) 之 ΔL 為 $\frac{3.16\ \text{nm}}{\text{精細度}} = 1.6\ \text{nm}$

(c) 若半峰全幅值可有 1% 之 resolution (解析度)，則此 Fabry-Perot 腔之解析度為 0.016 nm or 16 pm

Interferometry for GW detection: e.g. KAGRA

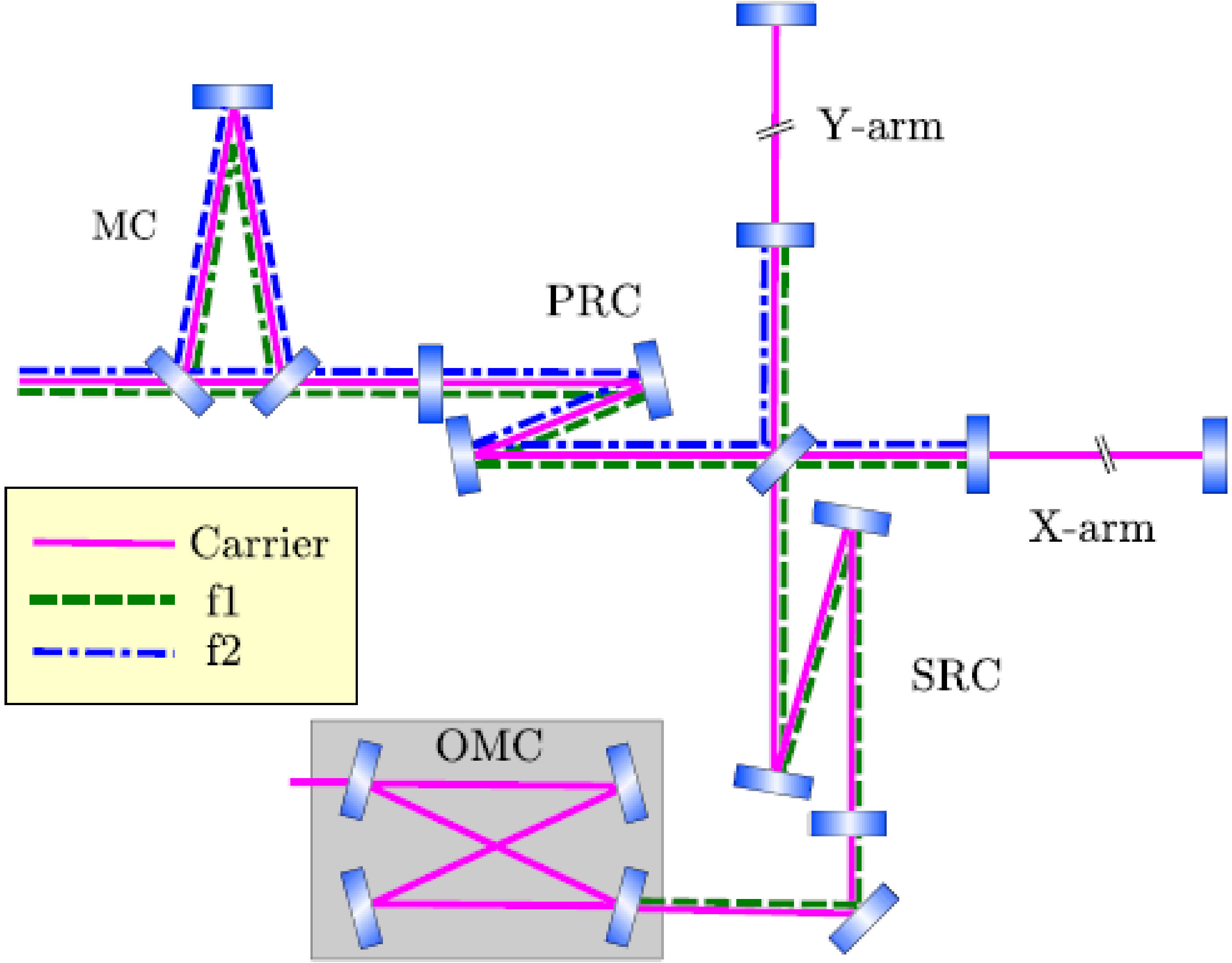

aLIGO achieved sensitivity

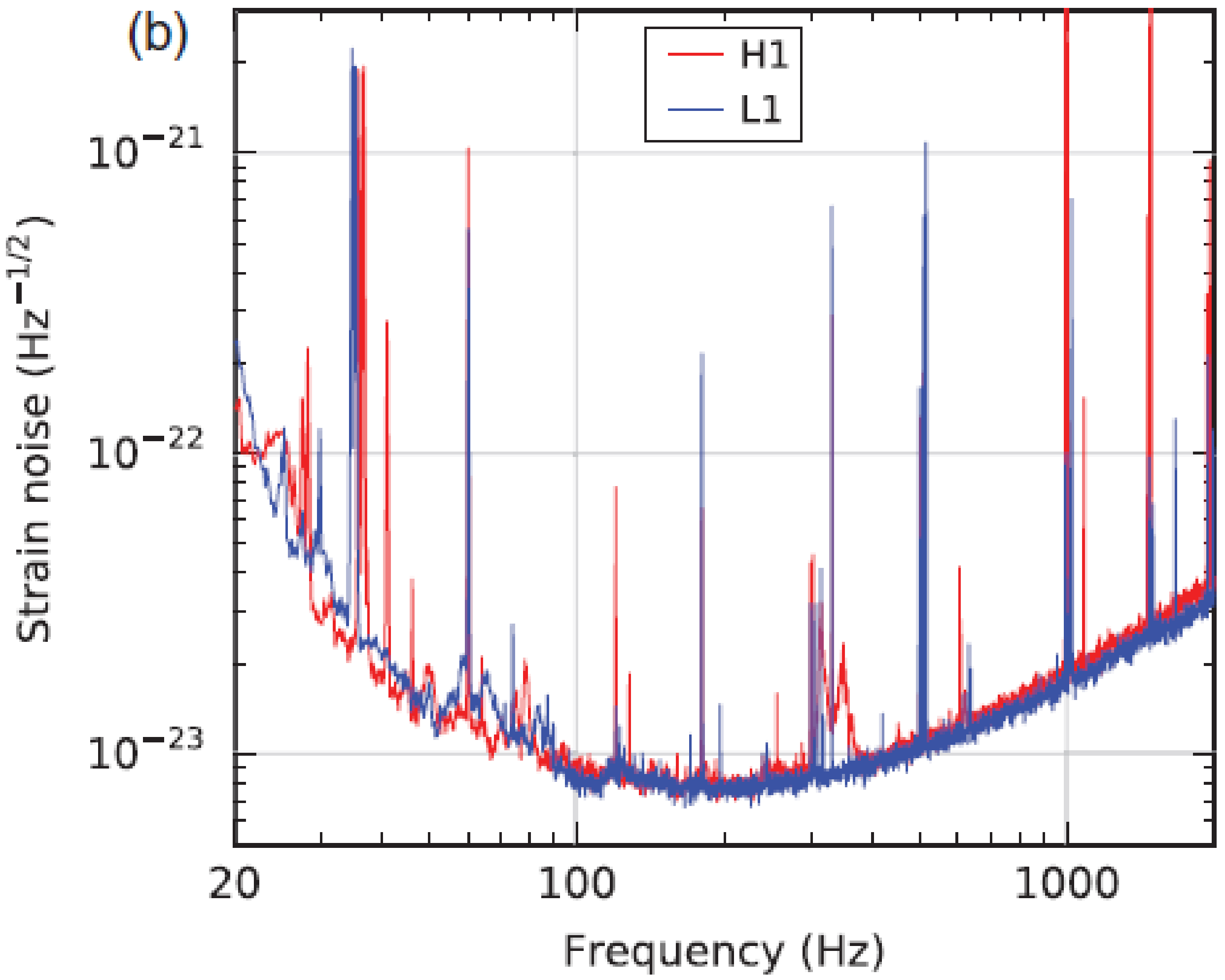

2016年2月11日宣布首探 Announcement of first detection

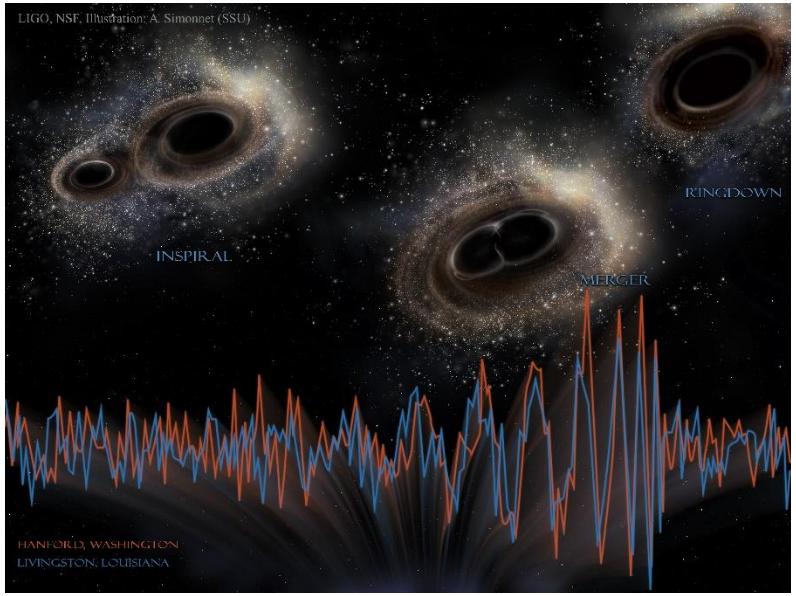

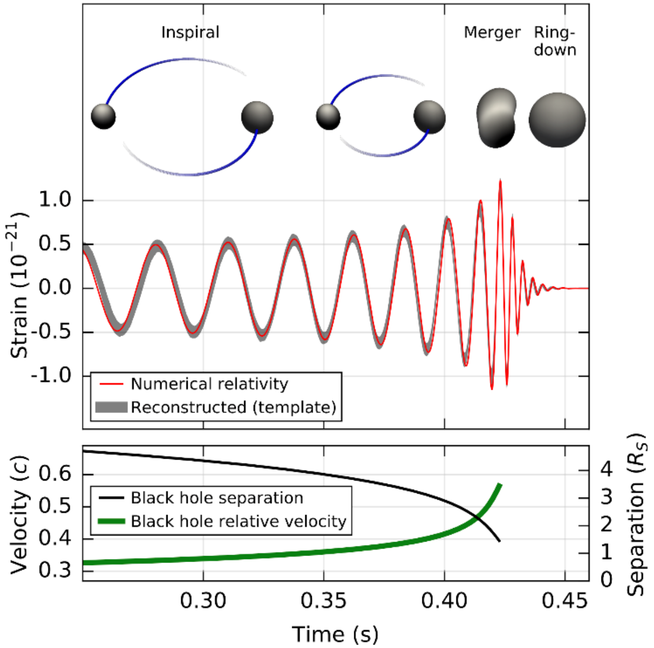

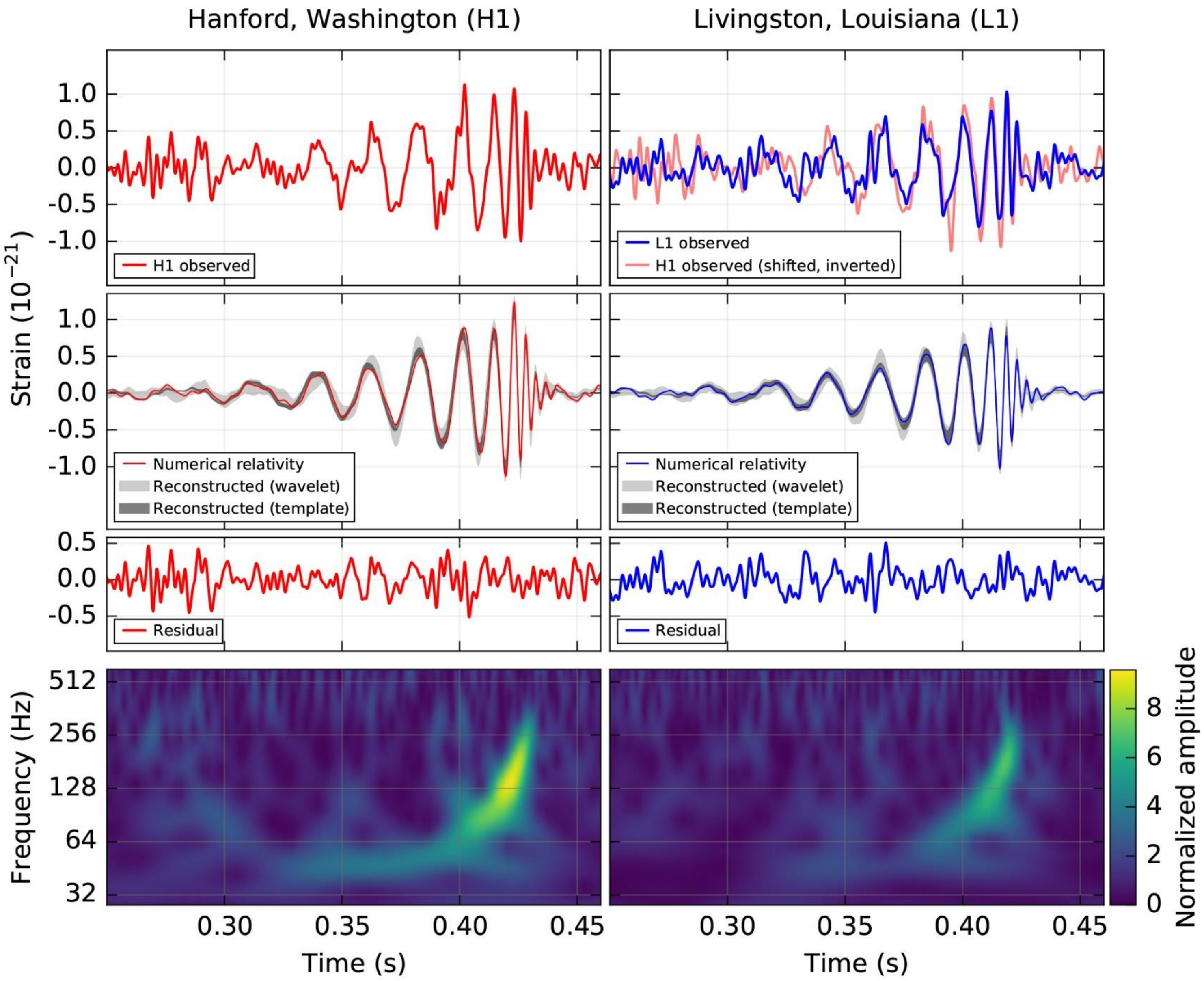

Advanced LIGO第一次觀測時期：

2015.9.12—2016.1.19 (51.5天-2 detectors/130天)

O1: 48.6天; PyCBC 46.1天; GstLAL 48.3天

Event	GW150914	GW151226	LVT151012
Signal-to-noise ratio ρ	23.7	13.0	9.7
False alarm rate FAR/yr^{-1}	$< 6.0 \times 10^{-7}$	$< 6.0 \times 10^{-7}$	0.37
p-value	7.5×10^{-8}	7.5×10^{-8}	0.045
Significance	$> 5.3\,\sigma$	$> 5.3\,\sigma$	$1.7\,\sigma$
Primary mass $m_1^{\mathrm{source}}/\mathrm{M}_\odot$	$36.2^{+5.2}_{-3.8}$	$14.2^{+8.3}_{-3.7}$	23^{+18}_{-6}
Secondary mass $m_2^{\mathrm{source}}/\mathrm{M}_\odot$	$29.1^{+3.7}_{-4.4}$	$7.5^{+2.3}_{-2.3}$	13^{+4}_{-5}
Chirp mass $\mathscr{M}^{\mathrm{source}}/\mathrm{M}_\odot$	$28.1^{+1.8}_{-1.5}$	$8.9^{+0.3}_{-0.3}$	$15.1^{+1.4}_{-1.1}$
Total mass $M^{\mathrm{source}}/\mathrm{M}_\odot$	$65.3^{+4.1}_{-3.4}$	$21.8^{+5.9}_{-1.7}$	37^{+13}_{-4}
Effective inspiral spin χ_{eff}	$-0.06^{+0.14}_{-0.14}$	$0.21^{+0.20}_{-0.10}$	$0.0^{+0.3}_{-0.2}$
Final mass $M_{\mathrm{f}}^{\mathrm{source}}/\mathrm{M}_\odot$	$62.3^{+3.7}_{-3.1}$	$20.8^{+6.1}_{-1.7}$	35^{+14}_{-4}
Final spin a_{f}	$0.68^{+0.05}_{-0.06}$	$0.74^{+0.06}_{-0.06}$	$0.66^{+0.09}_{-0.10}$
Radiated energy $E_{\mathrm{rad}}/(\mathrm{M}_\odot c^2)$	$3.0^{+0.5}_{-0.4}$	$1.0^{+0.1}_{-0.2}$	$1.5^{+0.3}_{-0.4}$
Peak luminosity $\ell_{\mathrm{peak}}/(\mathrm{erg\,s}^{-1})$	$3.6^{+0.5}_{-0.4} \times 10^{56}$	$3.3^{+0.8}_{-1.6} \times 10^{56}$	$3.1^{+0.8}_{-1.8} \times 10^{56}$
Luminosity distance $D_{\mathrm{L}}/\mathrm{Mpc}$	420^{+150}_{-180}	440^{+180}_{-190}	1000^{+500}_{-500}
Source redshift z	$0.09^{+0.03}_{-0.04}$	$0.09^{+0.03}_{-0.04}$	$0.20^{+0.09}_{-0.09}$
Sky localization $\Delta\Omega/\mathrm{deg}^2$	230	850	1600

2016年6月15日宣佈二探 Announcement of second detection

- GW151226 detected by the LIGO on December 26, 2015 at 03:38:53 UTC.
- identified within 70 s by an online matched-filter search targeting binary coalescences.
- GW151226 with S/N ratio of 13 and significance > 5σ.
- The signal ~ 1 s, about 55 cycles from 35 to 450 Hz, reached 3.4 (+0.7,−0.9) × 10^(−22). source-frame initial BH masses: 14.2 (+8.3,−3.7)$M_\odot$ and 7.5 (+2.3,−2.3)$M_\odot$, the final BH mass is 20.8 (+6.1,−1.7)$M_\odot$.
- 1 BH has spin greater than 0.2. luminosity distance 440 (+180,−190) Mpc redshift of 0.09 (+0.03,−0.04). **2σ**
- improved constraints on stellar populations and on deviations from general relativity.

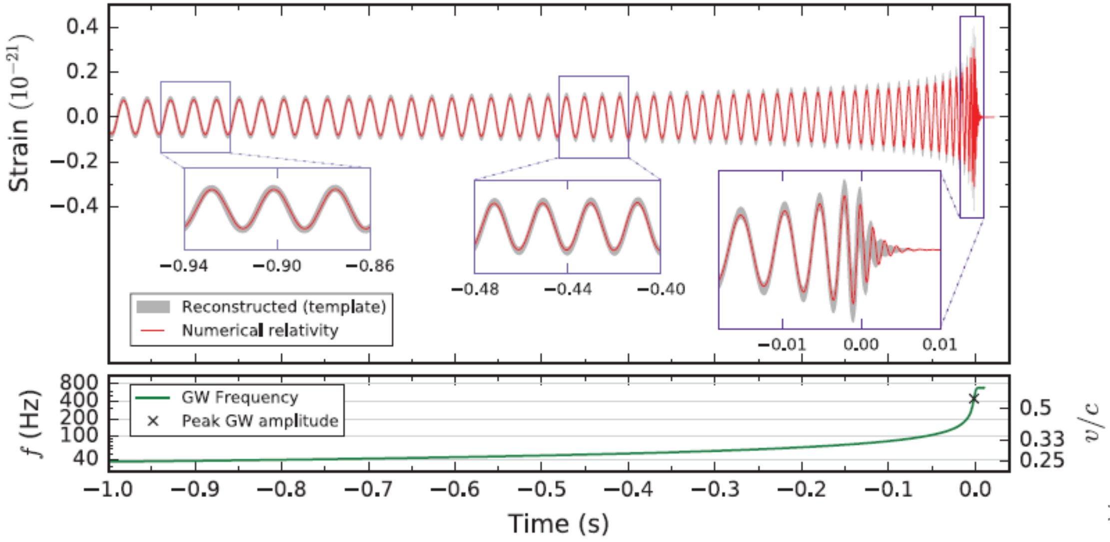

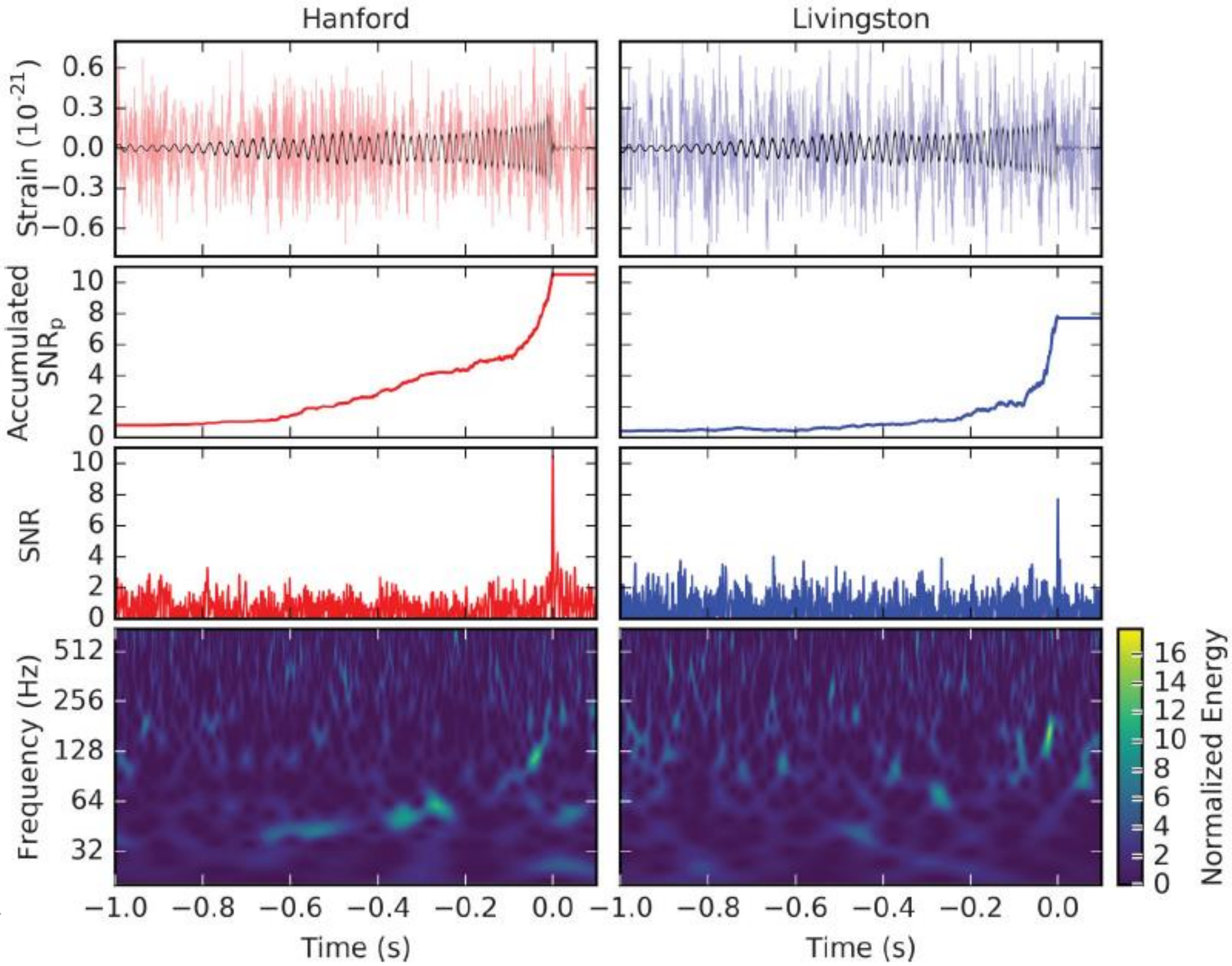

Characteristics of two GW events and one GW candidate deduced from LIGO O1 GW observations

Event	GW150914	GW151226	LVT151012 (candidate)
Signal-to-noise ratio ρ	23.7	13.0	9.7
Significance	$> 5.3\ \sigma$	$> 5.3\ \sigma$	$1.7\ \sigma$
Primary mass $m^{\mathrm{source}}{}_1/\mathrm{M}_\odot$	$36.2^{+5.2}{}_{-3.8}$	$14.2^{+8.3}{}_{-3.7}$	$23^{+18}{}_{-6}$
Secondary mass $m^{\mathrm{source}}{}_2/\mathrm{M}_\odot$	$29.1^{+3.7}{}_{-4.4}$	$7.5^{+2.3}{}_{-2.3}$	$13^{+4}{}_{-5}$
Effective inspiral spin χ_{eff}	$-0.06^{+0.14}{}_{-0.14}$	$0.21^{+0.20}{}_{-0.10}$	$0.0^{+0.3}{}_{-0.2}$
Final mass $M^{\mathrm{source}}{}_f/\mathrm{M}_\odot$	$62.3^{+3.7}{}_{-3.1}$	$20.8^{+6.1}{}_{-1.7}$	$35^{+14}{}_{-4}$
Final spin a_f	$0.68^{+0.05}{}_{-0.06}$	$0.74^{+0.06}{}_{-0.06}$	$0.66^{+0.09}{}_{-0.10}$
Radiated energy $E_{\mathrm{rad}}/(\mathrm{M}_\odot c^2)$	$3.0^{+0.5}{}_{-0.4}$	$1.0^{+0.1}{}_{-0.2}$	$1.5^{+0.3}{}_{-0.4}$
Peak luminosity $l_{\mathrm{peak}}/(\mathrm{erg\ s}^{-1})$	$3.6^{+0.5}{}_{-0.4} \times 10^{56}$	$3.3^{+0.8}{}_{-1.6} \times 10^{56}$	$3.1^{+0.8}{}_{-1.8} \times 10^{56}$
Luminosity distance D_L/Mpc	$420^{+150}{}_{-180}$	$440^{+180}{}_{-190}$	$1000^{+500}{}_{-500}$
Source redshift z	$0.09^{+0.03}{}_{-0.04}$	$0.09^{+0.03}{}_{-0.04}$	$0.2^{+0.09}{}_{-0.09}$

Q&A 3.5 m prototype

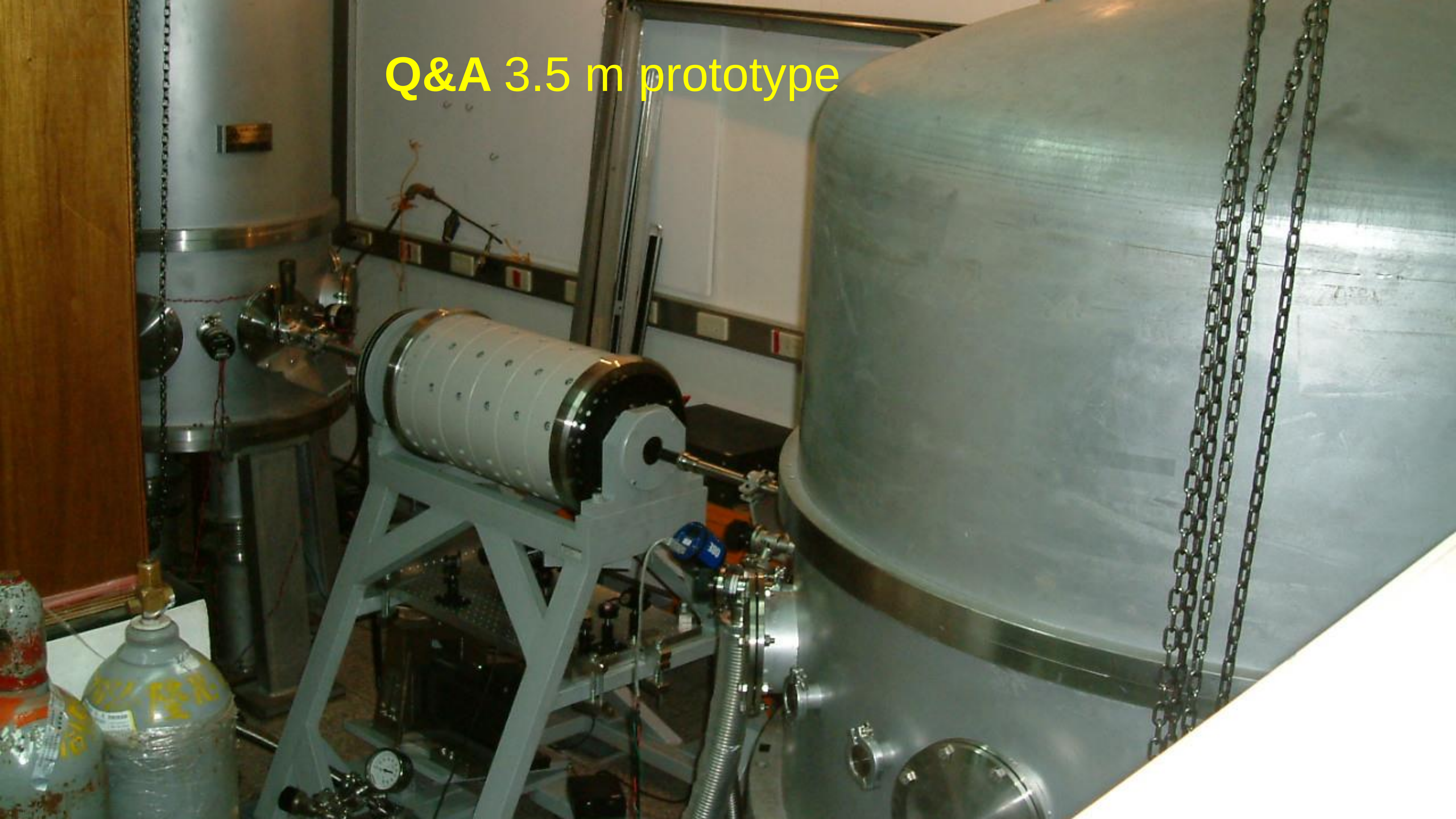

入射光学桌 *Injection Optical Bench*

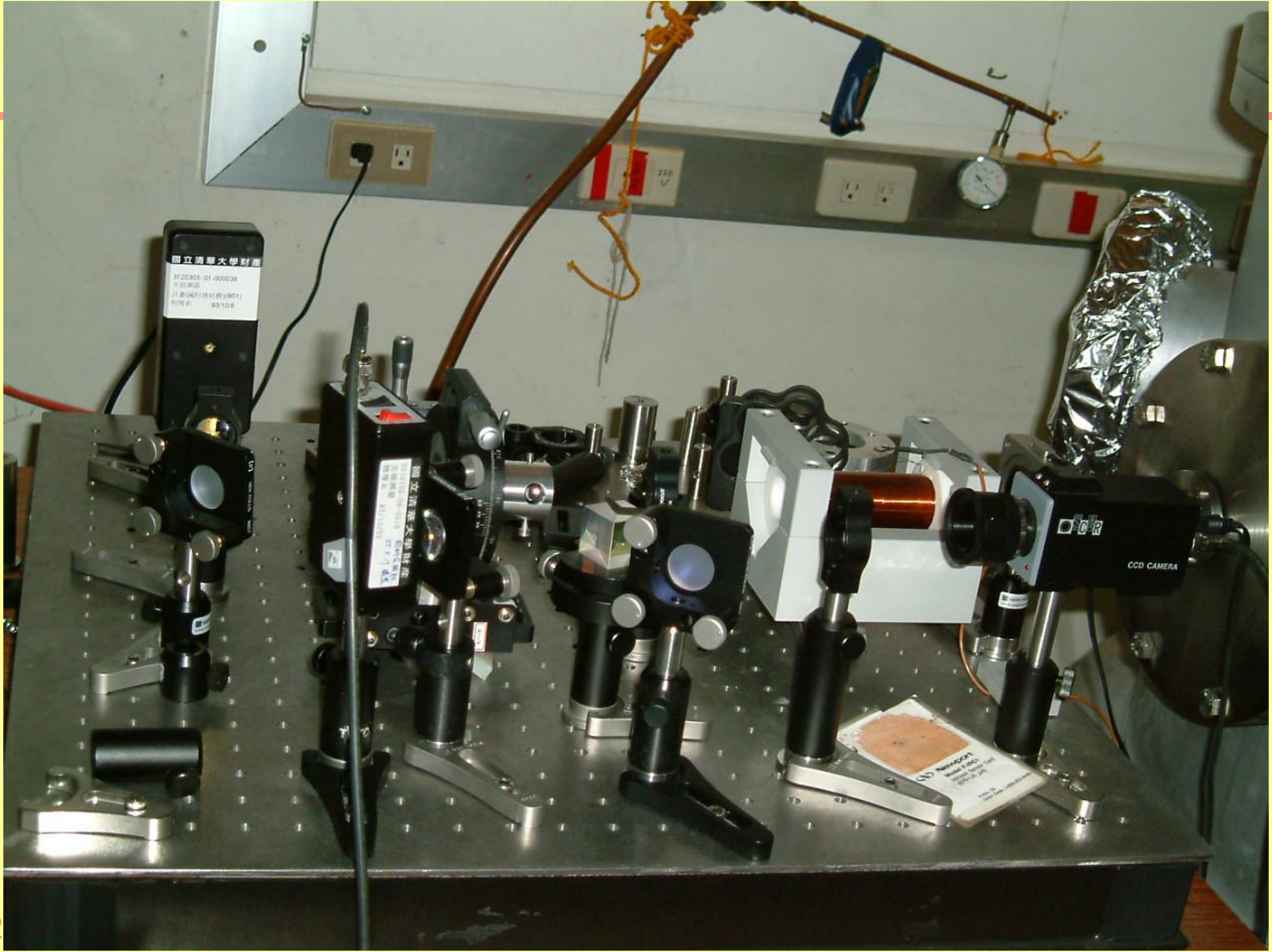
CCD CAMERA

悬吊系统 *Suspension System*

X摆和双摆 *X-Pendulum and double pendulum*

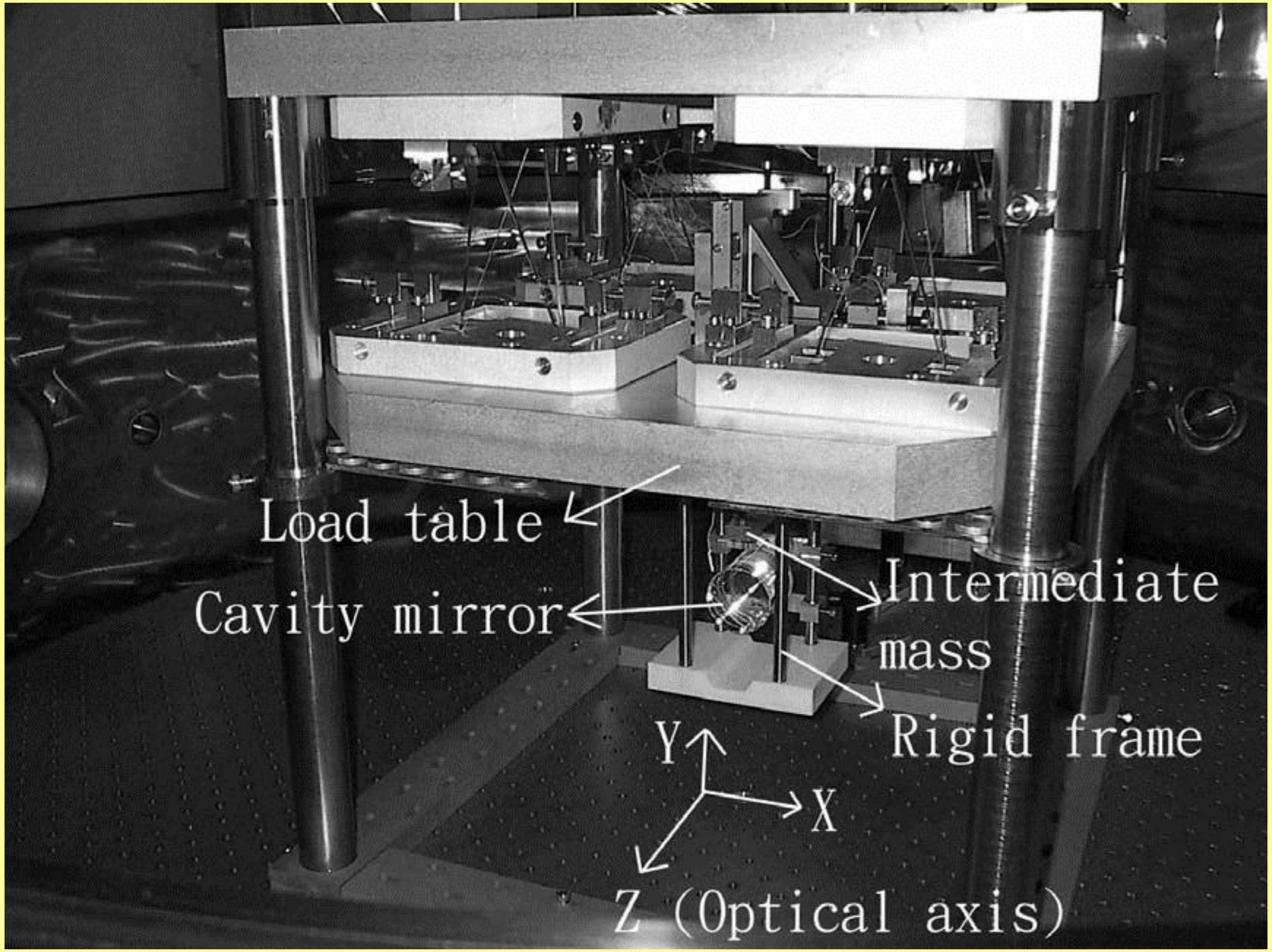

USST 9 m Q & A Interferometer

- Started construction this year

Scope: Goals –GW Astronomy & Fundamental Physics

Frequency band	GW sources / Possible GW sources	Detection method
Ultrahigh frequency band: above 1 THz	Discrete sources, Cosmological sources, Braneworld Kaluza-Klein (KK) mode radiation, Plasma instabilities	Terahertz resonators, optical resonators, and magnetic conversion detectors
Very high frequency band: 100 kHz – 1 THz	Discrete sources, Cosmological sources, Braneworld Kaluza-Klein (KK) mode radiation, Plasma instabilities	Microwave resonator/wave guide detectors, laser interferometers and Gaussian beam detectors
High frequency band (audio band)*: 10 Hz – 100 kHz	Conpact binaries [NS (Neutron Star)-NS, NS-BH (Black Hole), BH-BH], Supernovae	Low-temperature resonators and Earth-based laser-interferometric detectors
Middle frequency band: 0.1 Hz – 10 Hz	Intermediate mass black hole binaries, massive star (population III star) collapses	Space laser-interferometric detectors of arm length 1,000 km – 60,000 km
Low frequency band (milli-Hz band)†: 100 nHz – 0.1 Hz	Massive black hole binaries, Extreme mass ratio inspirals (EMRIs), Compact binaries	Space laser-interferometric detectors of arm length longer than 60,000 km
Very low frequency band (nano-Hz band): 300 pHz – 100 nHz	Supermassive black hole binary (SMBHB) coalescences, Stochastic GW background from SMBHB coalescences	Pulsar timing arrays (PTAs)
Ultralow frequency band: 10 fHz – 300 pHz	Inflationary/primordial GW background, Stochastic GW background	Astrometry of quasar proper motions
Extremely low (Hubble) frequency band: 1 aHz–10 fHz	Inflationary/primordial GW background	Cosmic microwave background experiments
Beyond Hubble-frequency band: below 1 aHz	Inflationary/primordial GW background	Through the verifications of primordial cosmological models

Scope: Researchers and Budget

- (i) Experimentalists (Experimental Astronomers, Engineers, Physicists), working on detectors and data processing;
- (ii) Multi-Messenger Astronomers, working on astrophysics;
- (iii) Theoretical Physicists/Cosmologists, working on fundamental physics and theoretical cosmology.

- Budget: grow up to 20 % - 30 % of Astronomy Budget

Precision

- Design sensitivity of **KAGRA**. DRSE, shown in the right-hand side figure is more sensitive at frequencies of less than 500Hz, while BRSE in the left-hand side figure is better at higher frequencies. (from [53])

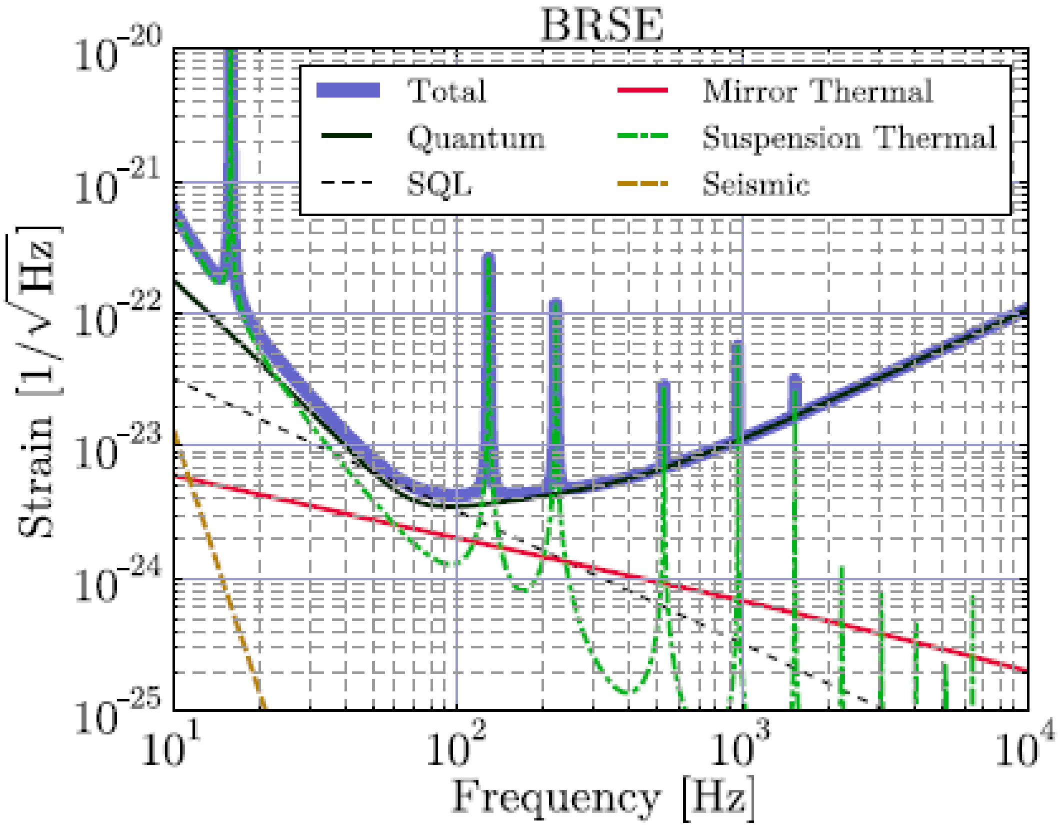

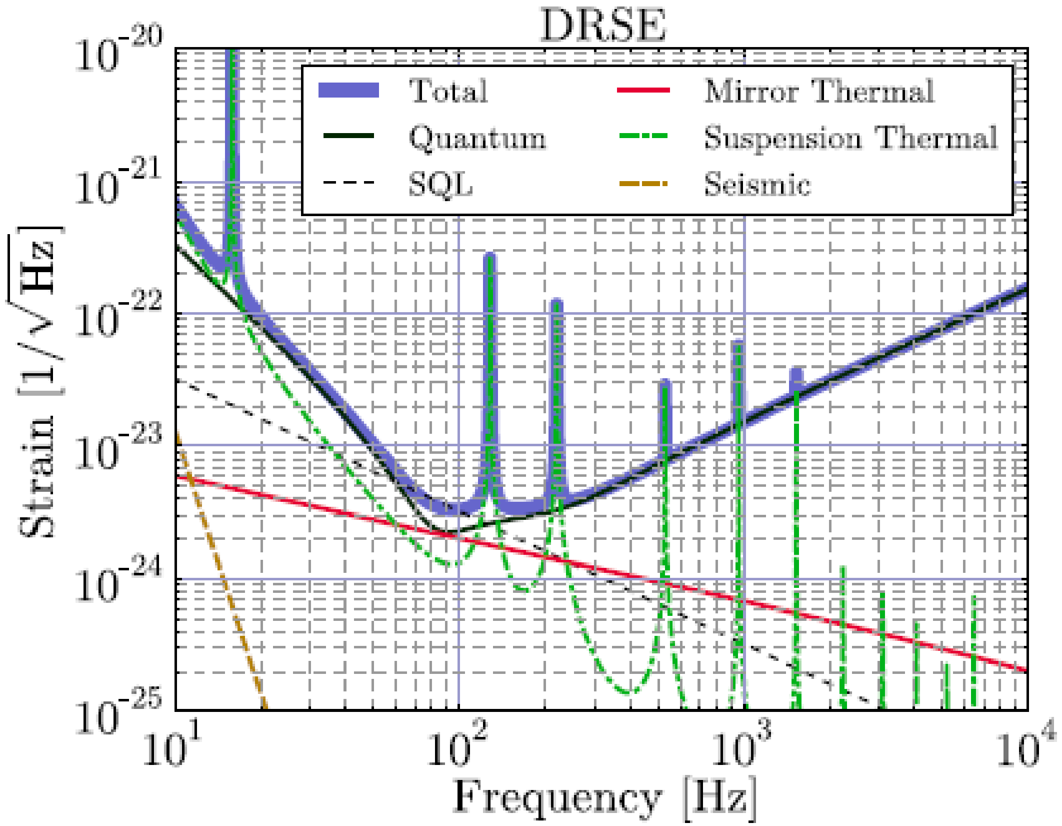

归一化引力波谱能量密度 Normalized GW spectral energy density Ω_{gw} vs. 频率 requency for GW detector sensitivities and GW sources

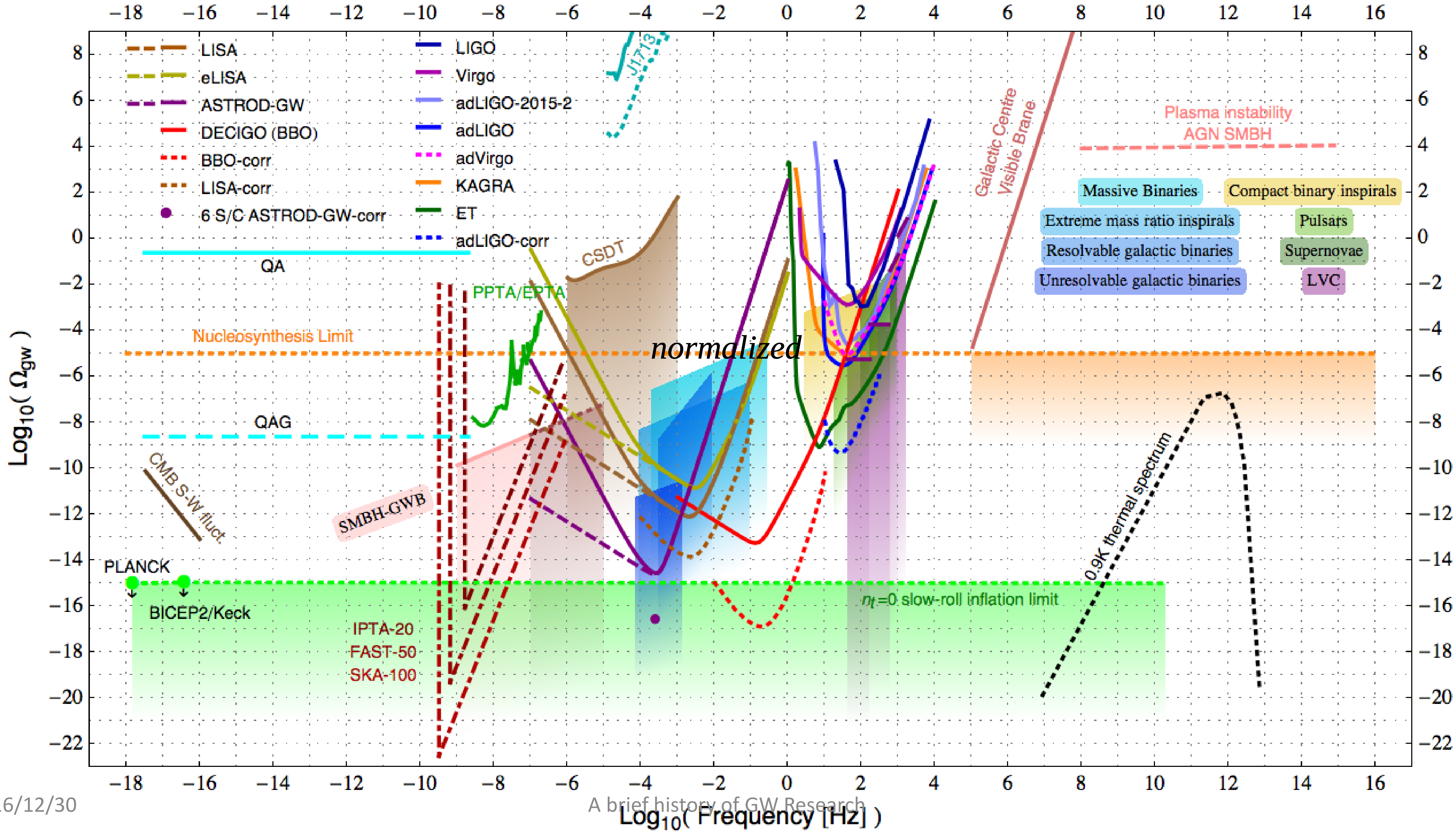

Innovation and Innovative Manufacturing

- production of large and homogeneous optical components
- optical diagnosis of large components
- high reflectance dielectric coating on large mirrors
- manufacturing of components for ultrahigh vacuum of large volume
- manufacturing of high attenuating vibration isolation system
- production of high-power high-stability single-frequency lasers
- production of high-resolution length measurement and positioning systems
- Drag-free technology
- Weak light phase locking and manipulation technology

Production of large and homogeneous optical components

- Example:
- For KAGRA, production of large sapphire mirrors with 220 mm/250 mm with the required homogeneity and absorption for cryogenic use at 20 K is still an issue.

- Although large boule of 100 kg could be produced, the quality is still an issue which needs more testing and innovation.

Optical diagnosis of large optical components

247th EFST

Requirements for Testing LIGO Optics

- **GENERAL:**
  - 1.06 μm wavelength
  - Fizeau phase shifting type
  - 150 mm diameter
  - Two fixed magnifications at two fixed focus locations
- **MEASUREMENT RANGE:**
  - Sample ROC: 5.5 km to 14.5 km
  - Sample reflectivity: 4%, 50% and above 90%
  - Spatial scale: 1 mm to 10 cm
- **ABSOLUTE ACCURACY:**
  - $\lambda/100$ PV for focus and astigmatism coefficient
  - $\lambda/1000$ RMS for residual surface after removal focus and astigmatism terms
  - ROC measurement accuracy: < 3%
  - Retrace error: 6 nm PV for 4 fringes of sample tilt

Optical diagnosis of large optical components

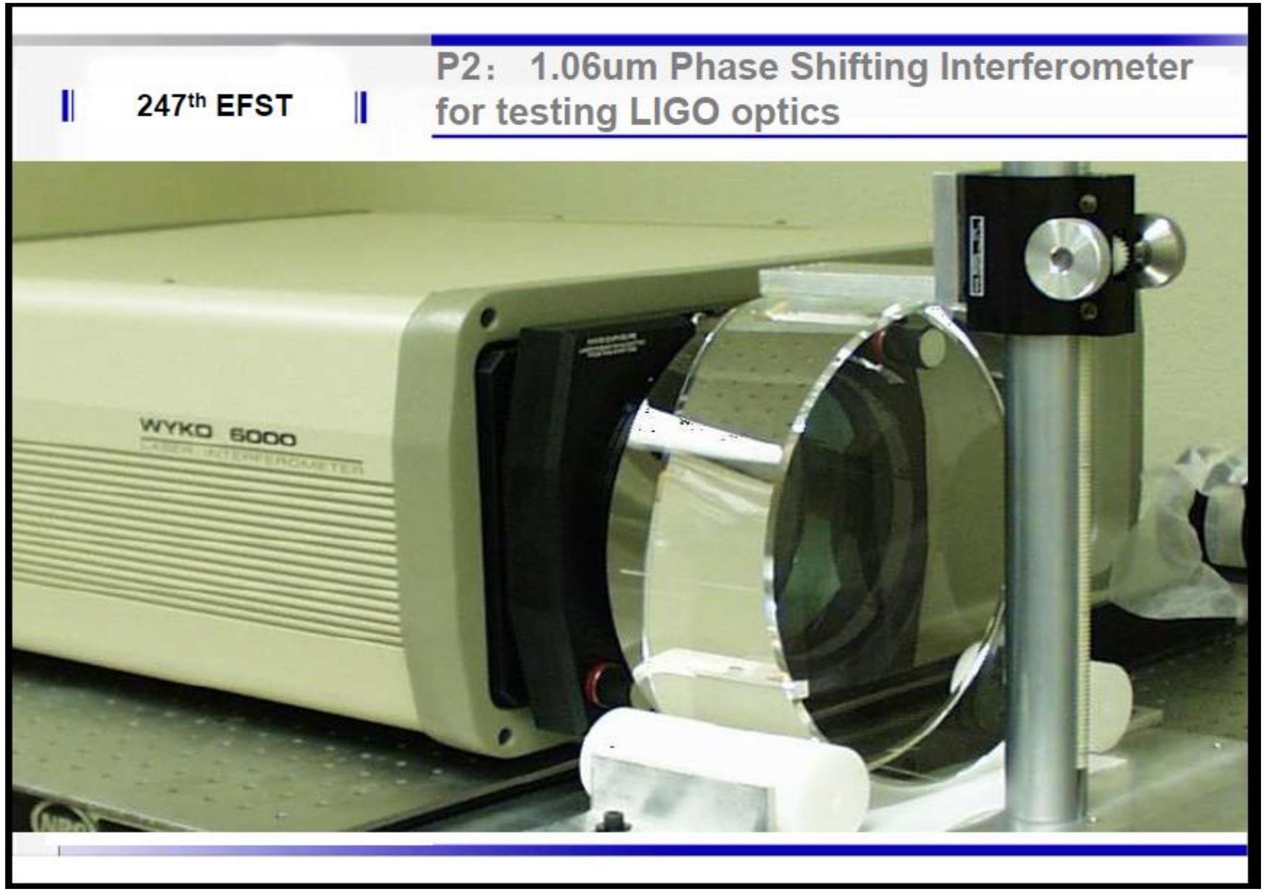

Low loss coating development at NTHU Prof. Chao Lab

At NTHU, we are **focusing on silicon-based amorphous coatings development** for the reasons:

(1) Silicon is likely to be the mirror substrate for next generation detector at 1550nm.

(2) 18" silicon wafer process technology is now matured in IC fabrication industry. (* 18" is larger than the mirror size of next generation detector)

(3) Taiwan has a strong and complete infrastructure and many vendors for silicon IC process.

We are studying amorphous silicon, silicon-nitride and silica thin films that can be deposited on silicon by chemical vapor deposition (CVD) methods.

http://www.examiner.com/article/transition-to-450mm-silicon-wafers-impact-on-analog-chips

PECVD system

LPCVD system

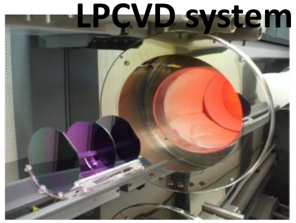

http://www.sil-tronix-st.com/deposition-on-silicon-wafers

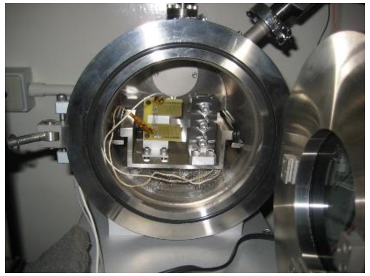

RT ring-down setup

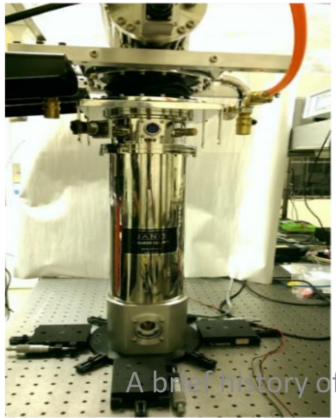

Cryogenic ring-down setup

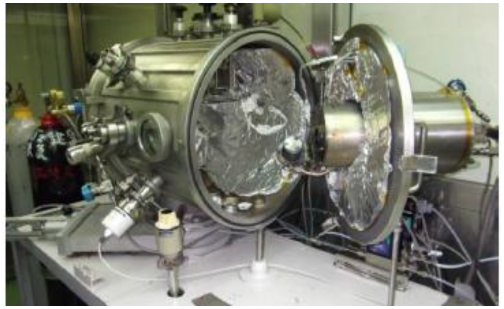

Ion-beam sputter

Configuration of vibration isolation system

Type-A: for cryogenic mirrors
Type-B: for room temperature mirrors
Type-Bp: simpler Type-B
Type-C: for small optics

Type-A

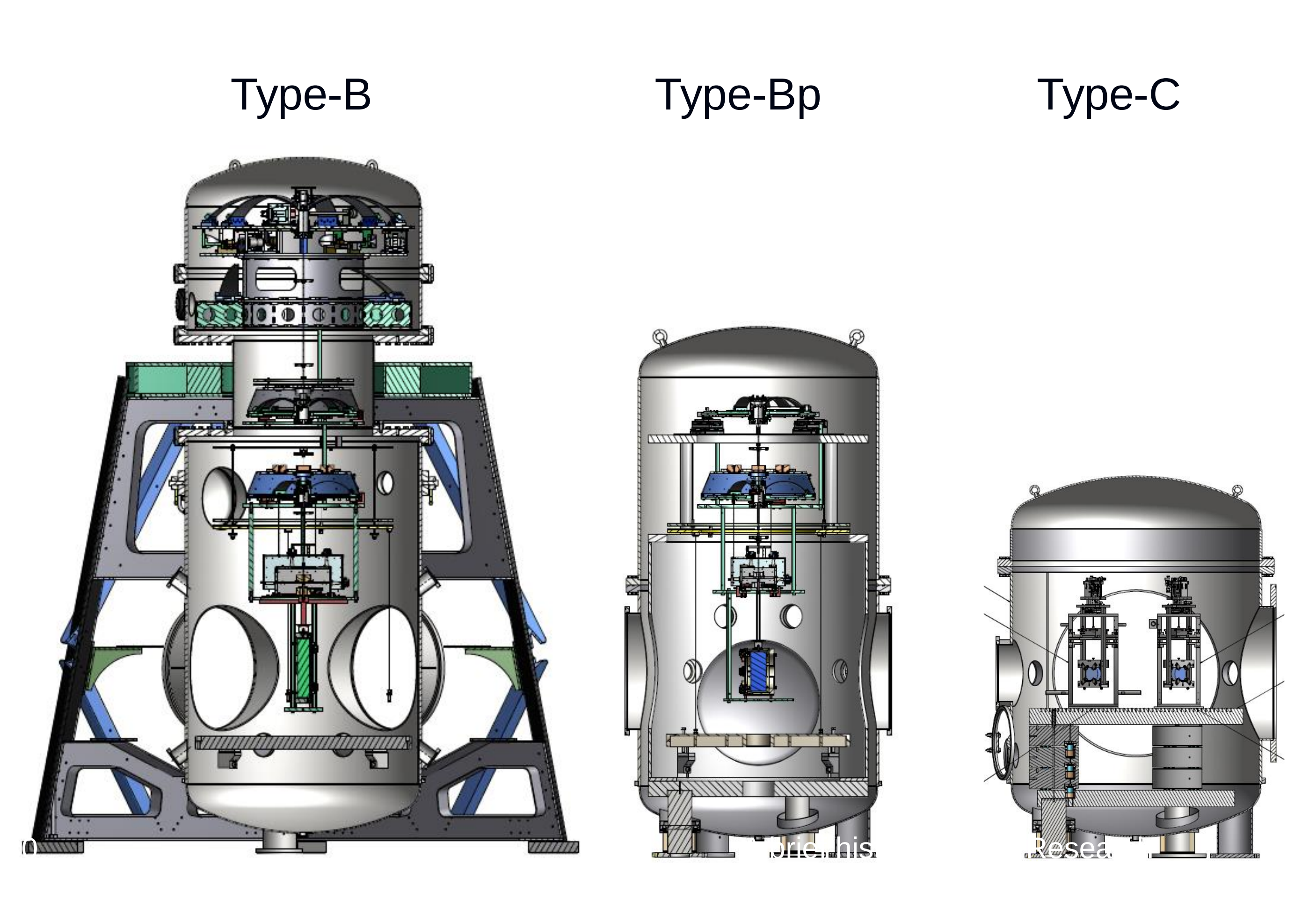

真空管与其遮避屋 Beam Pipe and Enclosure

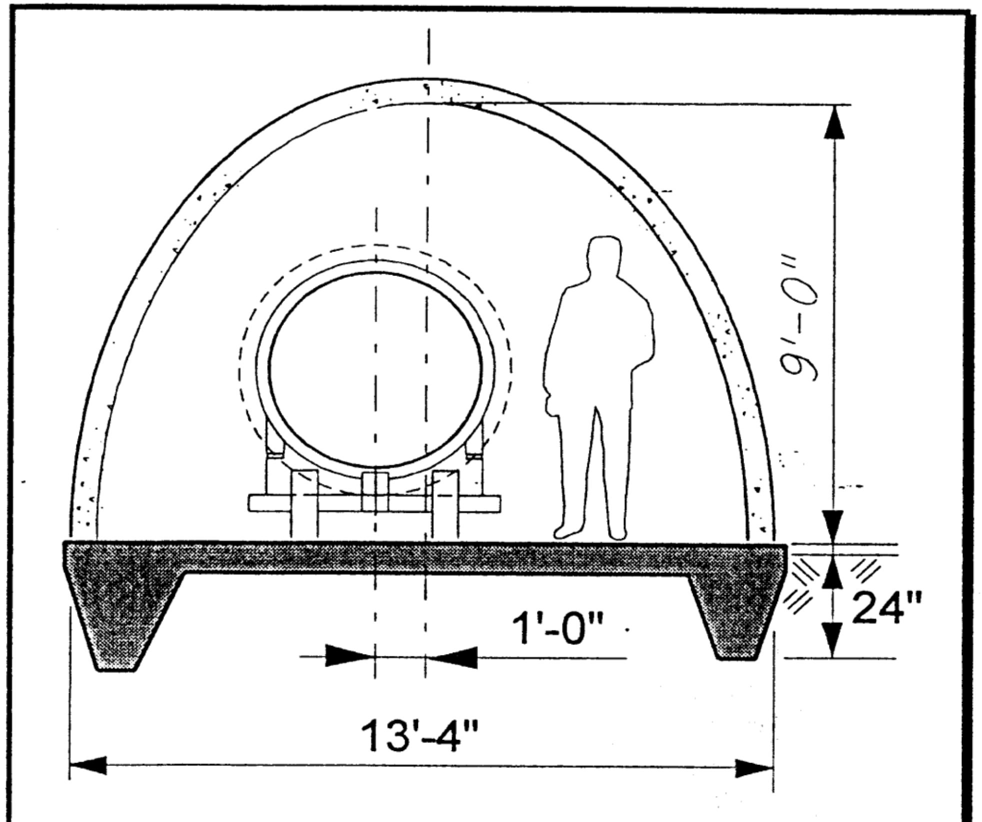

Figure 2.1-1 -- Cross Section of Design Baseline at Hanford

- Minimal Enclosure (no services)
- Beam Pipe
  - 1.2m diam; 3 mm stainless
  - 65 ft spiral weld sections
  - 50 km of weld (NO LEAKS!)

LIGO 真空管去气烘烤 Baking out the LIGO Beam Pipe

insulation

Fermilab Magnet Power Supply

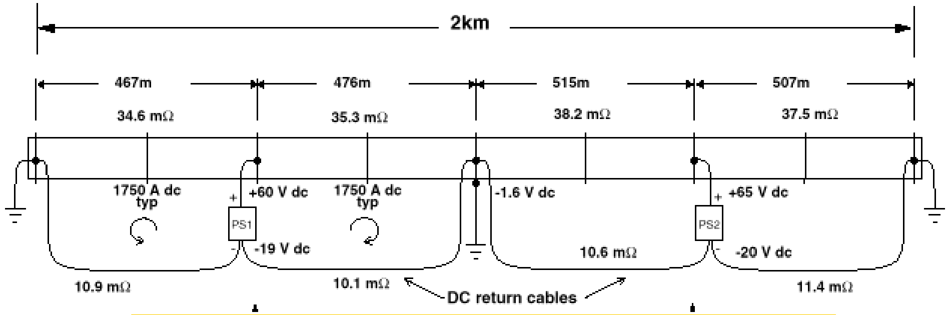

~ 2000 amps for one month

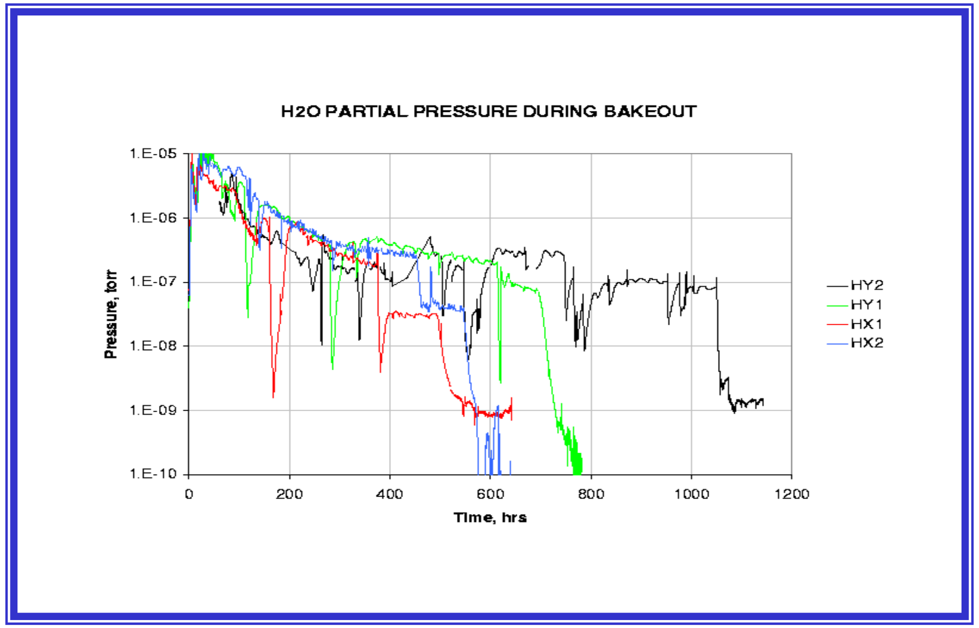

Production of high-power high-stability single-frequency lasers

- Production of high-power high-stability single frequency lasers up to 200 W becomes commercial.

- As the heating issues become lessened, higher power will be needed.

Production of high resolution length measurement and positioning systems

- In the drag-free control of spacecraft, we need precision metrology sensor to sense the position of the spacecraft relative to the proof mass. For this purpose, there are two choices – capacitance sensor and laser metrology sensor.[55]
- For a laser metrology sensor system, larger gap is possible. Hence, less local gravitational disturbances are incurred and better accuracy in controlling the deviation from the geodesics can be achieved.
- Sub-picometer accuracy achieved. Adaption to various situation needs development.

Drag-free technology

- Basically achieved.
- Needs industrialization.

Weak-light phase locking and manipulation technology

- Weak-light phase locking is crucial for long-distance space interferometry and for CW laser space communication. For LISA of arm length of 5 Gm (million km) the weak-light phase locking requirement is for 70 pW laser light to phase-lock with an onboard laser oscillator. For ASTROD-GW arm length of 260 Gm (1.73 AU) the weak-light phase locking requirement is for 100 fW laser light to lock with an onboard laser oscillator. Weak-light phase locking for 2 pW laser light to 200 μW local oscillator is demonstrated in our laboratory in Tsing Hua U.[6] Dick *et al.*[7] from their phase-locking experiment showed a PLL (Phase Locked Loop) phase-slip rate below one cycle slip per second at powers as low as 40 femtowatts (fW).

Looking into the future from announcement of first detection February 11, 2016 展望

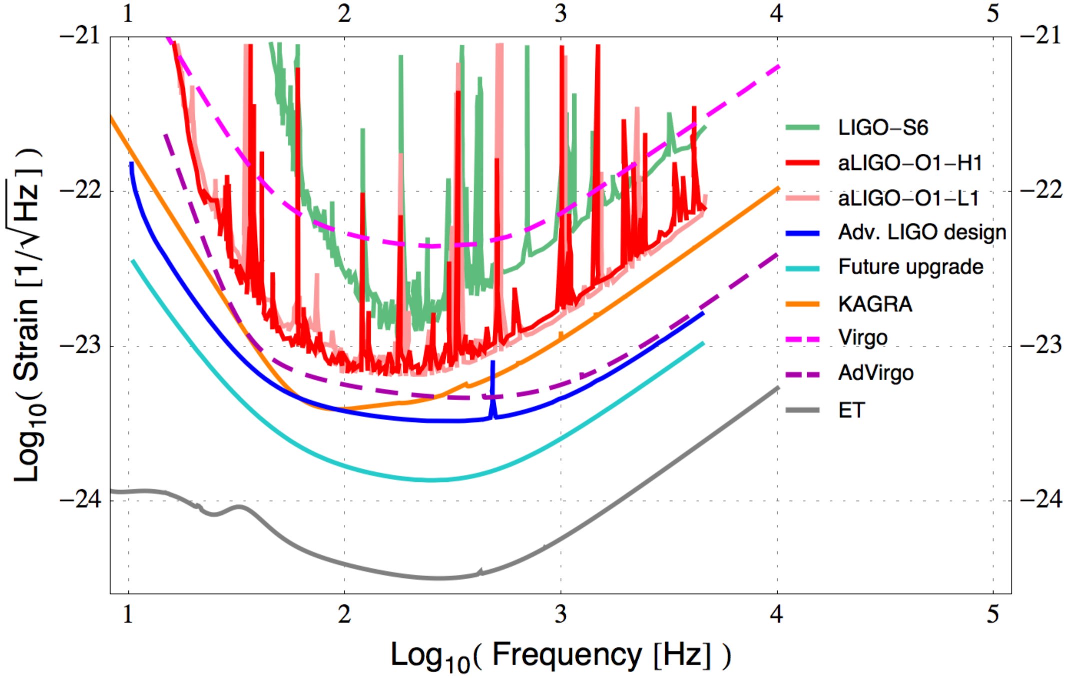

- Present aLIGO sensitivity: ~ two 5-σ event per 130 days.
- Goal second generation sensitivity: 100 5-σ events per year
- Improved 2nd gen.: x2, 800-1000 events/yr
- First generation sensitivity: several 3-σ events per year → one should look at the past data and try to search for them with better efforts and methods
- Third generation sensitivity → 100,000 or more 5-σ events per year Plenty compared to some other branches of physics and astronomy

Outlook

- GW astronomy has been an important drive to technology.

- Now it is growing.

- It will even be so. Let’s discern what will come in next 50-100 years.


Thank you

Looking into the future from announcement of first detection February 11, 2016 展望

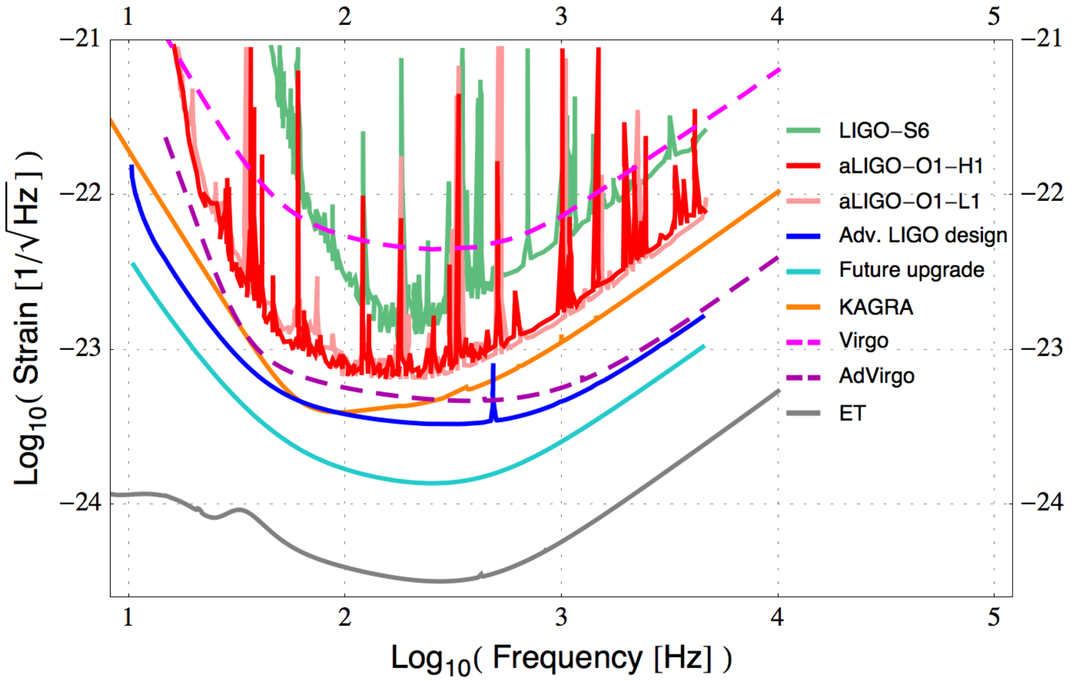

- Present aLIGO sensitivity: ~ two 5-σ event per 130 days.
- Goal second generation sensitivity: 100 5-σ events per year
- Improved 2nd gen.: x2, 800-1000 events/yr
- First generation sensitivity: several 3-σ events per year → one should look at the past data and try to search for them with better efforts and methods
- Third generation sensitivity → 100,000 or more 5-σ events per year Plenty compared to some other branches of physics and astronomy

Outlook

- GW astronomy has been an important drive to technology.

- Now it is growing.

- It will even be so. Let’s discern what will come in next 50-100 years.

Thank you

探测光学桌 *Detection Optical Bench*

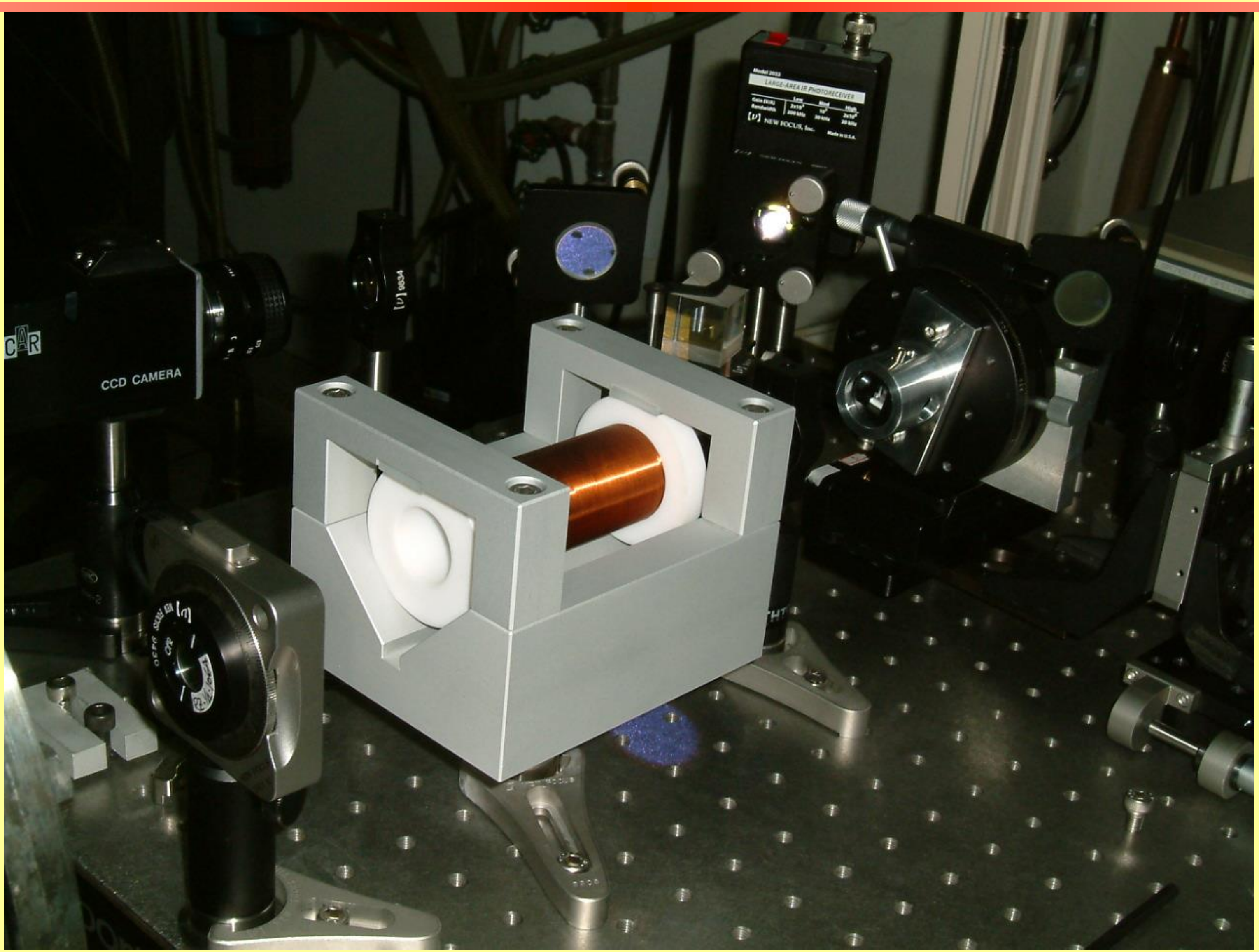

The ga


247th EFST
P1: First World-Wide 24” Phase Shifting Interferometer, Installed in Chengdu, China
WYKO 24”
PHASE SHIFTING INTERFEROMETER
WYKO
WYKO

► GENERAL:
- 1.06 mm wavelength
- Fizeau phase shifting type
- 150 mm diameter
- Two fixed magnifications at two fixed focus locations

► ABSOLUTE ACCURACY:
- l/100 PV for focus and astigmatism coefficient
- l/1000 RMS for residual surface after removal focus
A-C2 4R7othunEdFtSaTble

► MEASUREMENT RANGE:
- Sample ROC: 5.5 km to 14.5 km
- Sample reflectivity: 4%, 50% and above 90%
- Spatial scale: 1 mm to 10 cm and astigmatism terms
- ROC measurement accuracy: < 3%
- Retrace error: 6 nm PV for 4 fringes of sample tilt

真空腔与磁铁 Vacuum Chamber and Magnet

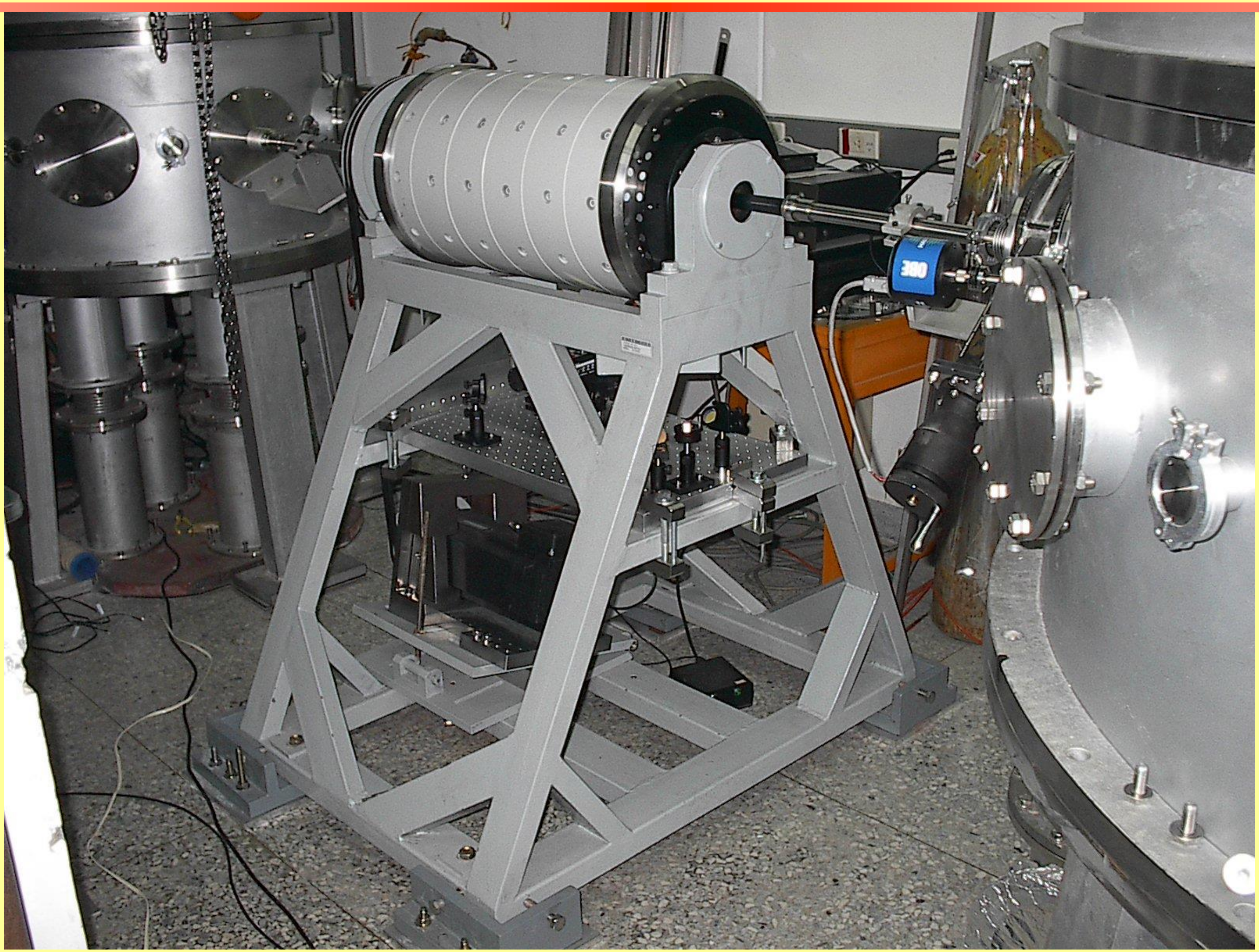

法布里-珀罗干涉仪 *Fabry-Perot Interferometer*

- Length: 3.5 m (Extendable to 7 m)
- Cavity Mirror Diameter: 50 mm
- Radius of Curvature of Cavity Mirror: 5 m and plano
- Laser: 1064 nm, frequency tunable, ~700mW
- Free Spectral Range: ~43 MHz
- Finesse: 30000

悬吊系统 *Suspension System*

›单摆的传递函数 *Transfer function of a simple pendulum*

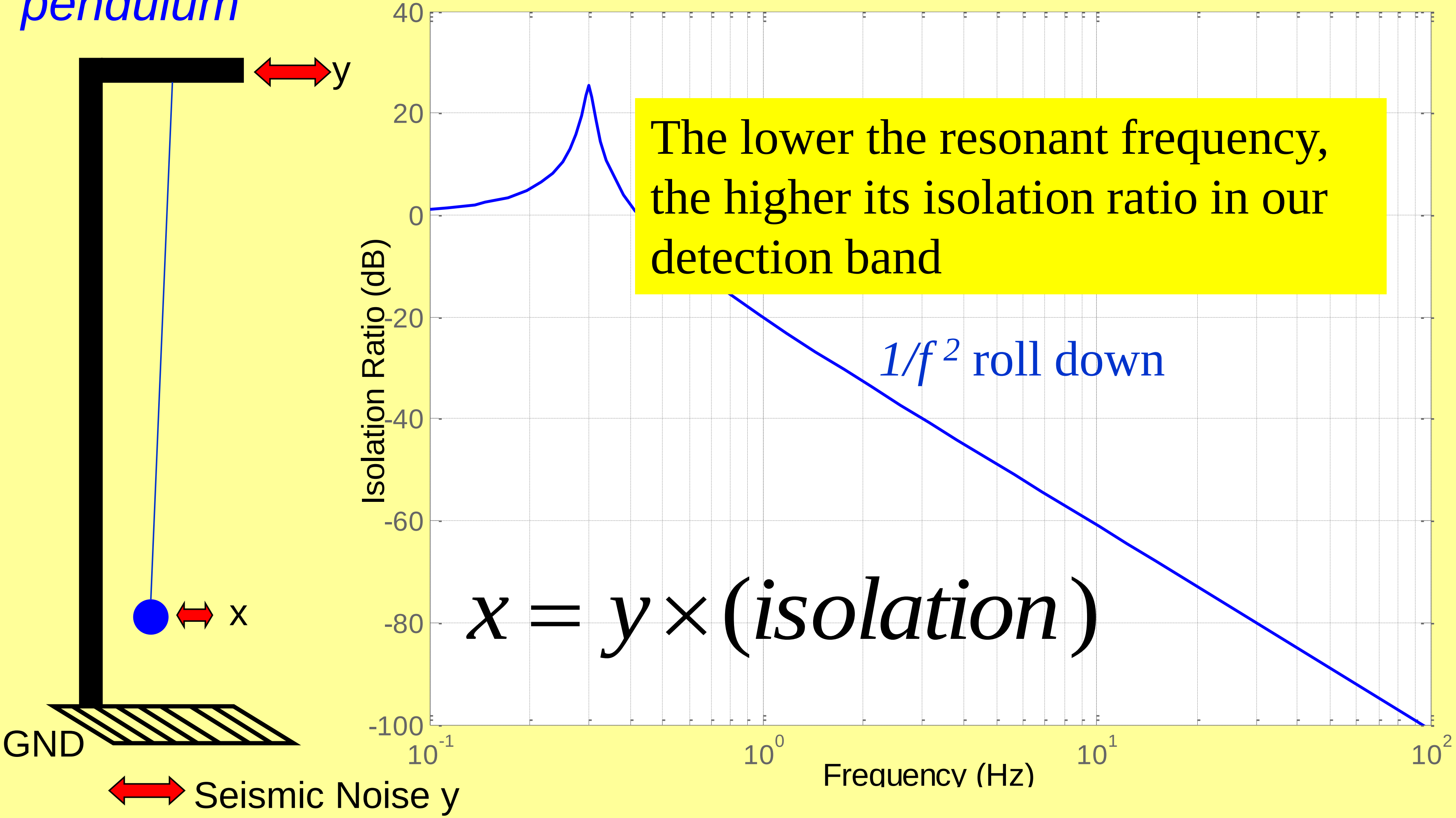

悬吊系统 *Suspension System*

›X摆 *X-Pendulum*

- Designed and developed by TAMA gravitation wave detection group, ICRR, Japan
- Resonant frequency
  - theoretically, can be infinitely low
  - ~0.3 Hz in our experiment
- Difficulties:
  - large resonant motion
  - ambiguous process of frequency tuning

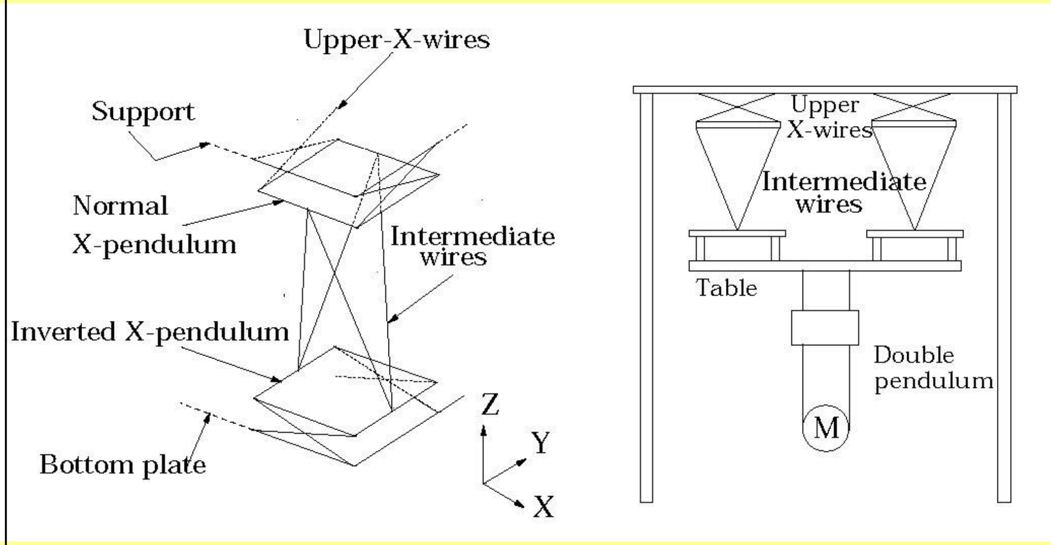

X摆 *X-Pendulum*

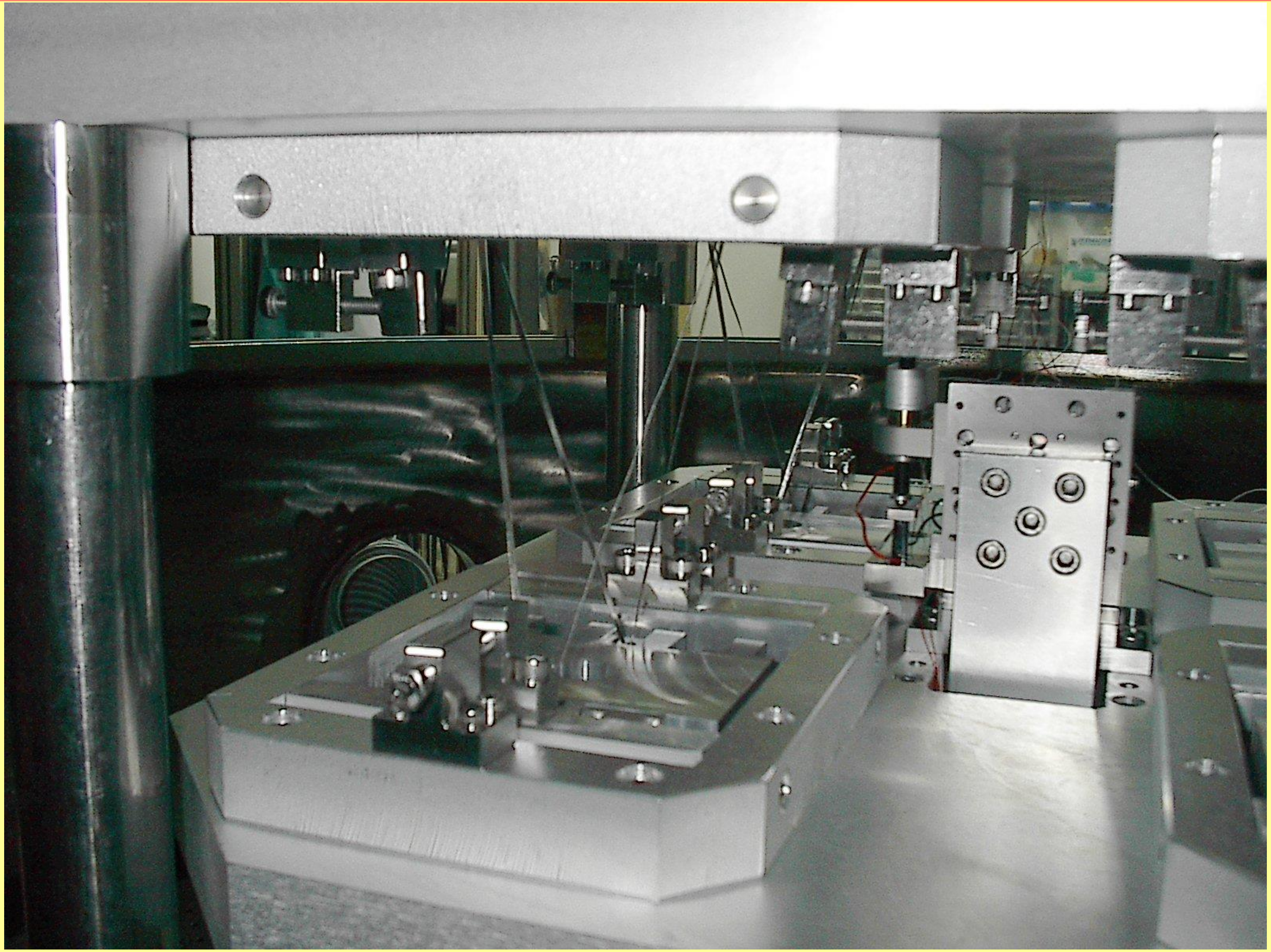

X摆 *X-Pendulum*

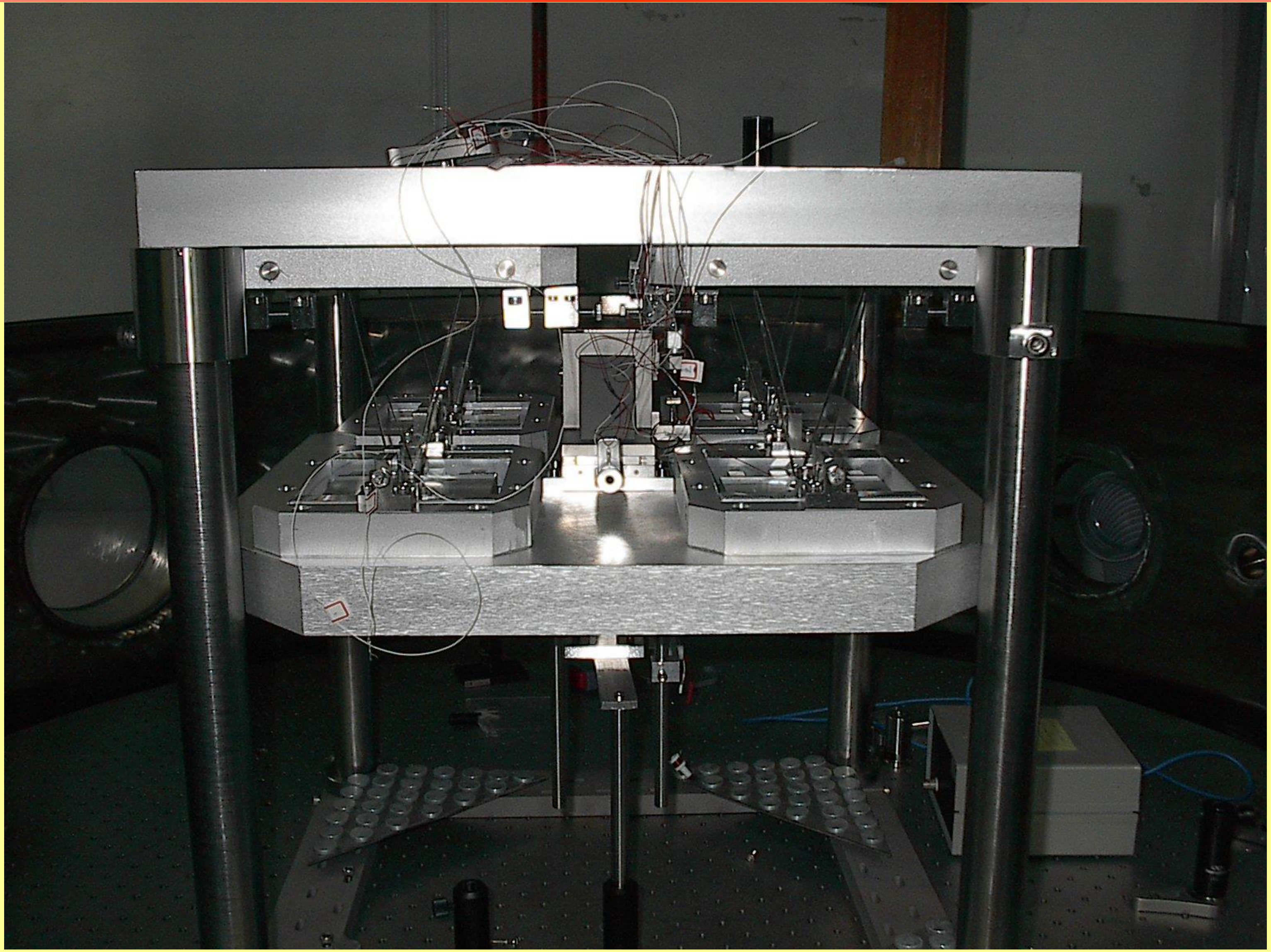

地基 Ground-based GW detectors

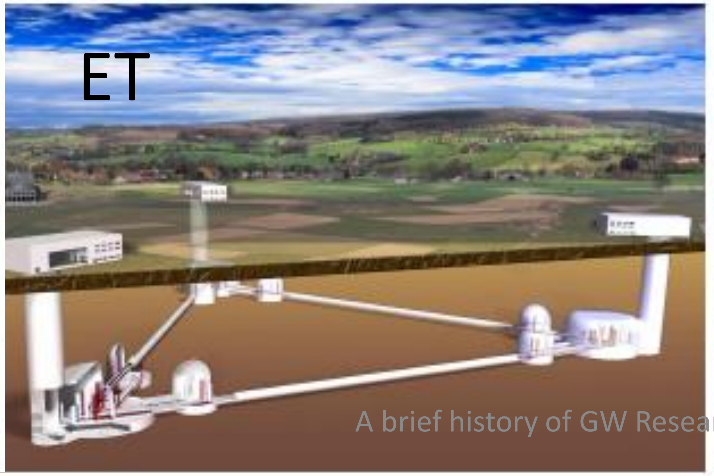

脉冲星计时数组

Pulsar Timing Arrays

PPTA, NANOGrav, EPTA, IPTA
FAST, SKA

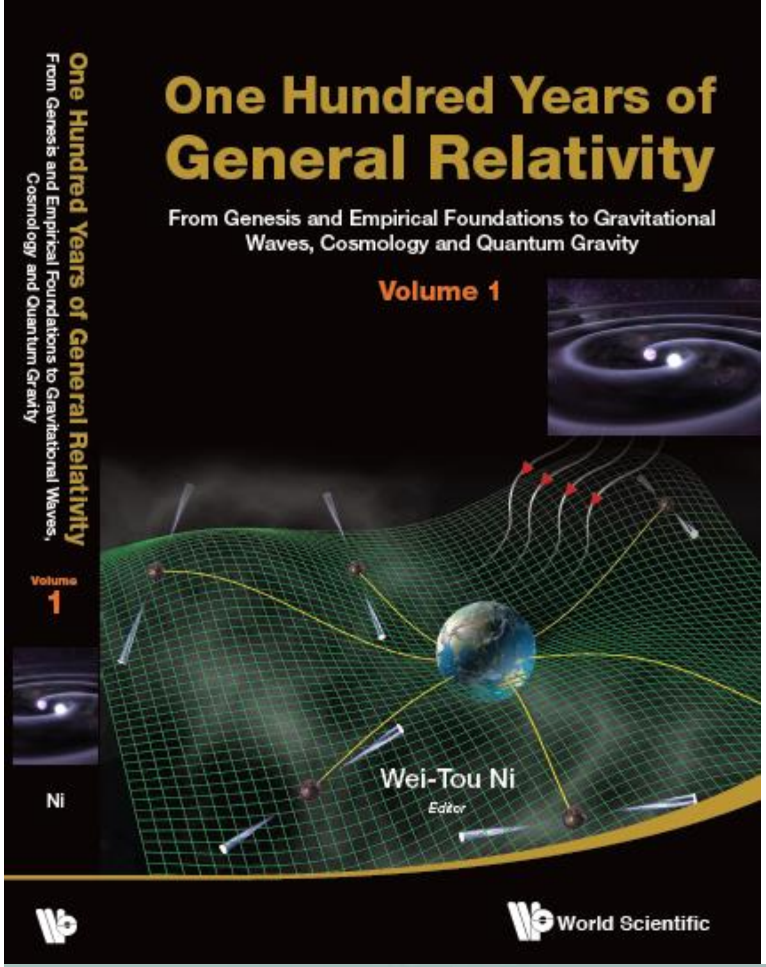

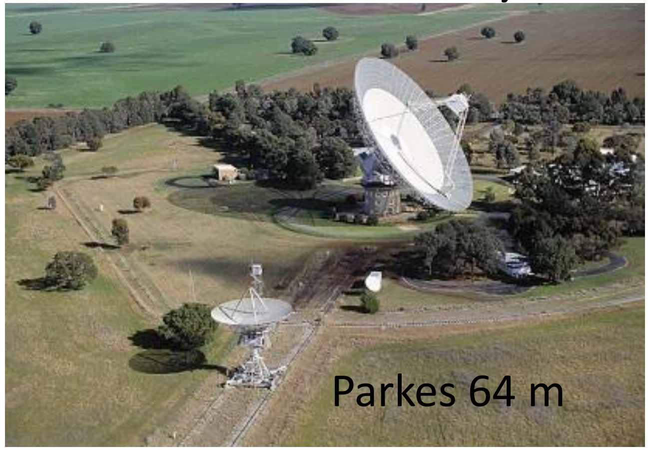

EPTA

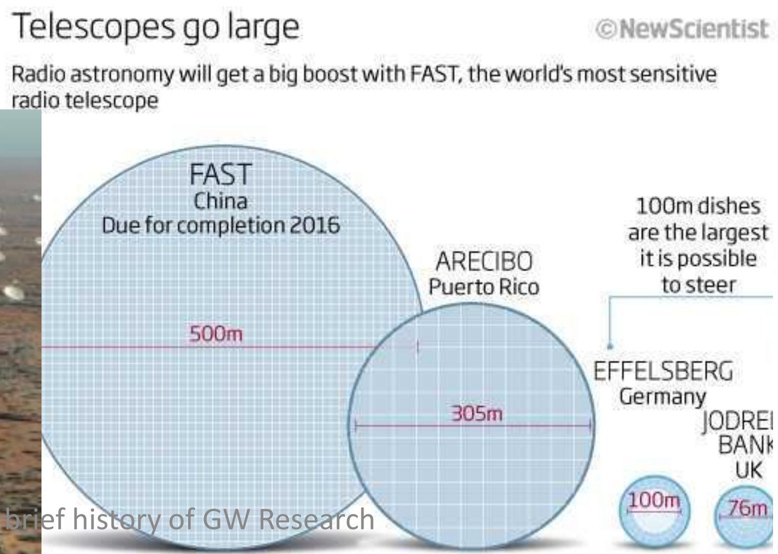

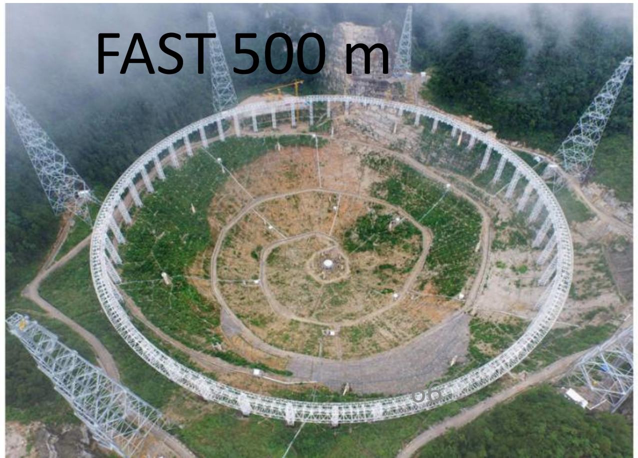

转换因子 Conversion factors among:
特征应变 the characteristic strain $h_c(f)$,
应变功率谱密度振幅 the strain psd (power spec. d.) $[S_h(f)]^{1/2}$
the normalized spectral energy density $\Omega_{gw}(f)$

- $h_c(f) = f^{1/2}\,[S_h(f)]^{1/2}$;
- 归一化引力波谱能量密度 *normalized GW spectral energy density* $\Omega_g(f)$: GW spectral energy density in terms of *the energy density per logarithmic frequency interval divided by the cosmic closure density* ρ_c for a cosmic GW sources or background, i.e.,
- $\Omega_{gw}(f) = (f/\rho_c)\, d\rho(f)/df$
- $\Omega_{gw}(f) = (2\pi^2/3H_0^2)\, f^3\, S_h(f) = (2\pi^2/3H_0^2)\, f^2\, h_c^2(f)$.

	Characteristic strain $h_c(f)$	Strain psd $[S_h(f)]^{1/2}$	Normalized spectral energy density $\Omega_{gw}(f)$
$h_c(f)$	$h_c(f)$	$f^{1/2}\,[S_h(f)]^{1/2}$	$[(3H_0^2/2\pi^2 f^2)\Omega_{gw}(f)]^{1/2}$
Strain psd $[S_h(f)]^{1/2}$	$f^{-1/2} h_c(f)$	$[S_h(f)]^{1/2}$	$[(3H_0^2/2\pi^2 f^3)\Omega_{gw}(f)]^{1/2}$
$\Omega_{gw}(f)$	$(2\pi^2/3H_0^2)\, f^2\, h_c^2(f)$	$(2\pi^2/3H_0^2)\, f^3\, S_h(f)$	$\Omega_{gw}(f)$

应变功率谱密度振幅 Strain power spectral density (psd) amplitude vs. 频率 frequency for various GW detectors and GW sources

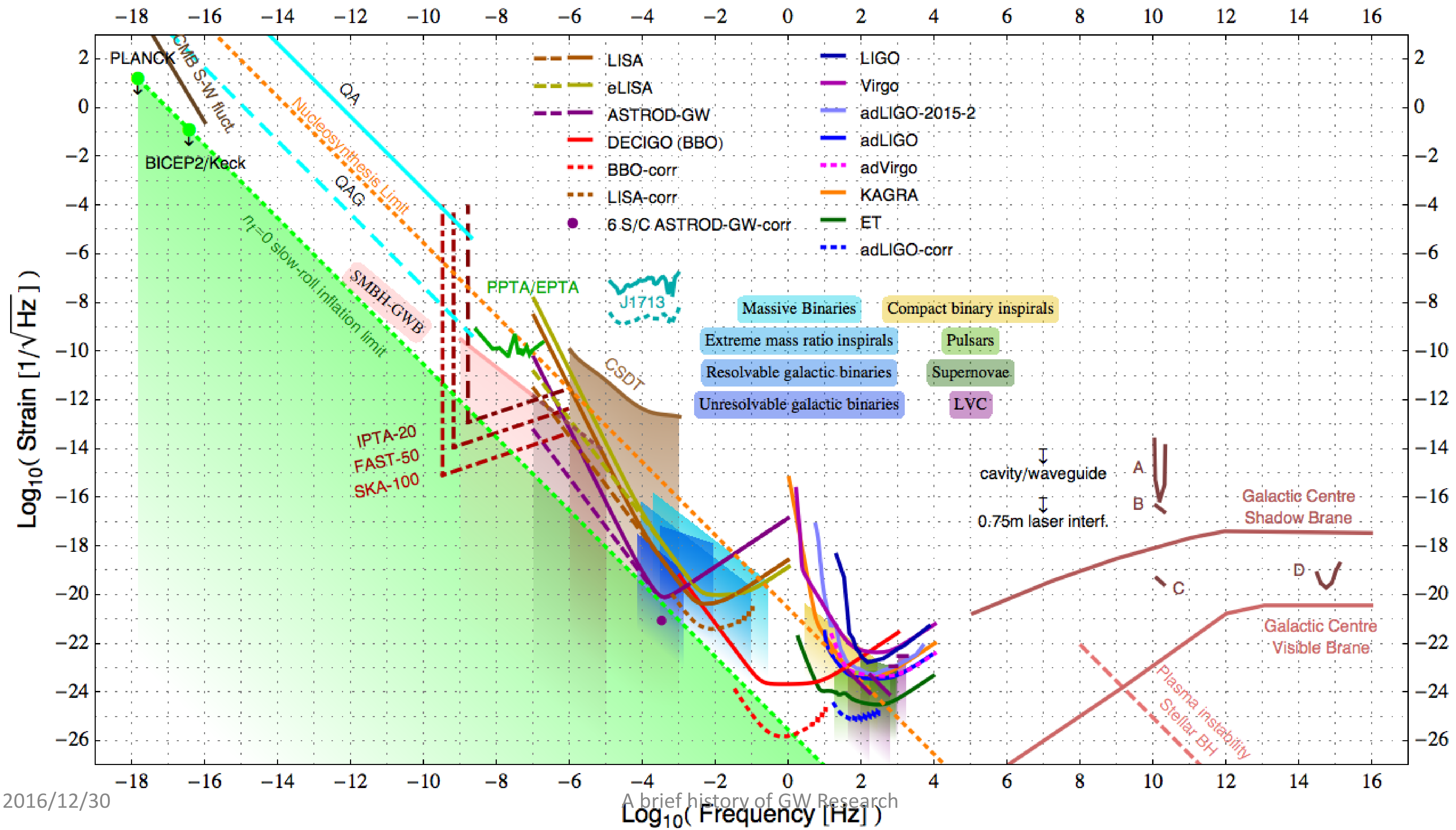

Characteristic strain h_c vs. frequency for various GW detectors and sources. [QA: Quasar Astrometry; QAG: Quasar Astrometry Goal; LVC: LIGO-Virgo Constraints; CSDT: Cassini Spacecraft Doppler Tracking; SMBH-GWB: Supermassive Black Hole-GW Background.]

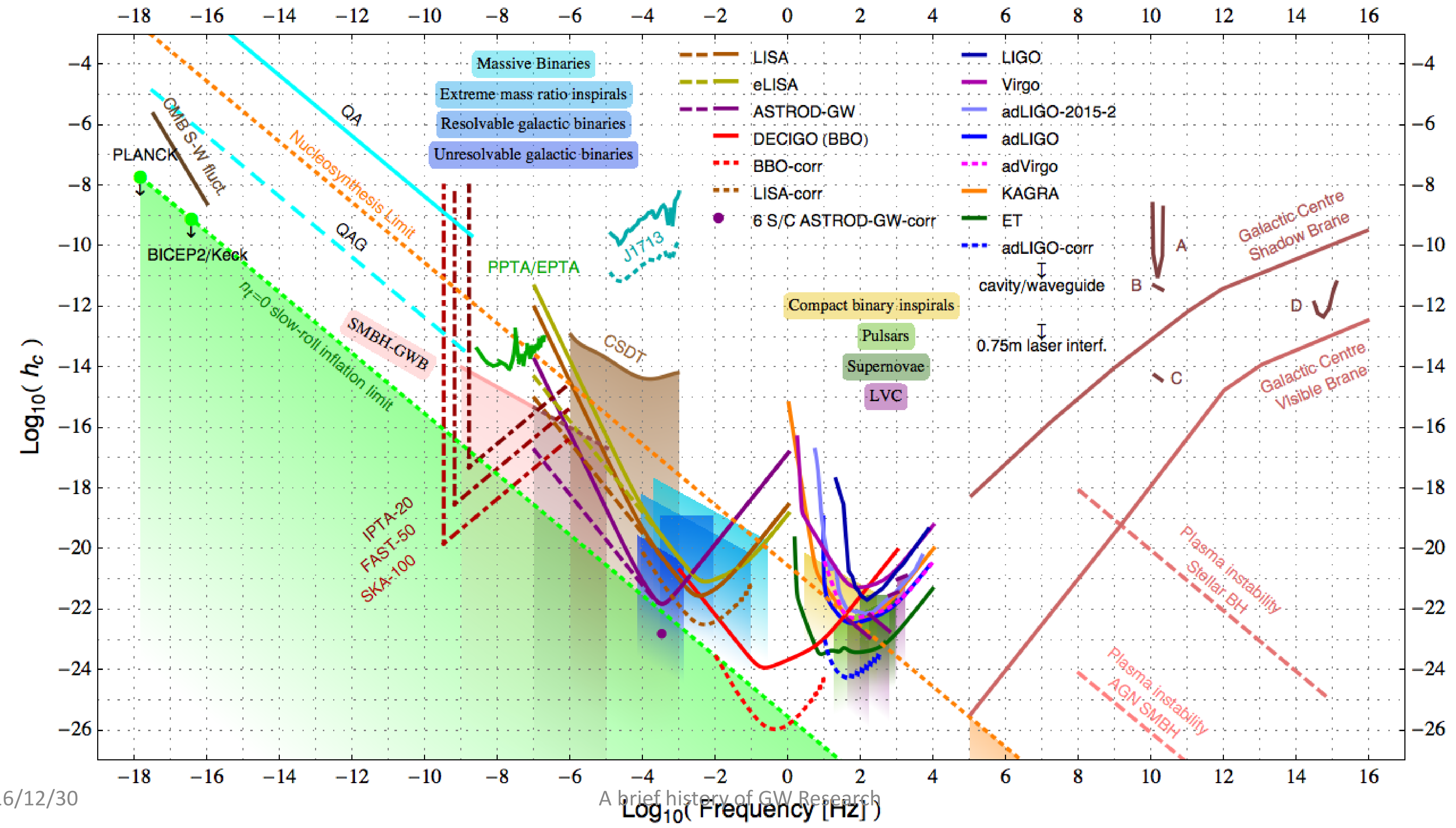

归一化引力波谱能量密度 Normalized GW spectral energy density Ω_{gw} vs. 频率 requency for GW detector sensitivities and GW sources

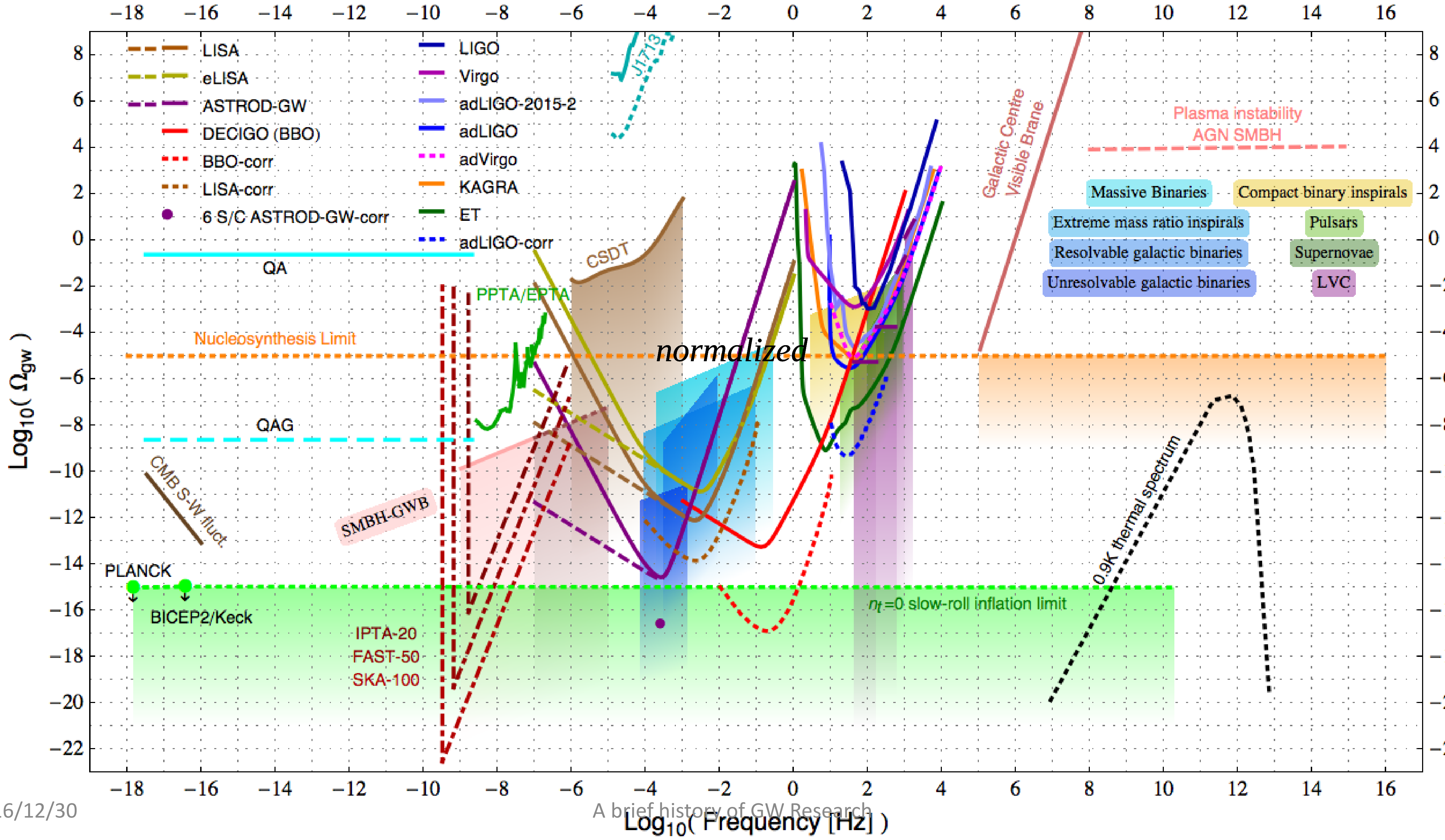

引力波谱分类 The Gravitation-Wave (GW) Spectrum Classification

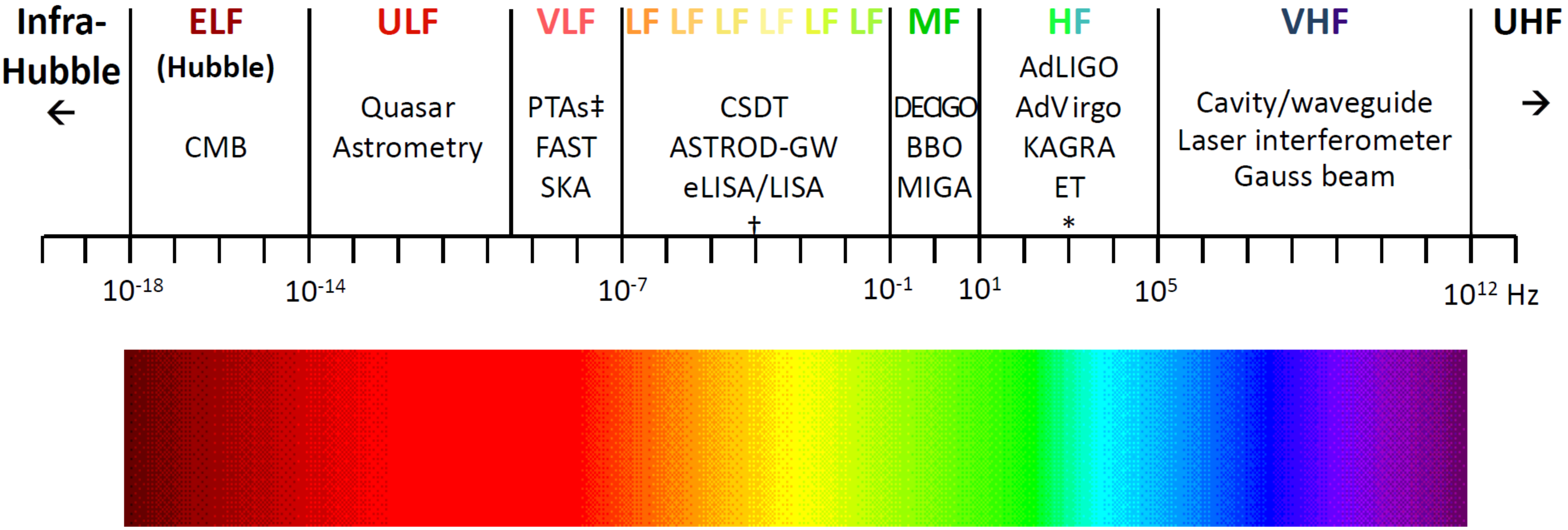

* AIGO, AURIGA, EXPLORER, GEO, NAUTILUS, MiniGRAIL, Schenberg.

† OMEGA, gLISA/GEOGRAWI, GADFLI, TIANQIN, ASTROD-EM, LAGRANGE, ALIA, ALIA-descope.

‡ EPTA, NANOGrav, PPTA, IPTA.

引力波－时空中的涟漪

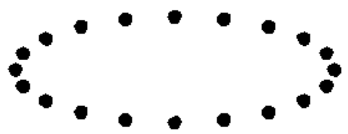

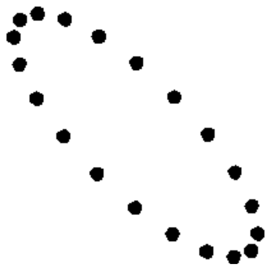

$$[\epsilon^{(1)}]_{ij} = \begin{pmatrix} 0 & 0 & 0 \\ 0 & 0 & 0 \\ 0 & 0 & 1 \end{pmatrix} \qquad [\epsilon^{(2)}]_{ij} = \begin{pmatrix} 0 & 0 & 1 \\ 0 & 0 & 0 \\ 1 & 0 & 0 \end{pmatrix}$$

$$[\epsilon^{(3)}]_{ij} = \begin{pmatrix} 0 & 0 & 0 \\ 0 & 0 & 1 \\ 0 & 1 & 0 \end{pmatrix} \qquad [\epsilon^{(4)}]_{ij} = \text{GR} \begin{pmatrix} 1 & 0 & 0 \\ 0 & -1 & 0 \\ 0 & 0 & 0 \end{pmatrix}$$

$$[\epsilon^{(5)}]_{ij} = \text{GR} \begin{pmatrix} 0 & 1 & 0 \\ 1 & 0 & 0 \\ 0 & 0 & 0 \end{pmatrix} \qquad [\epsilon^{(6)}]_{ij} = \begin{pmatrix} 1 & 0 & 0 \\ 0 & 1 & 0 \\ 0 & 0 & 0 \end{pmatrix}.$$

GW propagation direction: z

- 单频 Monochromatic

  A single frequency plane GW

- Wave form in time t,

  Spectral form in frequency f

- Noise power amplitude

$<n^2(t)> = \int_0^\infty (df)\, S_n(f),\; h_n(f) \equiv [f\, S_n(f)]^{1/2}$

- Characteristic amplitude

$$G_{\mu\nu} = \kappa\, T_{\mu\nu},\; R_{\mu\nu} = 8\pi G_N\, [T_{\mu\nu} - (1/2)(g_{\mu\nu} T)]$$

$$A_{\mu,\beta}{}^{\beta} = 4\pi J_\mu,$$

$$h_{\mu\nu,\beta}{}^{\beta} = -16\pi G_N [T_{\mu\nu} - (1/2)(\eta_{\mu\nu} T)] + O(h^2)$$

with gauge condition

$$h_{\mu\nu} = -[(4G_N)/(c^4)] \int \{[T_{\mu\nu} - (1/2)\, g_{\mu\nu} T]/r\}_{\text{retarded}}\, (d^3x') + O(h^2)$$

$$A_{\alpha,}{}^{\alpha} = 0.$$

In harmonic gauge

The retarded solution of equation (12) is

$$A_\mu = \int (J_\mu / r)_{\text{retarded}}\, (d^3x').$$

plane GW $h_{\mu\nu}(n_x x + n_y y + n_z z - ct) = h_{\mu\nu}(U)$

$$h_{\mu\nu}(u, t) \equiv h_{\mu\nu}(U) = \int_{-\infty}^{\infty} {}^{(f)}h_{\mu\nu}(f) \exp(2\pi i f U/c)\, (df) = \int_0^\infty 2f\, |{}^{(f)}h_{\mu\nu}(f)| \cos(2\pi f U/c)\, d(\ln f)$$

$$h_{\mu\nu}(U) = \int_0^\infty 2|{}^{(f)}h_{\mu\nu}(f)| \cos(2\pi f U/c)\, (df)$$

$$= \int_0^\infty 2f\, |{}^{(f)}h_{\mu\nu}(f)| \cos(2\pi f U/c)\, d(\ln f).$$

$$h_{\mu\nu}(x, y, z, t) = (c/2\pi)^3 \int {}^{(k)}h_{\mu\nu}(k_x, k_y, k_z) \exp(ik_x x + ik_y y + ik_z z - 2\pi i f t)\, (dk_x dk_y dk_z)$$

$h_c(f) \equiv 2\, f\, [(|{}^{(f)}h_+(f)|^2 + |{}^{(f)}h_\times(f)|^2)]^{1/2};\; h_{cA}(f) \equiv 2\, f\, |{}^{(f)}h_A(f)|$

首探并没有对非广义相对论偏振态制约

The first detection has “No constraints on non-GR polarization states” (LSC and VC)

- Because of the similar orientations of the Hanford and Livingston LIGO instruments, our data cannot exclude the presence of non-GR polarization states in GW150914.
- As an illustration, LSC and VC use the BayesWave GW-transient analysis algorithm [51] to reconstruct the GW150914 signal, assuming the simplest nonphysical case in which the signal model consists of purely a scalar mode.

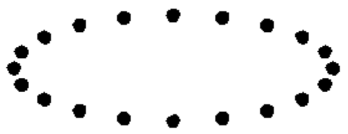

真空腔与防震 Vacuum Chambers and Seismic Isolation

Vacuum Chambers

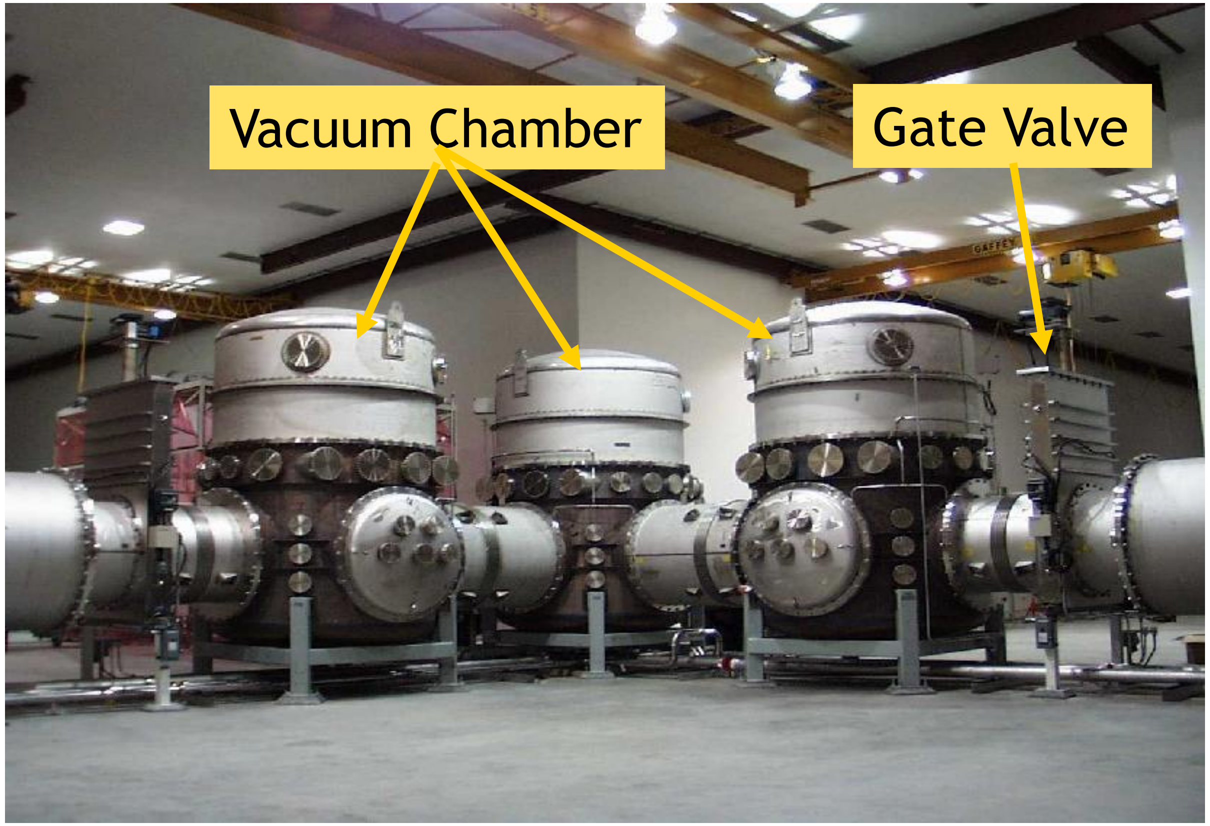

constrained layer damped springs

passive isolation

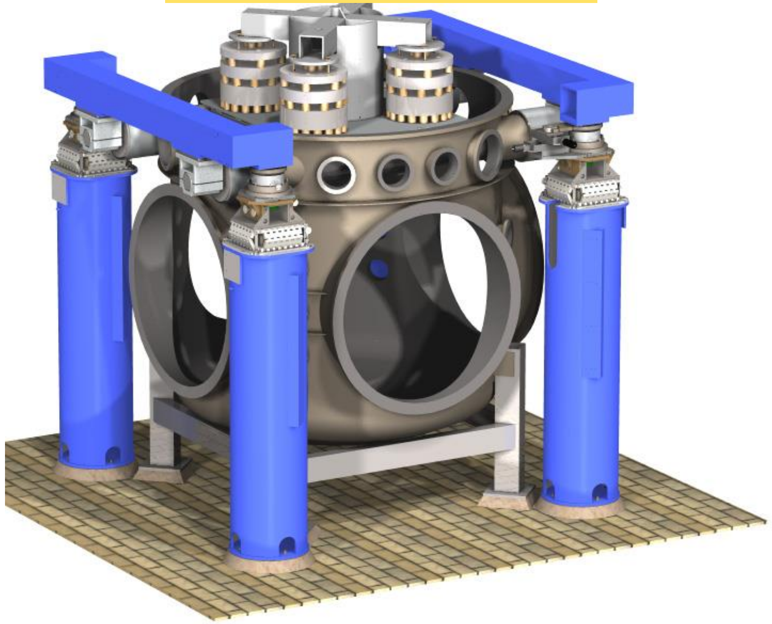

悬吊与光学系统 LIGO I Suspension and Optics

Single suspension 0.31mm music wire

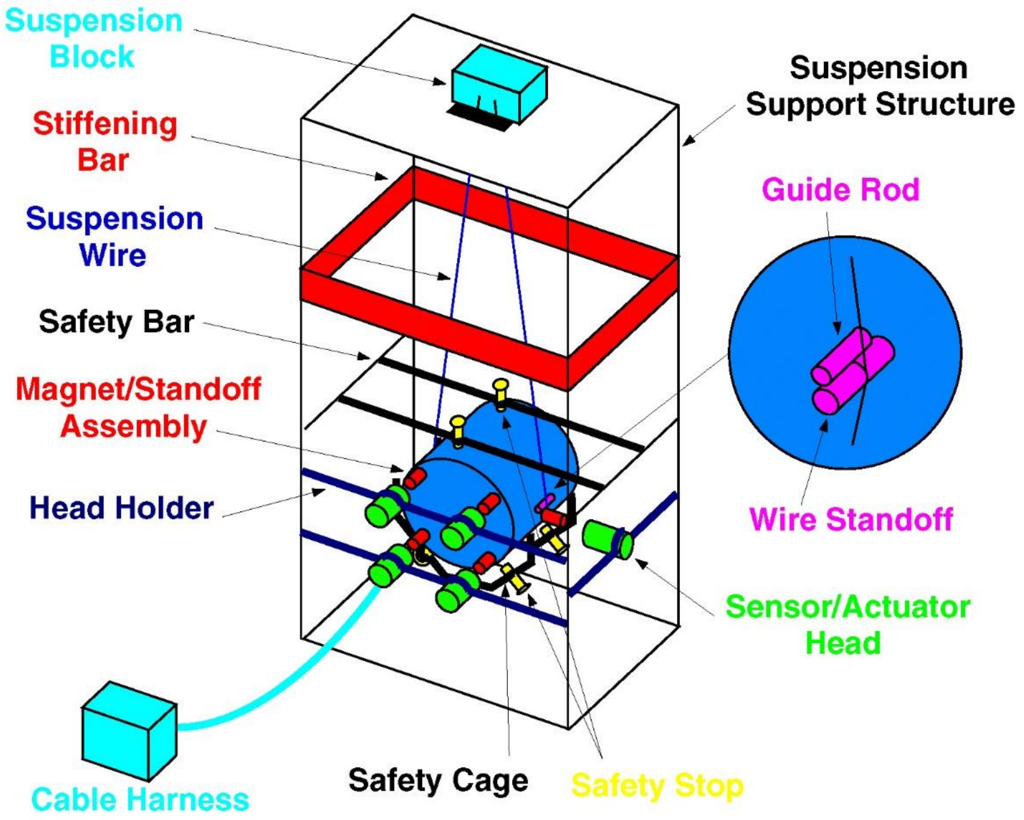

fused silica

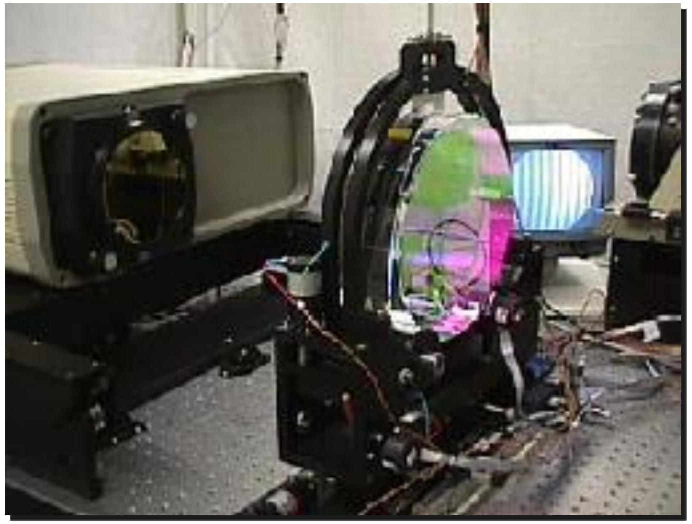

Surface figure = λ/ 6000

- surface uniformity < 1nm rms
- scatter < 50 ppm
- absorption < 2 ppm
- internal Q's > 2 10^6

子系统调试 Commissioning the LIGO I Subsystems

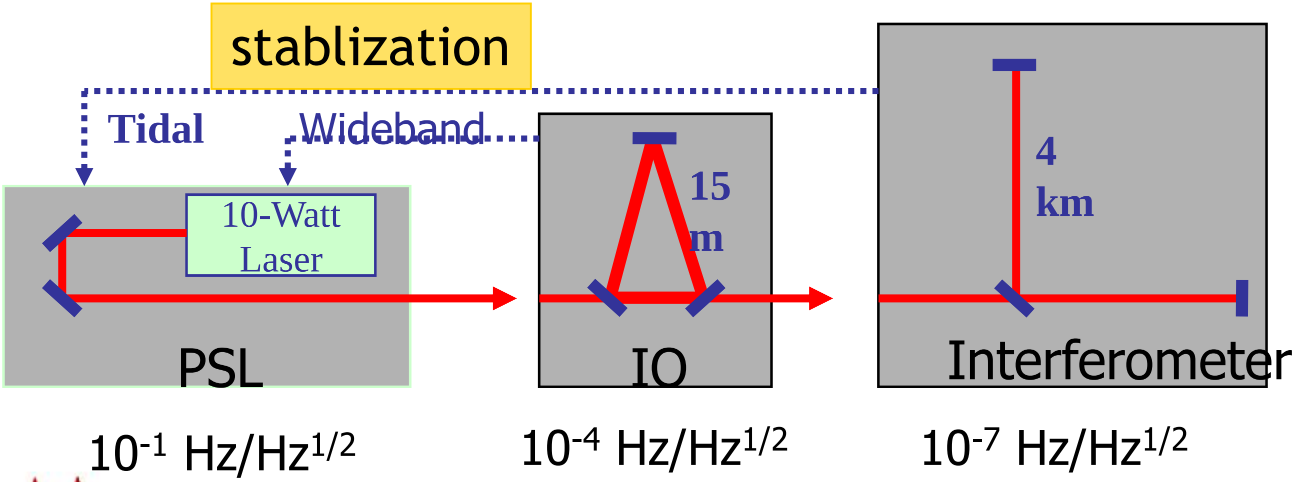

Nd:Yag 1.064 mm
Output power
>8 Watt
TEM00 mode

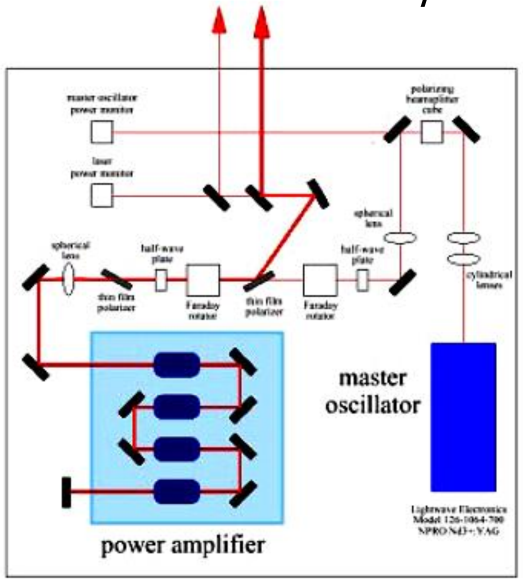

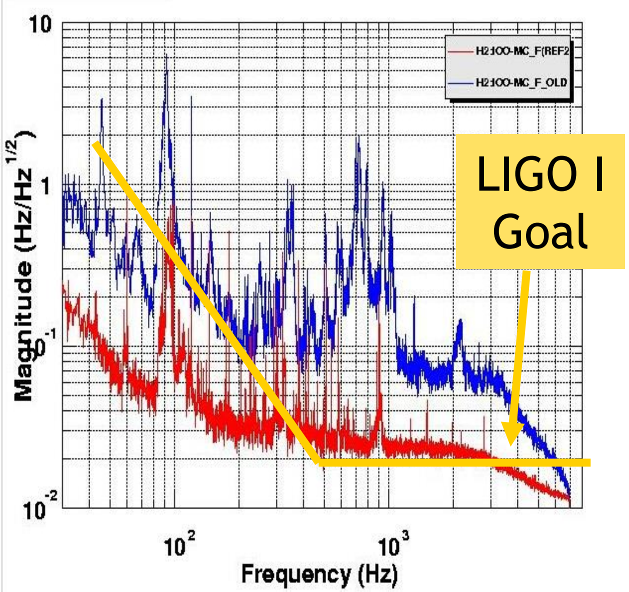

光学器件、悬吊与防震 Optics, suspension and seismic isolation

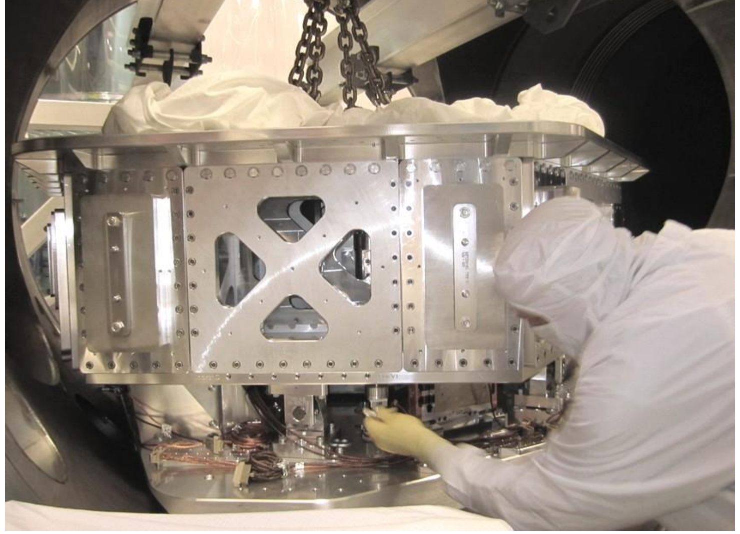

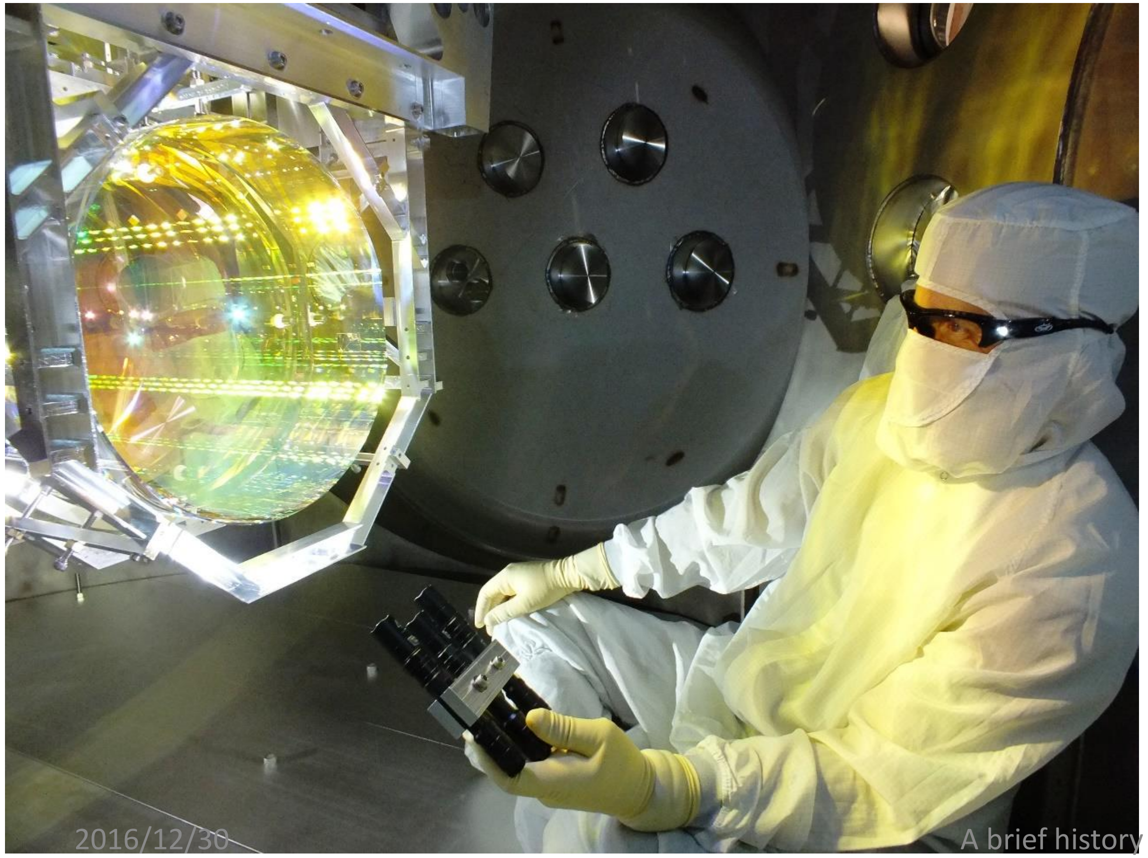

已达成与规划的灵敏度
The achieved and planned Sensitivities

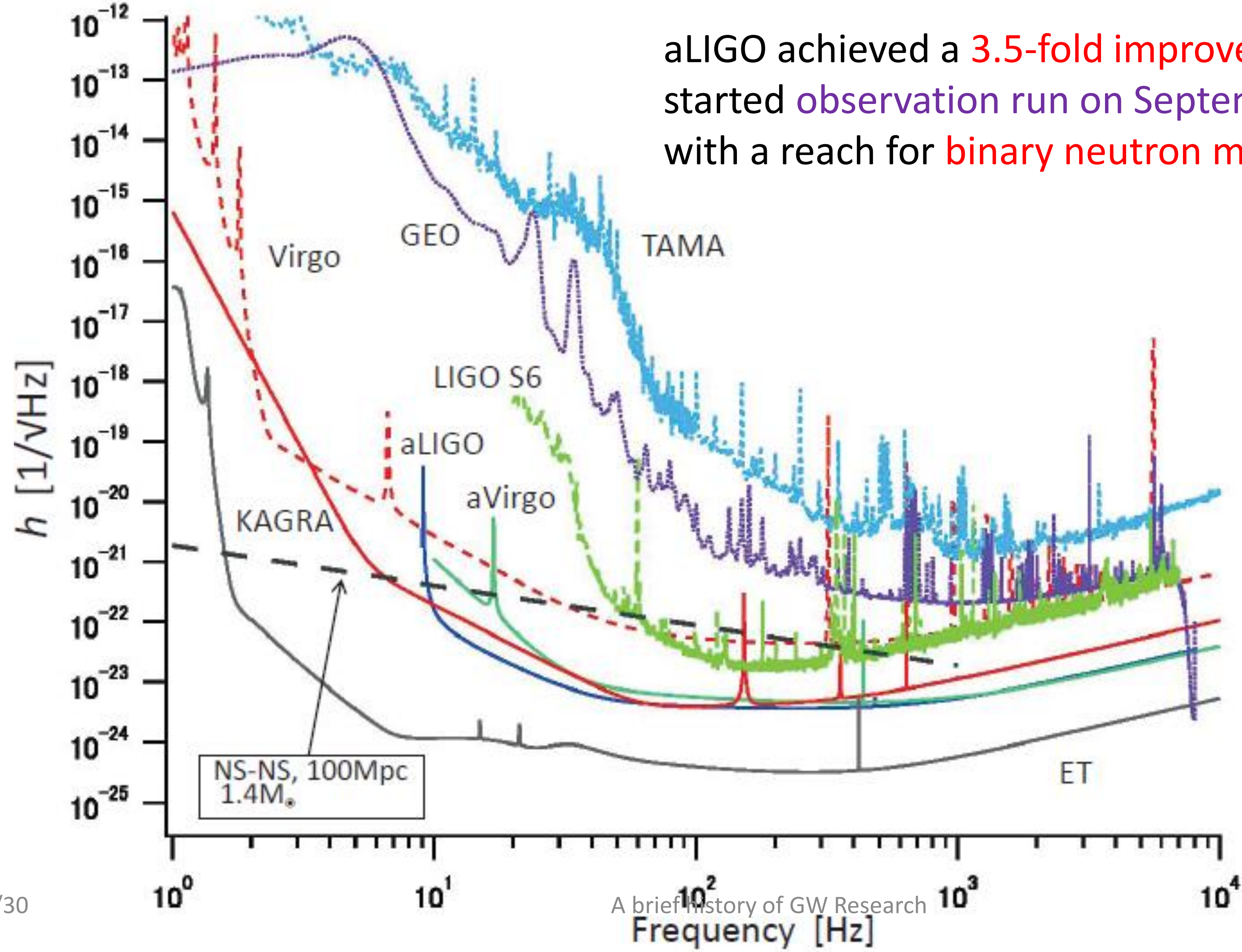

aLIGO achieved a 3.5-fold improvement and started observation run on September 18, 2015 with a reach for binary neutron merger to 70 Mpc.

However, before the first observation run, the first GW detection on September 14, 2015

first direct detection of gravitational waves (GW) and first direct observation of a black hole binary

observed by	LIGO L1, H1
source type	black hole (BH) binary
date	14 Sept 2015
time	09:50:45 UTC
likely distance	0.75 to 1.9 Gly 230 to 570 Mpc
redshift	0.054 to 0.136
signal-to-noise ratio	24
false alarm prob.	< 1 in 5 million
false alarm rate	< 1 in 200,000 yr
Source Masses	M⊙
total mass	60 to 70
primary BH	32 to 41
secondary BH	25 to 33
remnant BH	58 to 67

duration from 30 Hz	~ 200 ms
# cycles from 30 Hz	~10
peak GW strain	1×10^{-21}
peak displacement of interferometers arms	±0.002 fm
frequency/wavelength at peak GW strain	150 Hz, 2000 km
peak speed of BHs	~ 0.6 c
peak GW luminosity	3.6×10^{56} erg s^{-1}
radiated GW energy	2.5-3.5 M⊙
remnant ringdown freq.	~ 250 Hz
remnant damping time	~ 4 ms
remnant size, area	180 km, 3.5×10^{5} km^{2}
consistent with general relativity?	passes all tests performed
graviton mass bound	$< 1.2 \times 10^{-22}$ eV

mass ratio	0.6 to 1
primary BH spin	< 0.7
secondary BH spin	< 0.9
remnant BH spin	0.57 to 0.72
signal arrival time delay	arrived in L1 7 ms before H1
likely sky position	Southern Hemisphere
likely orientation	face-on/off
resolved to	~600 sq. deg.

coalescence rate of binary black holes	2 to 400 $\mathrm{Gpc}^{-3}\,\mathrm{yr}^{-1}$
online trigger latency	~ 3 min
# offline analysis pipelines	5
CPU hours consumed	~ 50 million (=20,000 PCs run for 100 days)
papers on Feb 11, 2016	13
# researchers	~1000, 80 institutions in 15 countries

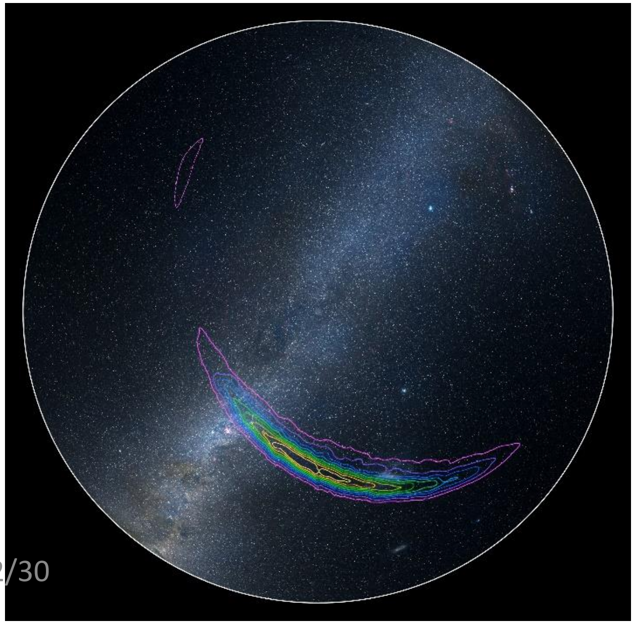

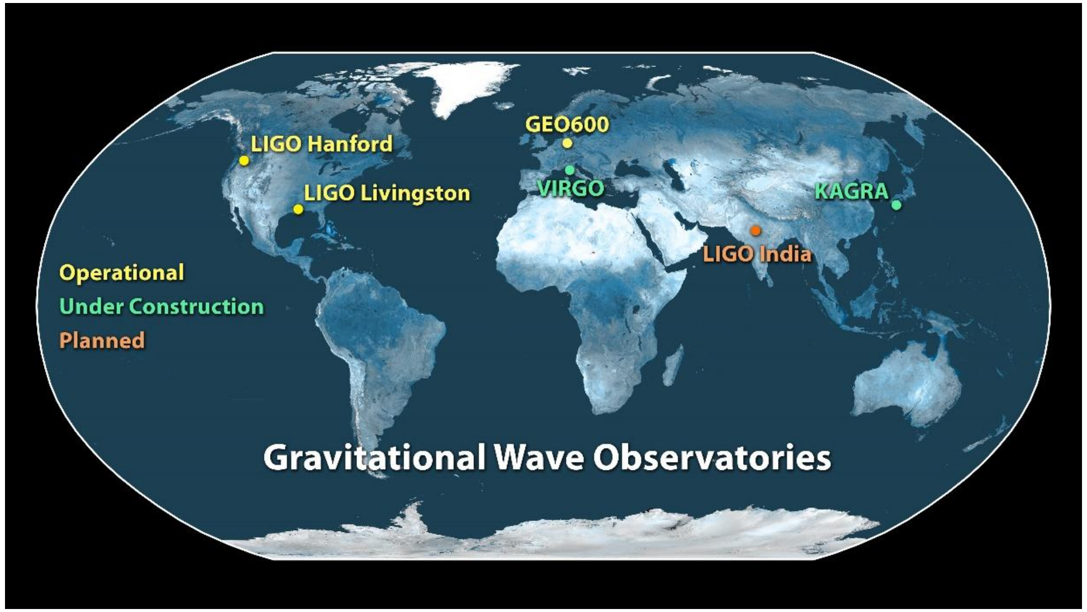

Looking into the future from announcement of first detection February 11, 2016 展望

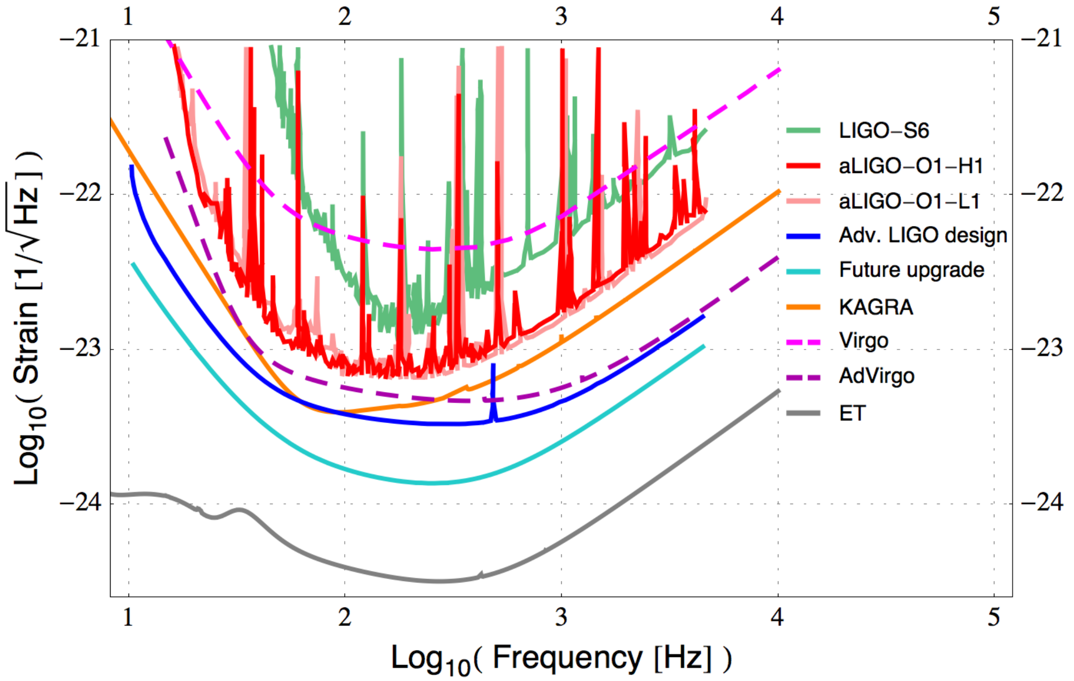

- Present aLIGO sensitivity: ~ one 5-σ event per 3 months.
- Goal second generation sensitivity: 100 5-σ events per year
- Improved 2nd gen.: x2, 800-1000 events/yr
- First generation sensitivity: several 3-σ events per year → one should look at the past data and try to search for them with better efforts and methods
- Third generation sensitivity → 100,000 or more 5-σ events per year

  Plenty compared to some other branches of physics and astronomy


JGW-G1604972
LIGO-G1600682
KAGRA
Large-scale cryogenic gravitational-wave telescope in Japan:
KAGRA
Tomotada Akutsu
National Astronomical Observatory of Japan
for the KAGRA Collaboration
LVC meeting, Hilton Pasadena, Pasadena, CA, USA (March 14-18, 2016)
1

KAGRA project

Previously known as LCGT

- Laser interferometric gravitational-wave detector with 3-km arms
- Now under construction in the Kamioka mine, Gifu, Japan

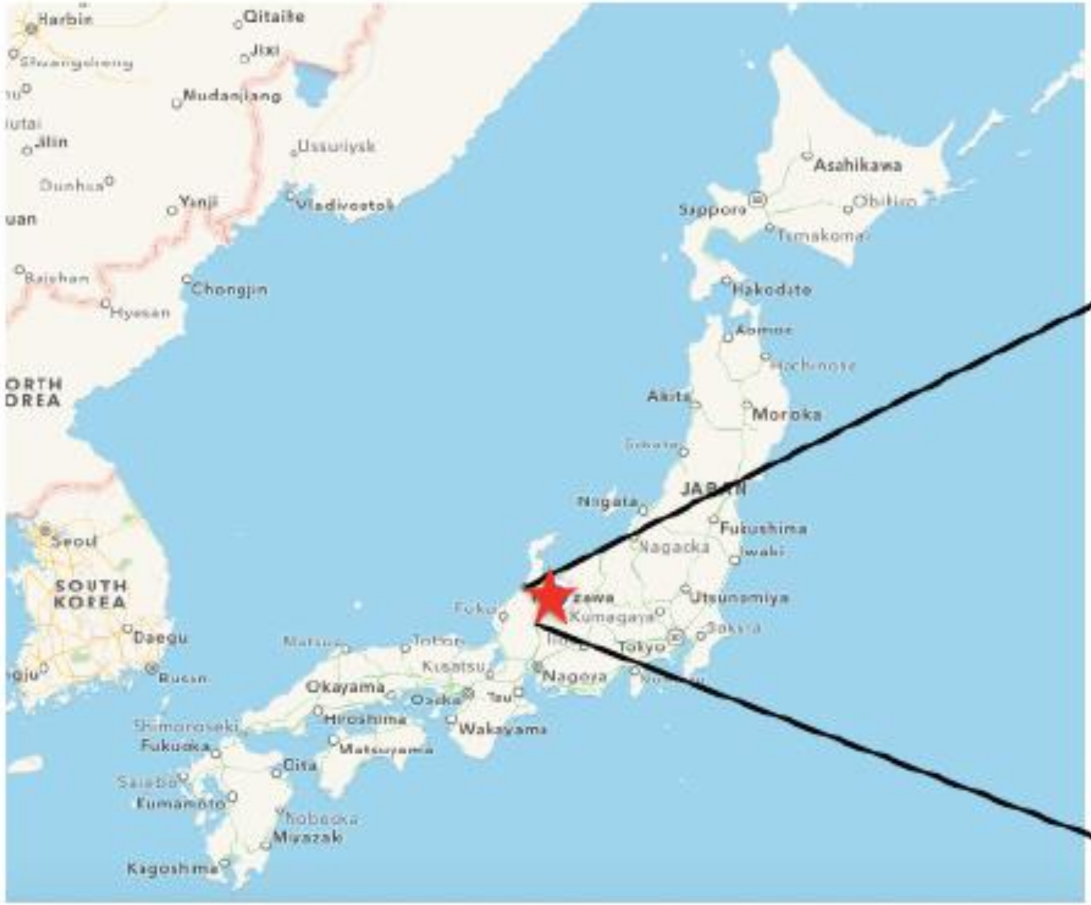

Tokyo-Toyama

By K. Kokeyama

In collaboration

- Host: ICRR, Univ. of Tokyo
- Co-Hosts: KEK and NAOJ
- Over 200 collaborators from more than 60 universities and institutes in Japan and abroad.

+more…

Kamioka site

Main Features

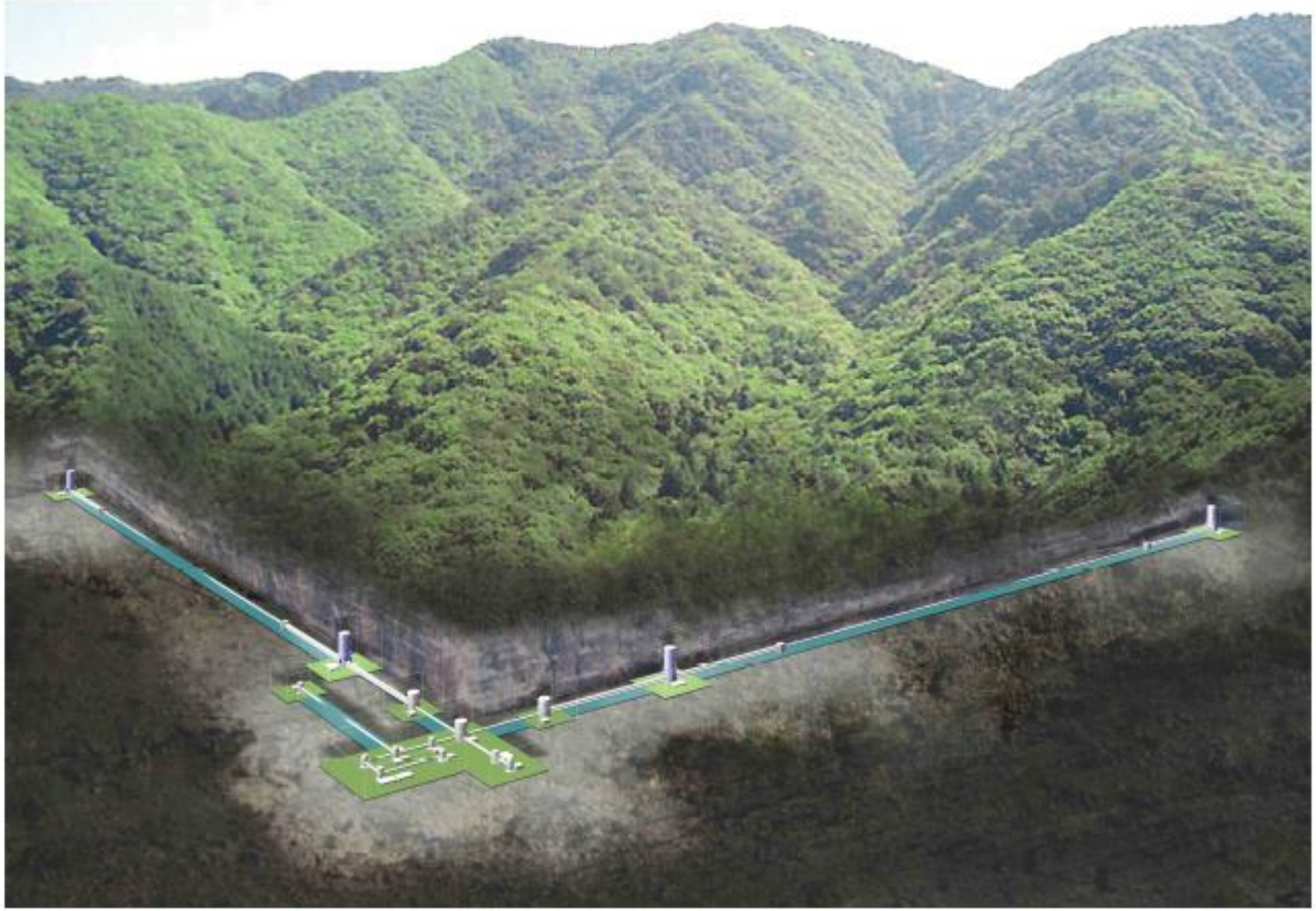

LVC meeting, Hilton Pasadena, Pasadena, CA, USA (March 14-18, 2016)

5

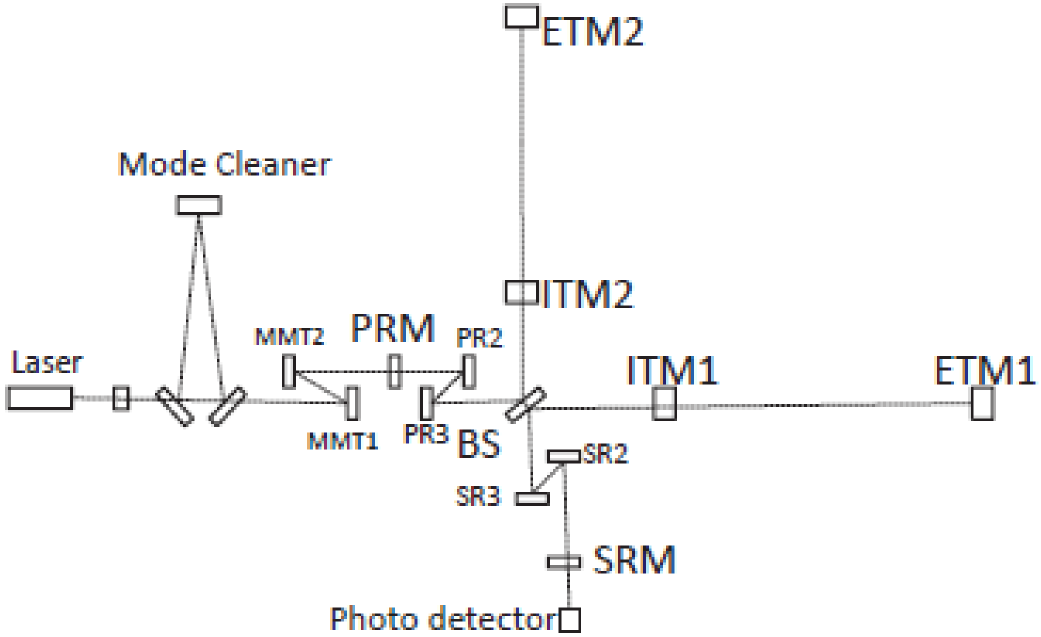
ETM2
Mode Cleaner
ITM2
Laser
MMT2
PRM
PR2
ITM1
ETM1
MMT1
PR3
BS
SR2
SR3
SRM
Photo detector

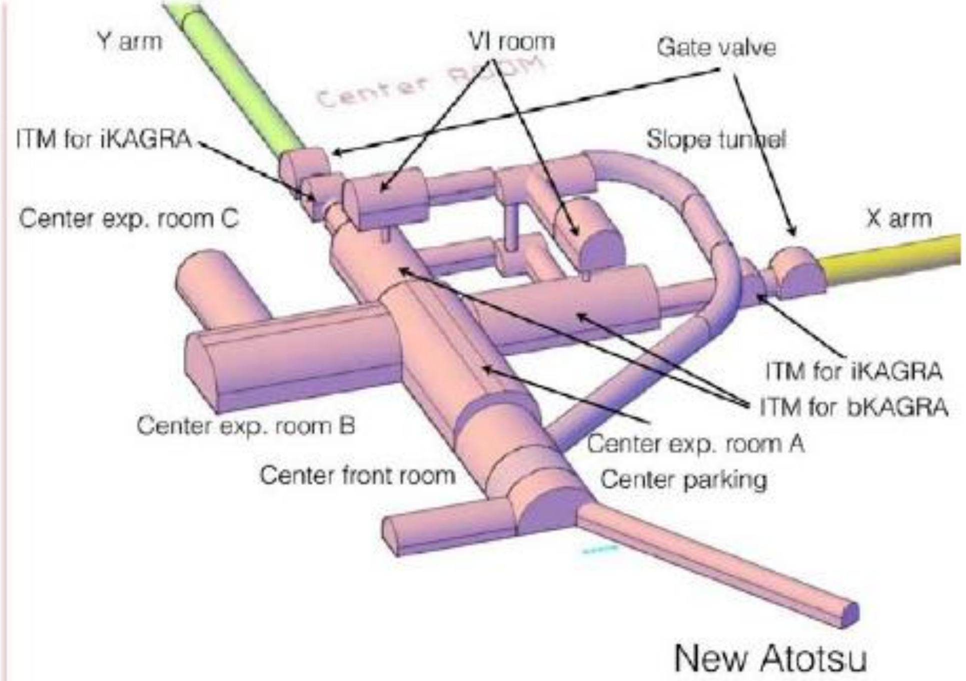
Y arm
VI room
Gate valve
ITM for iKAGRA
Slope tunnel
Center exp. room C
X arm
ITM for iKAGRA
ITM for bKAGRA
Center exp. room B
Center exp. room A
Center front room
Center parking
New Atotsu

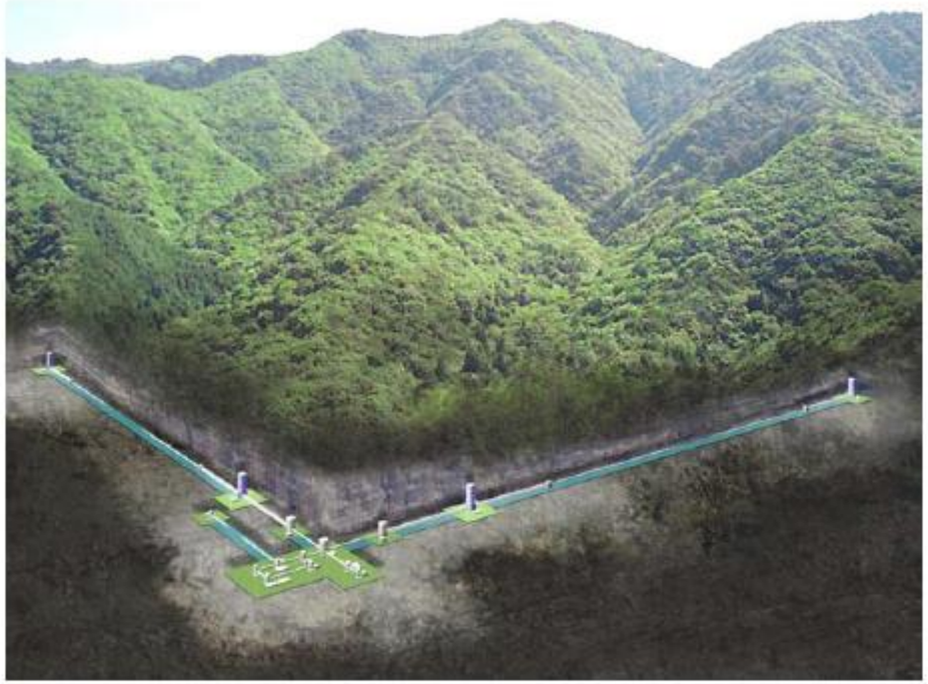

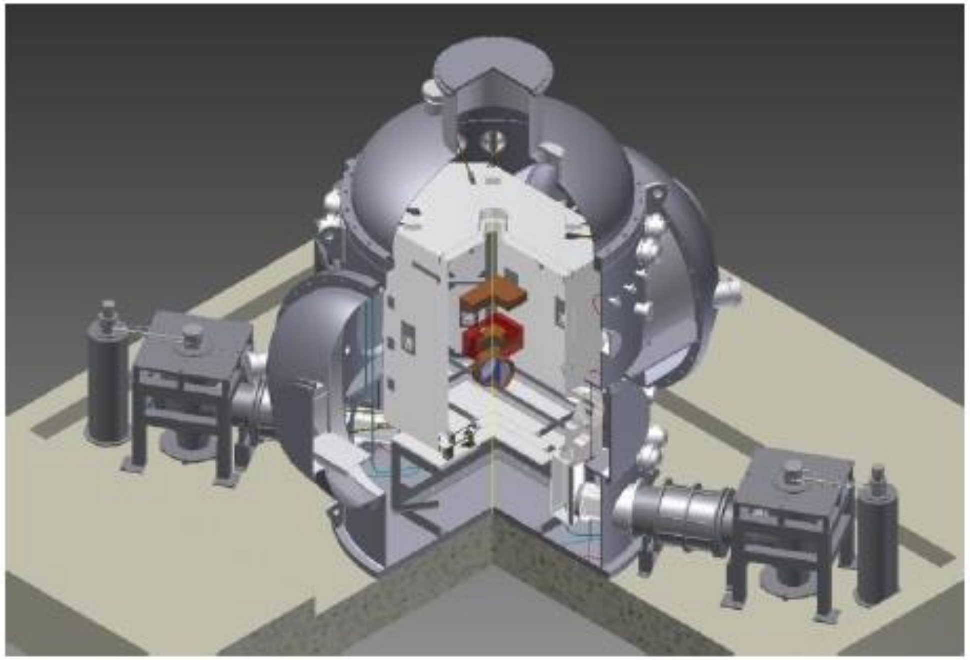

KAGRA

Kamioka GW Detector

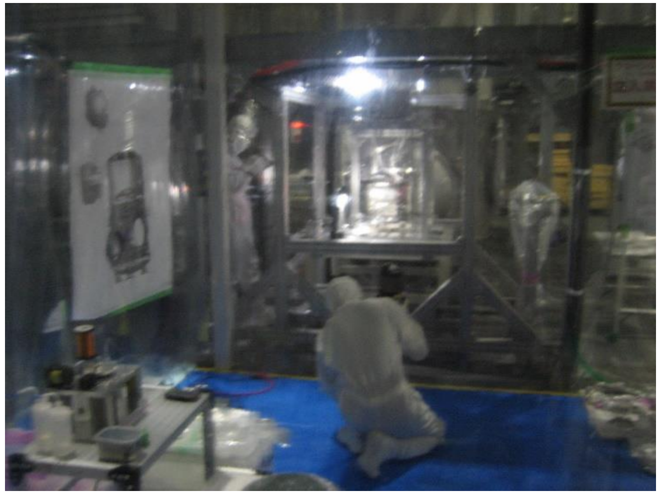

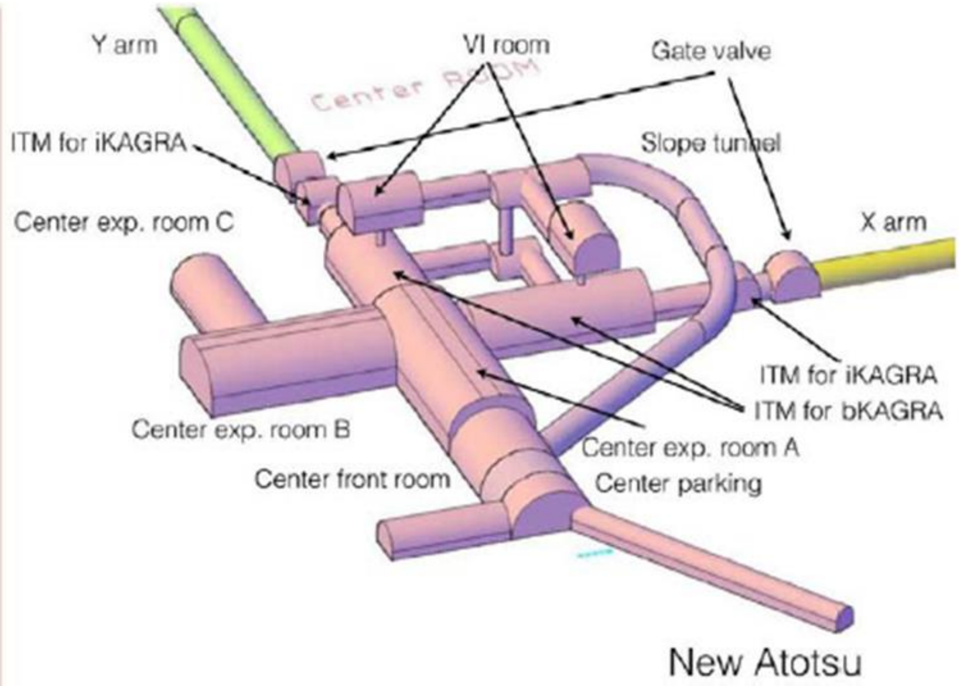

KAGRA Office 茂住 Mozumi Branch

KAGRA Site at 神岡 Kamioka Mine

富山 Toyama

国际暨中德双边激光天文动力学研讨会

Hulse-Taylor Binary PSR1913+16

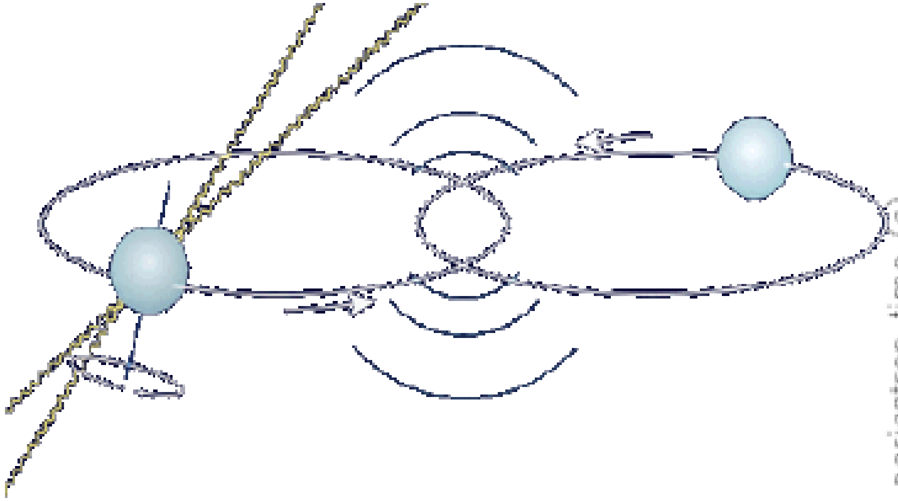

- Observed loss of energy matches prediction of GW emission to (0.13 ± 0.21)%   0.997±0.002(2010)
- Indirect evidence of gravitational waves
- Frequency 70 μHz, amplitude 7×10-[23] ⇒ outside detector sensitivity

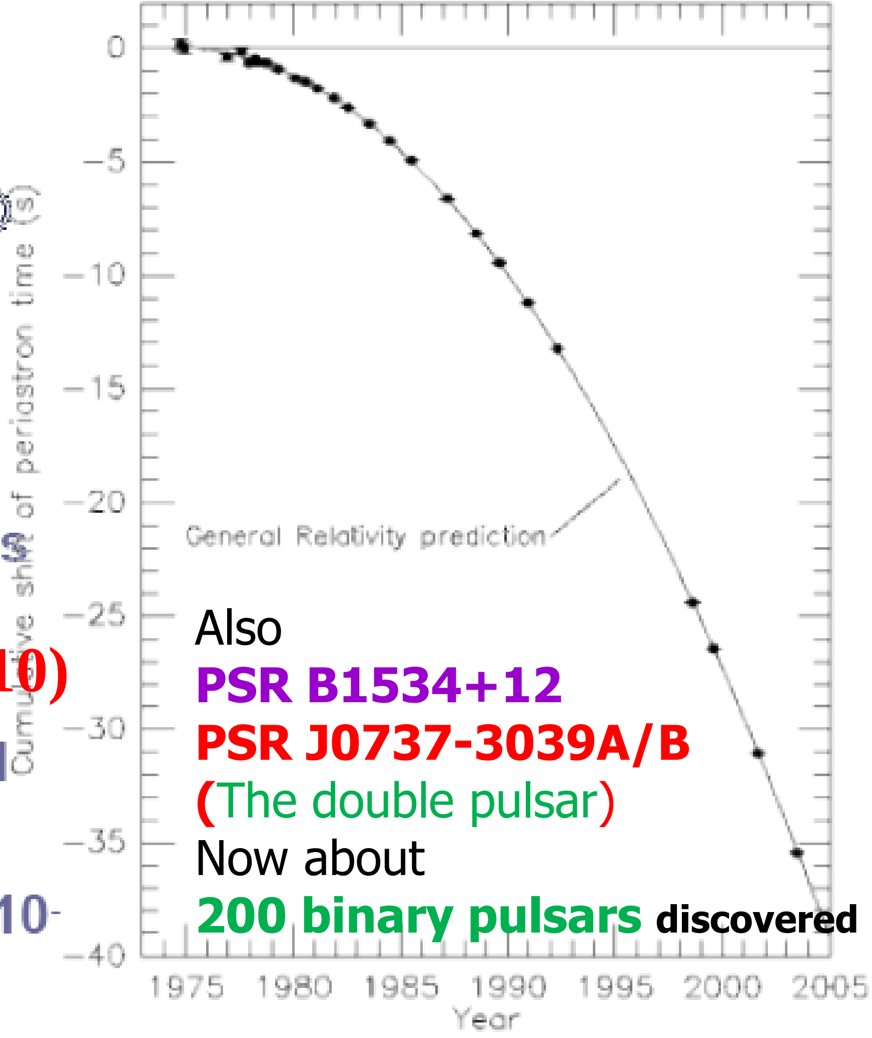

Also
PSR B1534+12
PSR J0737-3039A/B
(The double pulsar)
Now about
200 binary pulsars discovered

第二代引力波空间计划概念
Second Generation GW Mission Concepts

- DECIGO
- BBO
- Super-ASTROD

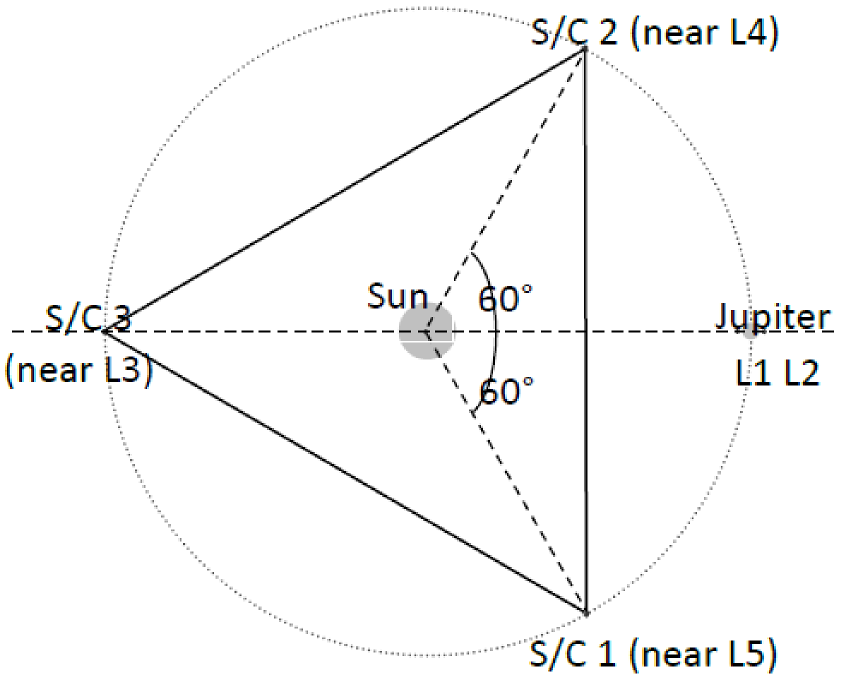

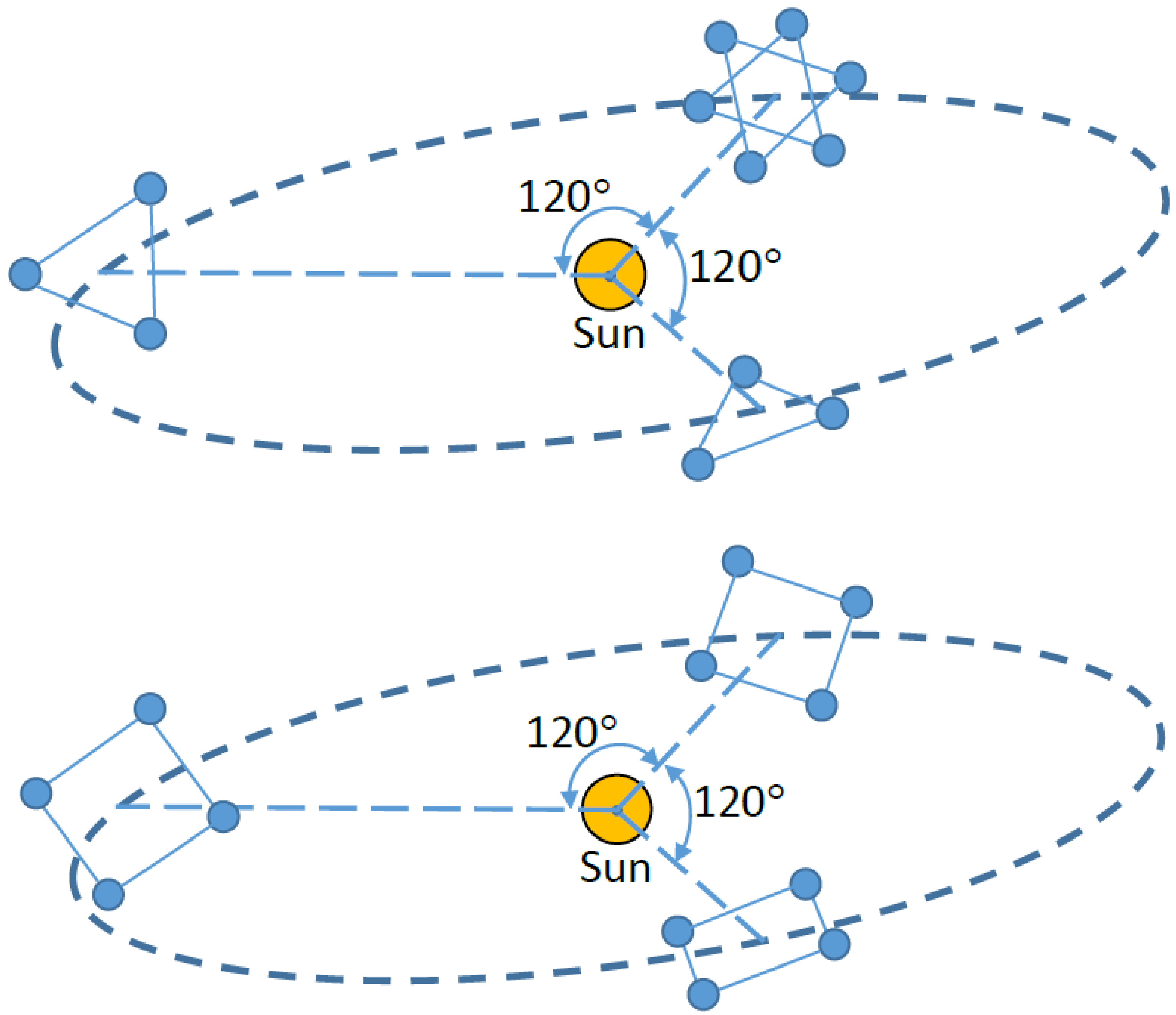

Strain power spectral density (psd) amplitude vs. frequency for various GW detectors and GW sources. [CSDT: Cassini Spacecraft Doppler Tracking; SMBH-GWB: Supermassive Black Hole-GW Background.]

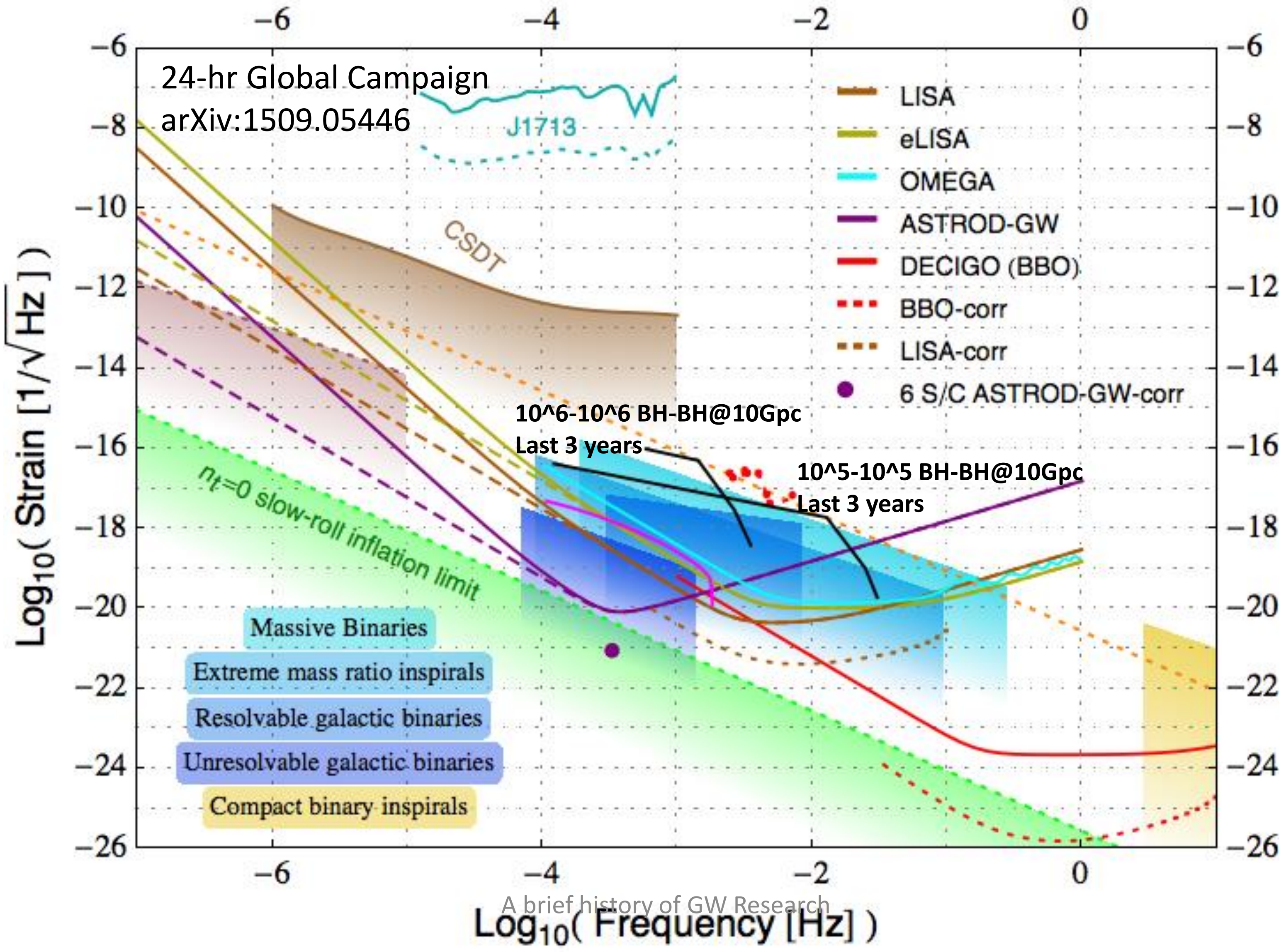

（超）大质量黑洞系统 Massive Black Hole Systems: 大质量黑洞合生 Massive BH Mergers & 极端质量比合生 Extreme Mass Ratio Mergers (EMRIs)

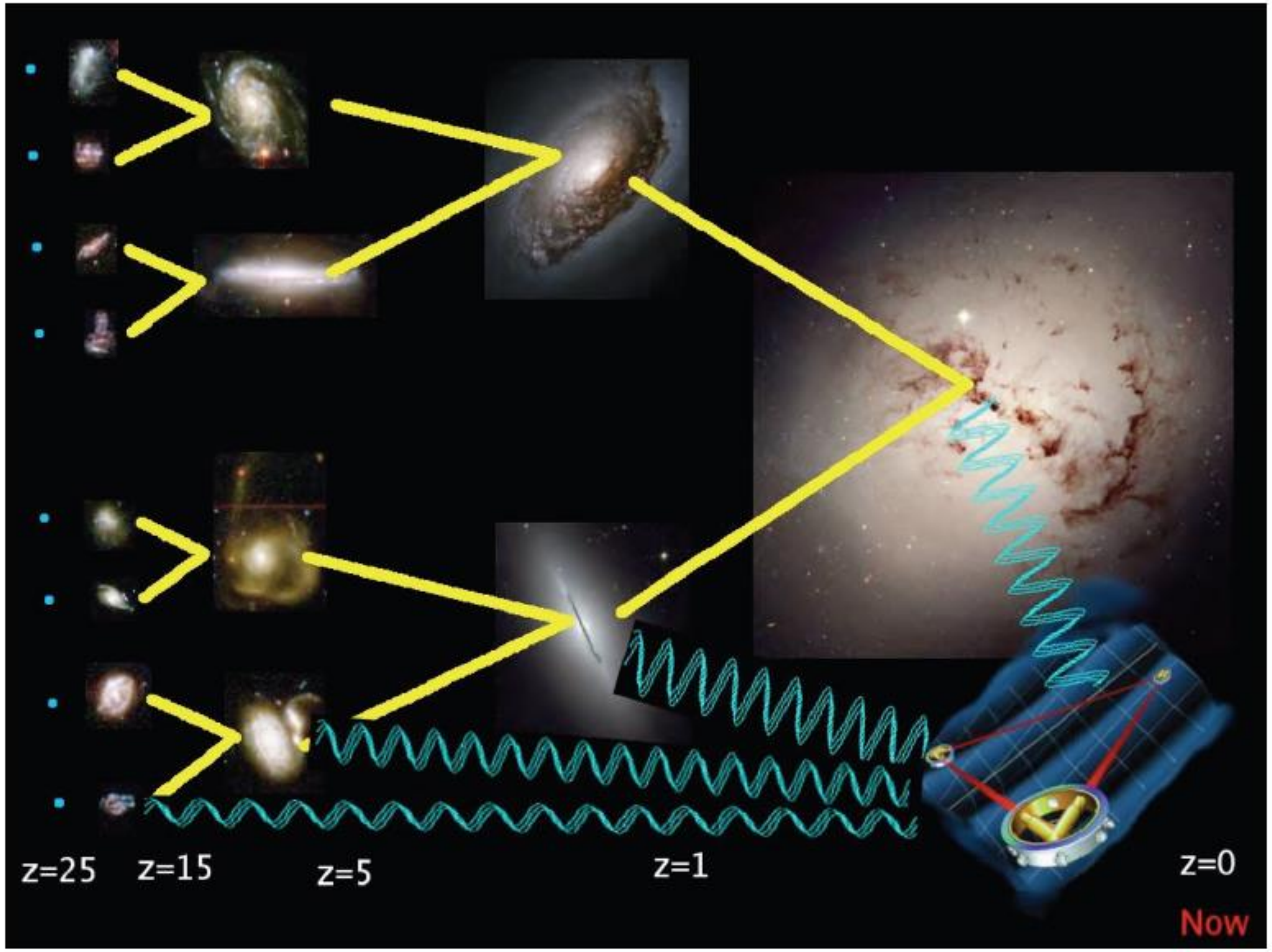

极低频 Very low frequency band (300 pHz – 100 nHz)

$$h_c(f) = A_{yr}\,[f/(1\ \mathrm{yr}^{-1})]^{\alpha}$$

Table 4. Upper limits on the isotropic stochastic background from 3 pulsar timing arrays.

	No. of pulsars included	No. of years observed	Observation radio band [MHz]	Constraint on characteristic strain $h_c(f)$ [$= A_{yr}\,[f/(1\mathrm{yr}^{-1})]^{-(2/3)}$, ($f = 10^{-9}$-$10^{-7}$ Hz)]
EPTA[102]	6	18	120-3000	$A_{yr} < 3 \times 10^{-15}$
PPTA[103]	4	11	3100	$A_{yr} < 1 \times 10^{-15}$
NANOGrav[104]	27	9	327-2100	$A_{yr} < 1.5 \times 10^{-15}$

Table 5. Sensitivities of IPTA, FAST and SKA to monochromatic GWs.

	No. of pulsars	No. of years of observation	Timing accuracy (ns)	Sensitivity in characteristic strain $h_c(f)$ [$= B_{yr}\,(f\,/\,\mathrm{yr}^{-1})$] for monochromatic GWs
IPTA[106]	36	20	100	$B_{yr} = 1 \times 10^{-16}$
FAST[107]	50	50	50	$B_{yr} = 1.5 \times 10^{-17}$
SKA[108]	100	100	20	$B_{yr} = 1.5 \times 10^{-18}$

归一化引力波谱能量密度 Normalized GW spectral energy density Ω_{gw} vs. 频率 requency for GW detector sensitivities and GW sources

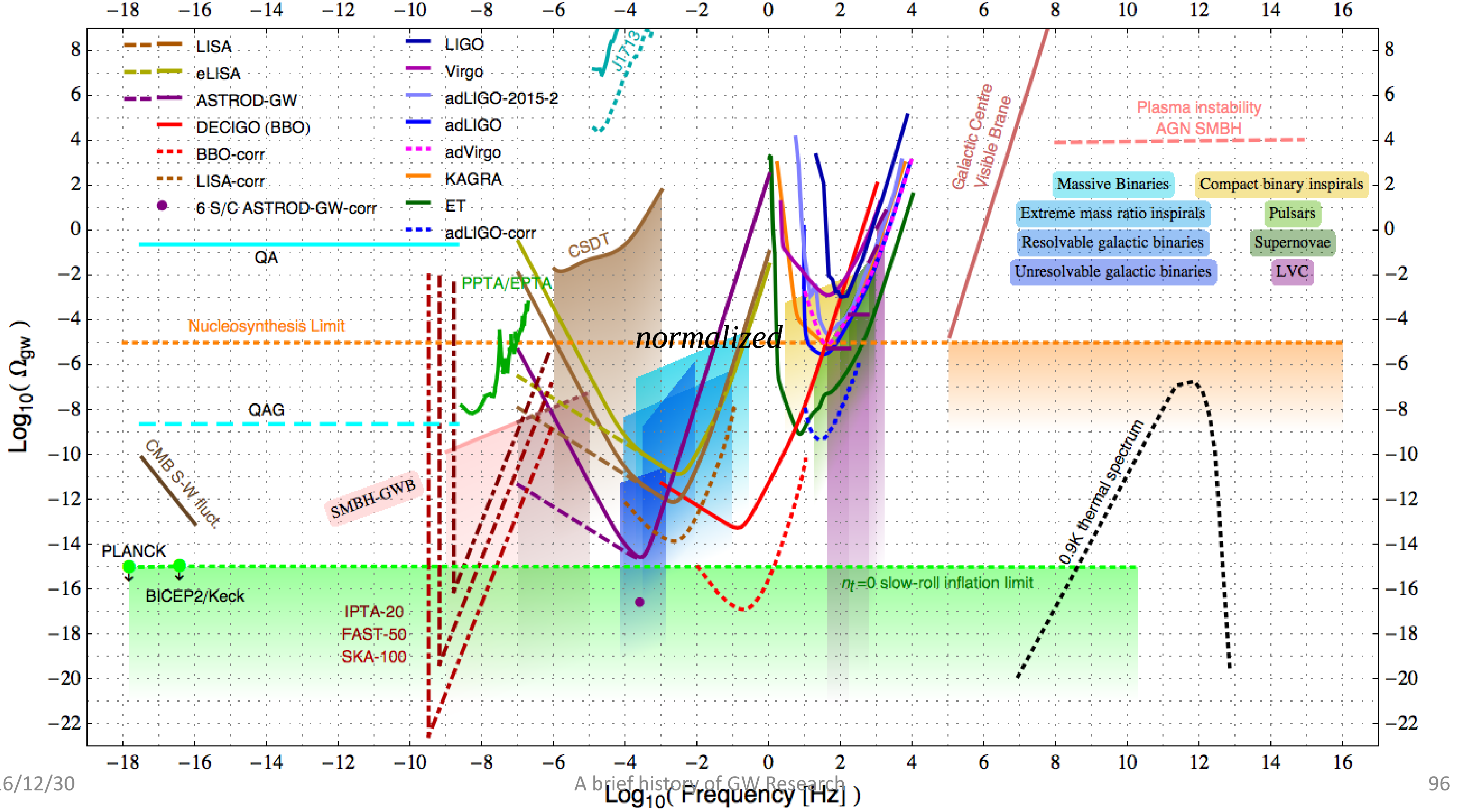

引力波谱分类 The Gravitation-Wave (GW) Spectrum Classification

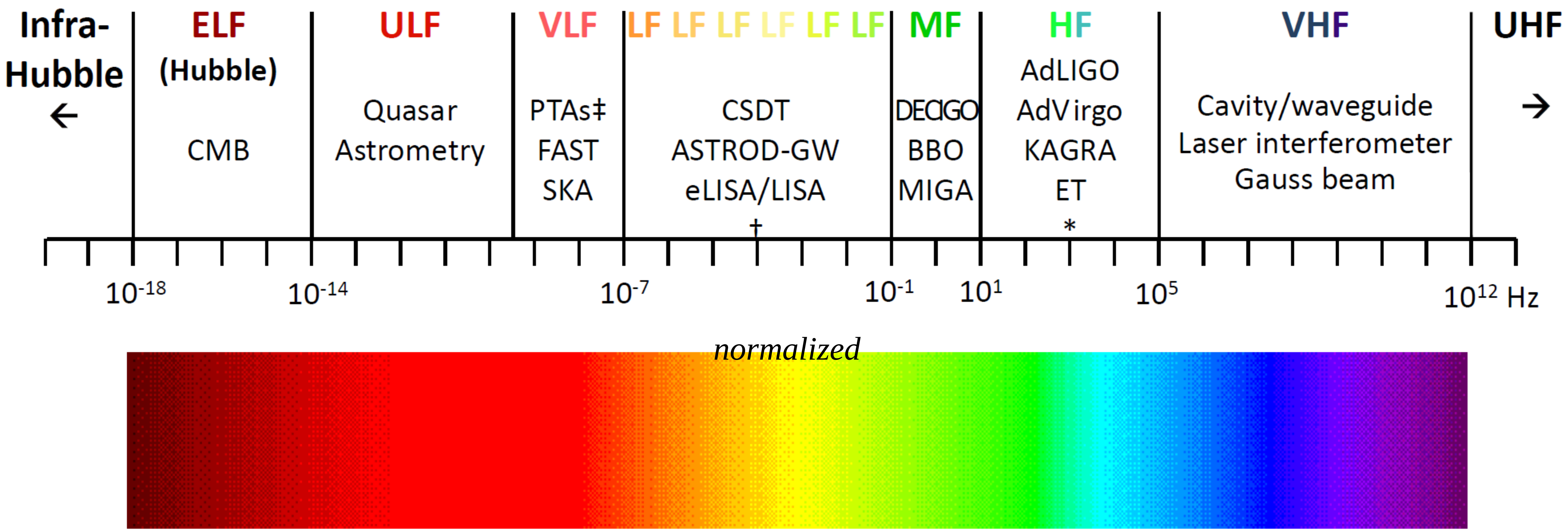

* AIGO, AURIGA, EXPLORER, GEO, NAUTILUS, MiniGRAIL, Schenberg.

† OMEGA, gLISA/GEOGRAWI, GADFLI, TIANQIN, ASTROD-EM, LAGRANGE, ALIA, ALIA-descope.

‡ EPTA, NANOGrav, PPTA, IPTA.

归一化引力波谱能量密度 Normalized GW spectral energy density Ω_{gw} vs. 频率 requency for GW detector sensitivities and GW sources

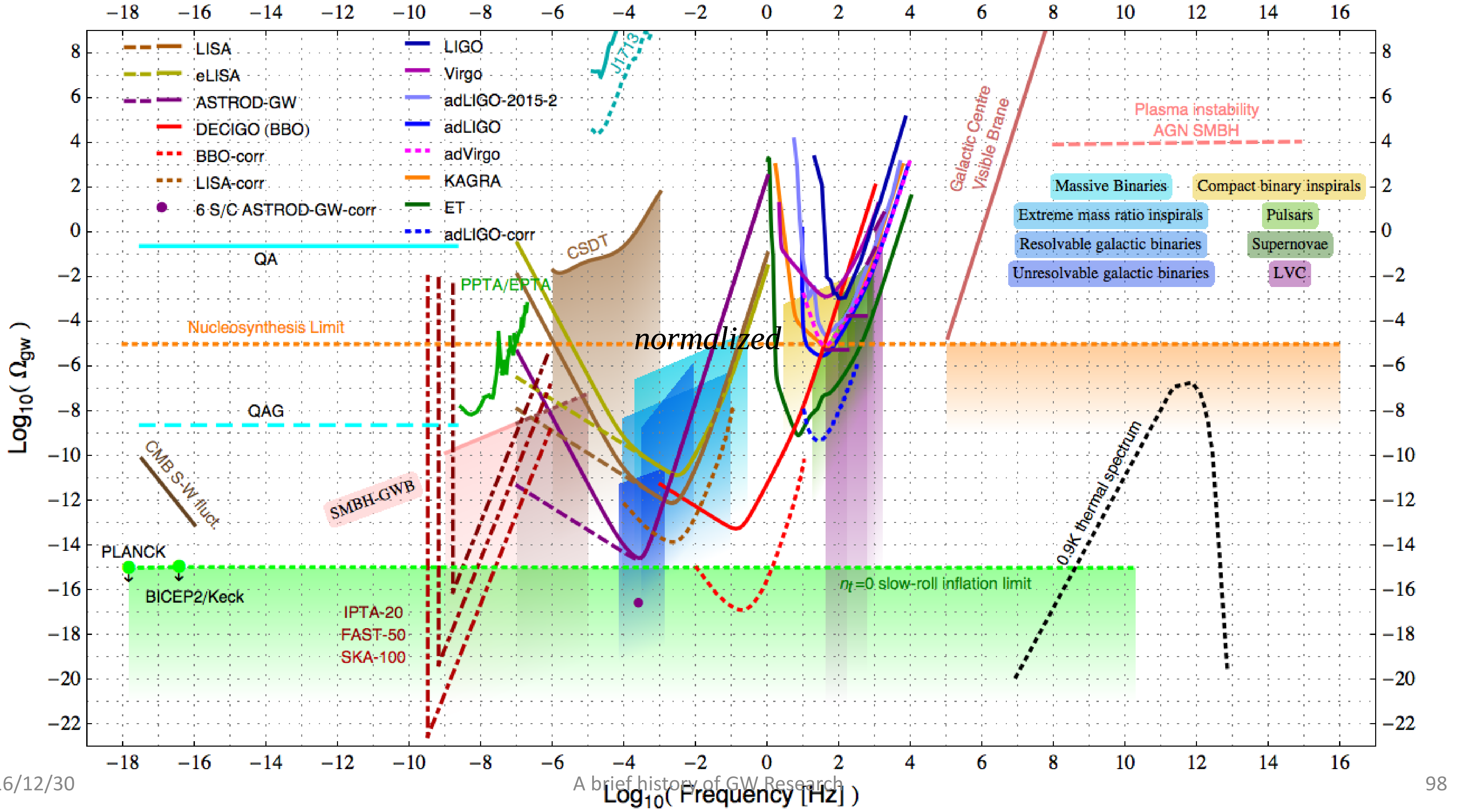

Very high frequency band (100 kHz – 1 THz) and ultrahigh frequency band (above 1 THz)

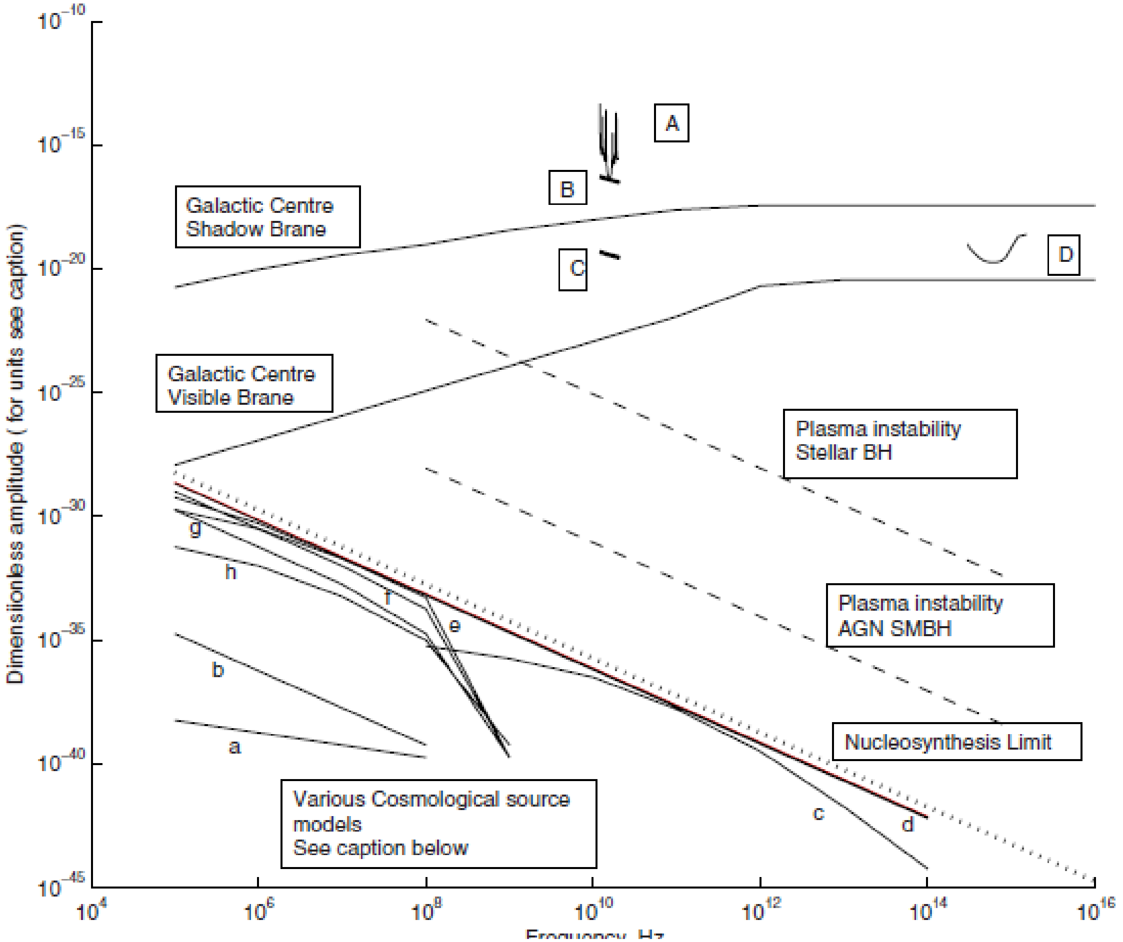

- A M Cruise

  The potential for very high-frequency gravitational wave detection

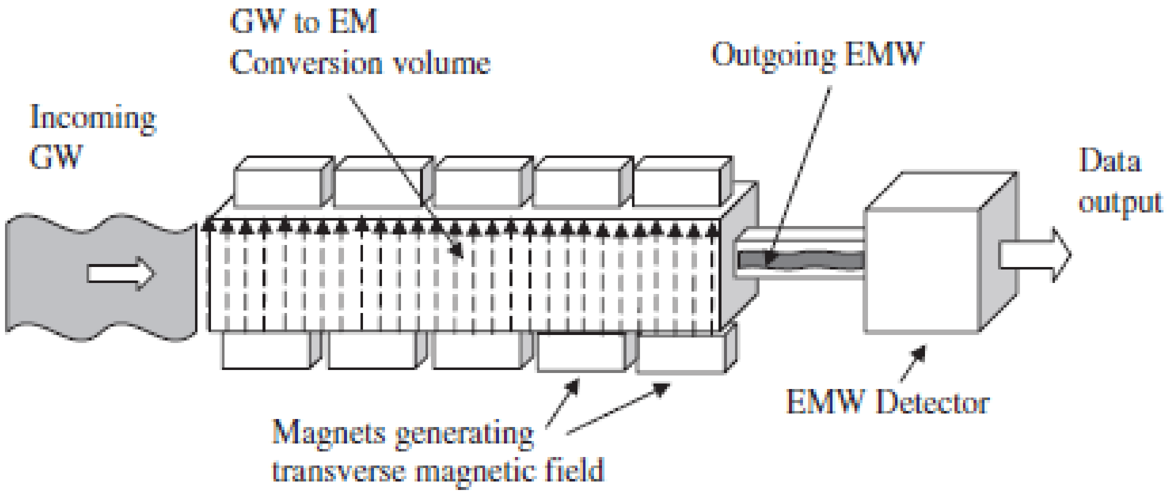

Figure 2. A generic diagram of a magnetic conversion detector.

应变功率谱密度振幅 Strain power spectral density (psd) amplitude vs. 频率 frequency for various GW detectors and GW sources

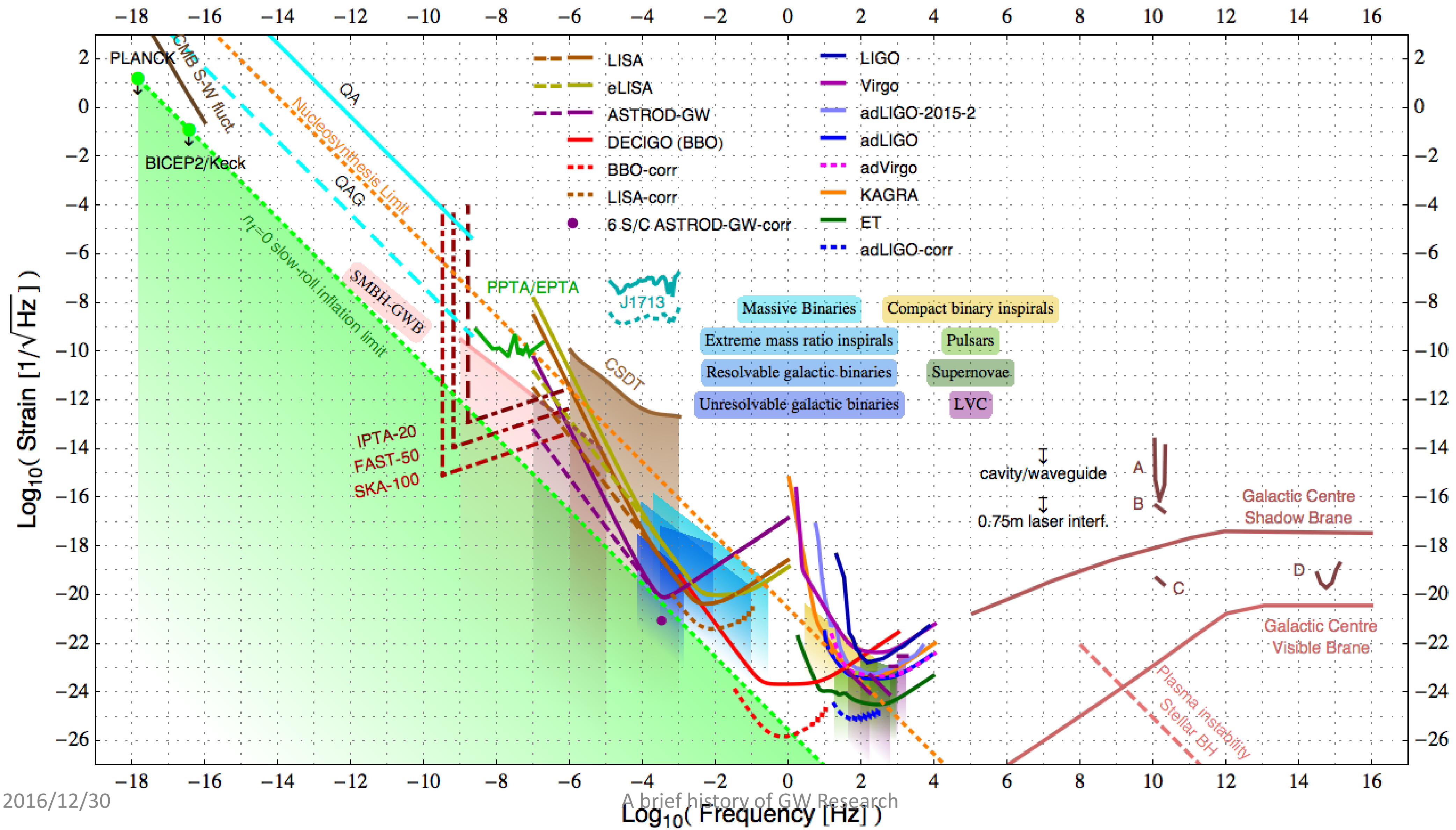

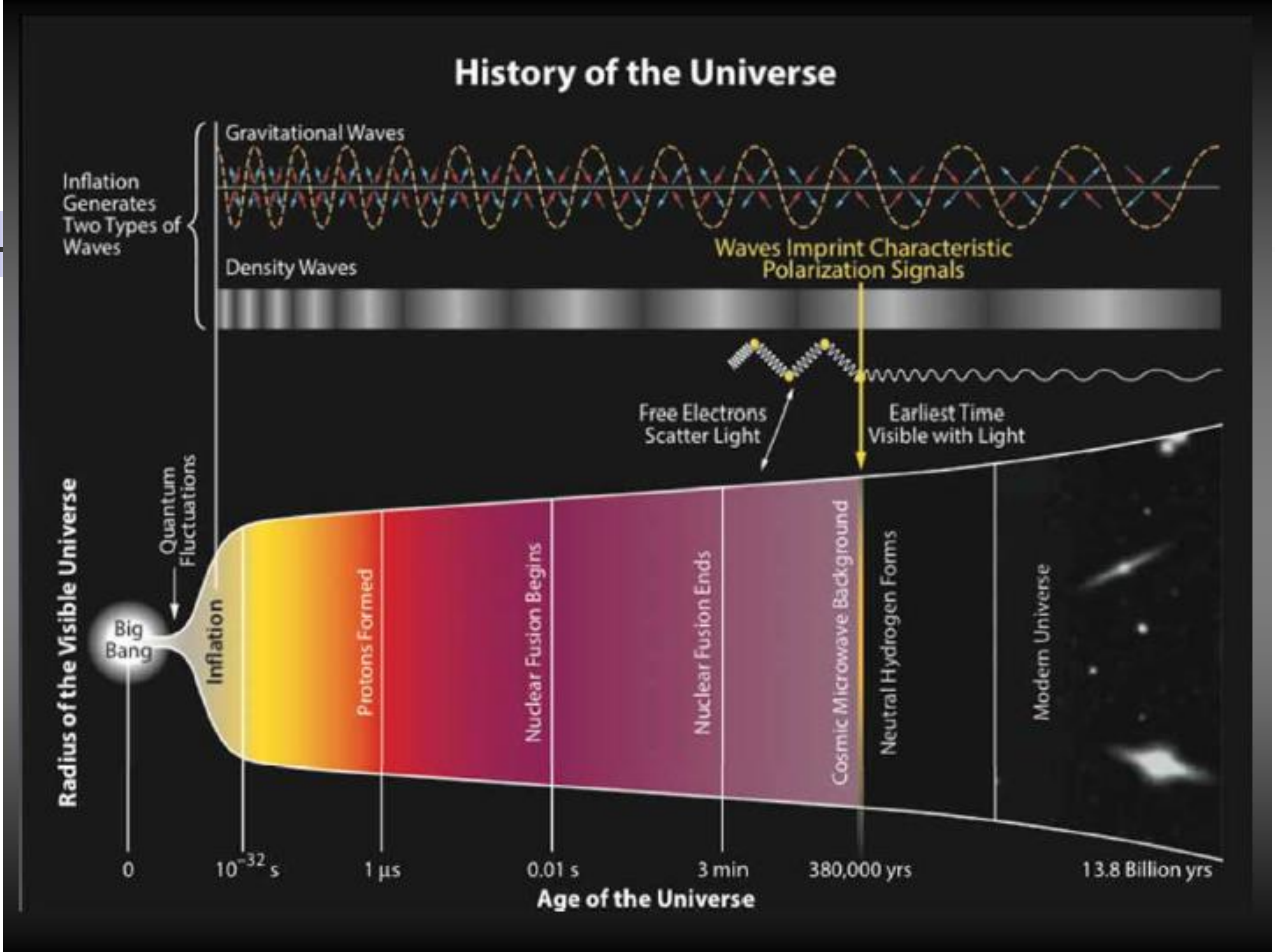
History of the Universe
Gravitational Waves
Inflation Generates Two Types of Waves
Density Waves
Waves Imprint Characteristic Polarization Signals
Free Electrons Scatter Light
Earliest Time Visible with Light
Radius of the Visible Universe
Quantum Fluctuations
Big Bang
Inflation
Protons Formed
Nuclear Fusion Begins
Nuclear Fusion Ends
Cosmic Microwave Background
Neutral Hydrogen Forms
Modern Universe
0
10^-32 s
1 µs
0.01 s
3 min
380,000 yrs
13.8 Billion yrs
Age of the Universe

产生观测到的B模偏振之4个过程
Four processes could produce CMB B-mode polarization observed

- (i) gravitational lensing from E-mode polarization (Zaldarriaga & Seljak 1997),
- (ii) local quadrupole anisotropies in the CMB within the last scattering region by large scale GWs (Polnarev 1985)
- (iii) cosmic polarization rotation (CPR) due to pseudoscalar-photon interaction (Ni 1973; for a review, see Ni 2010). (The CPR has also been called Cosmological Birefringence)
- (iv) Dust alignment

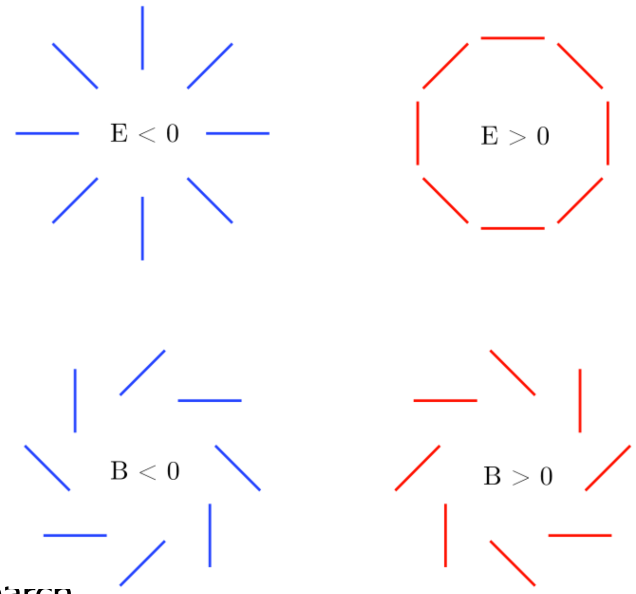

对哈伯频段引力波的制约
The constraints for Hubble frequency band

- CMB S-W fluct.: The COBE microwave-background quadrupole anisotropy measurement gives a limit Ωgw (1 aHz) ~ 10-9 on the extremely-low-frequency GW background.
- WMAP improves on the COBE constraints; the constraint on Ωgw for the higher frequency end of this band is better than 10^(-14).
- The analysis of *Planck*, SPT, and ACT temperature data together with WMAP polarization; the scalar index is $n_s = 0.959 \pm 0.007$, the tensor-to-scalar perturbation ratio r is less than 0.11
- The combined analysis of BICEP2/Keck Array and Planck Collaboration: the tensor-to-scalar perturbation ratio r is constrained to less than 0.12 (95% CL; no running). The pivot scale of this constraint is 0.05 Mpc−1, corresponding to GW frequency *f* at 3.8 x 10^(−17) Hz at present.
- Most recent: $r < 0.07$ (2 σ) (Chao-Lin Kuo, Dec. 9 talk at NCTS; his talk in LeCosPA Symposium12/17/15)

BB power spectrum from SPTpol, ACTpol, BICEP2/Keck, and POLARBEAR. The solid gray line shows the expected lensed BB spectrum from the Planck+lensing+WP+highL best-fit model. The dotted line shows the nominal 150 GHz BB power spectrum of Galactic dust emission derived from an analysis of polarized dust emission in the BICEP2/Keck field using Planck data. The dash-dotted line shows the sum of the lensed BB power and dust BB power.

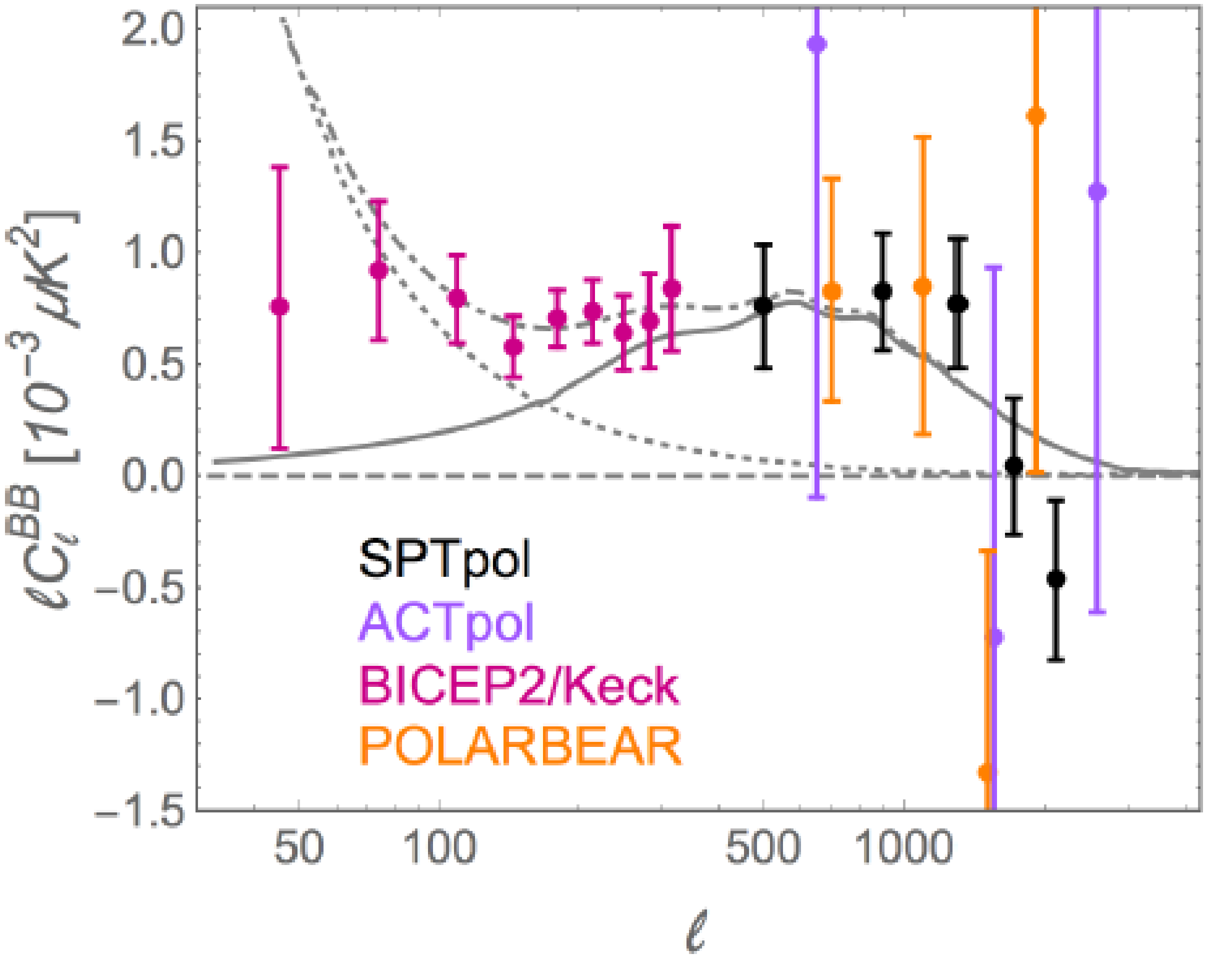

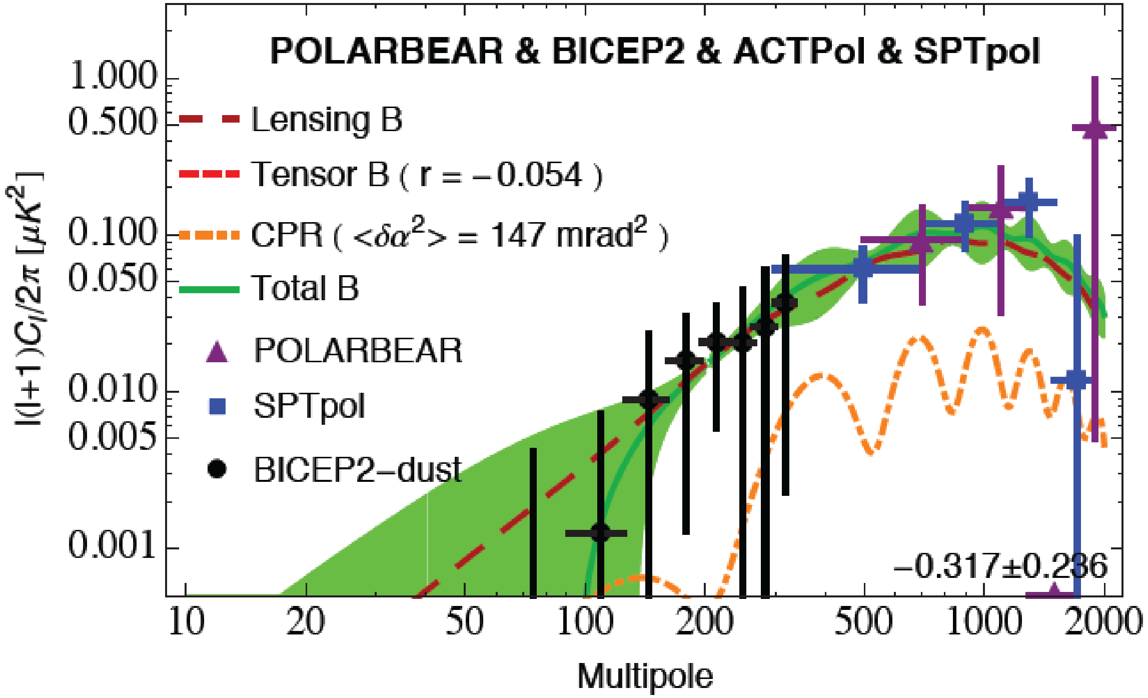

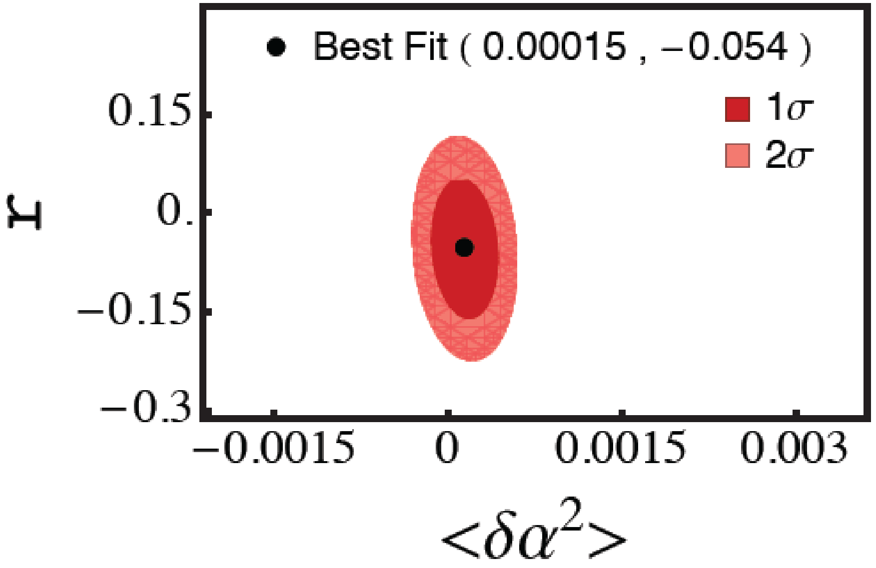

第二届 LeCosPA 会议 OT session (first 2 talks)

- r ≈ - 0.05±0.1
- $<\delta\alpha^2> = 100 \pm 500$ mrad^2
- Fluctuation amplitude bound: 17 mrad (1 degree)

The indirect GW limits are from CMB temperature and polarization power spectra, lensing, BAOs, and BBN. Models predicting a power-law spectrum that intersect with an observational constraint are ruled out at > 95% confidence. We show five predictions for the GW background, each with r = 0:11, and with nt = 0:68 (orange curve), nt = 0:54 (blue), nt = 0:36 (red), nt = 0:34 (magenta), and the consistency relation, nt = r/8 (green), corresponding to minimal inflation. Paul D. Lasky et al.1511.05994

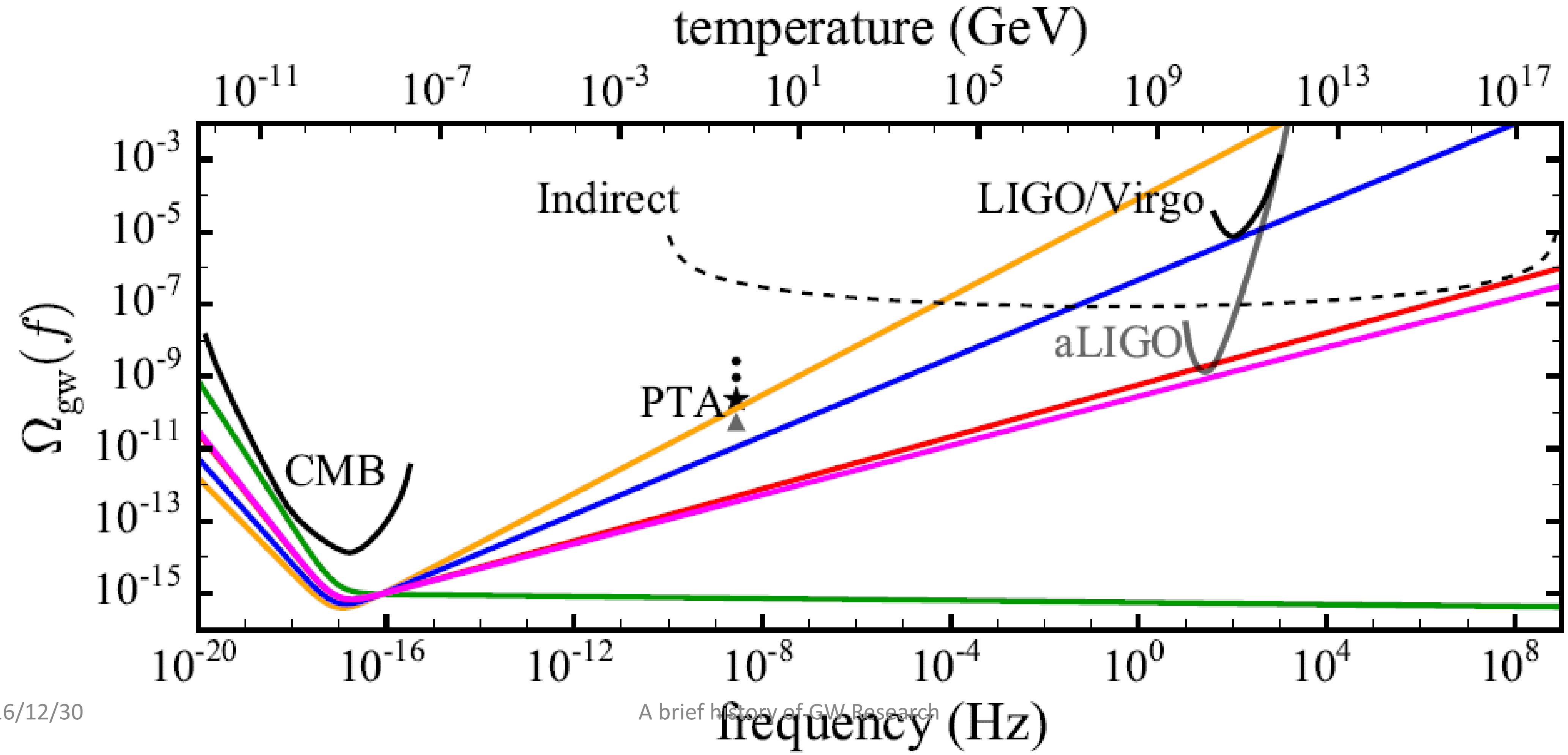

展 望 Outlook

- Advanced LIGO has detected GWs from stellar-mass binary black hole mergers. We will see a global network of second generation km-size interferometers for GW detection soon. Scaling with the achieved detection, third generation detectors would be to detect more than 100,000 5-σ GW events per year.
- Advanced LIGO has achieved 3.5 times better sensitivities with a reach to neutron star binary merging event at 70 Mpc and began its first observing run (O1) on September 18, 2015 searching for GWs.
- Another avenue for real-time direct detection is from the PTAs. The PTA bound on stochastic GW background already excludes most theoretical models; this may mean we could detect very low frequency GWs anytime too with a longer time scale.
- Although the prospect of a launch of space GW is only expected in about 20 years, the detection in the low frequency band may have the largest signal to noise ratios. This will enable the detailed study of black hole co-evolution with galaxies and with the dark energy issue. LISA Pathfinder has been launched on December 3, 2015. This will pave the technology road for GW space missions.
- Foreground separation and correlation detection method need to be investigated to achieve the sensitivities 10^{-16}-10^{-17} or beyond in Ω_{gw} to study the primordial GW background for exploring very early universe and possibly quantum gravity regimes.

将来的 3 类引力波研究者
Three Kinds of GW Researchers in future

- 实验研究者 Experimentalists (Experimental Astronomers/Physicists):
  working on detectors and data processing
- 多波段天文学家 Multi-Messenger Astronomers: Working on astrophysics
- 理论物理学家/宇宙学者 Theoretical Physicists/Cosmologists: Working on fundamental physics and theoretical cosmology
- 经费 Budget: grow up to 20 % - 30 % of Astronomy Budget

欢迎参加引力波探测研究 What you could do if you would like to join this field

- 实验 Experiments: 一种途径是参加 KAGRA One way is to join KAGRA
  理由 Reason: (i) KAGRA as a 2.1 -2.5 generation GW detector has a future
  (ii) KAGRA needs manpower and it is easier to start and to join
  (iii) (Logistics provided) Just get trained in CMS and go (10 round trip plane tickets will be provided)

- 多波段天文学家 Multi-Messenger Astronomy: Working on astrophysics

- 理论物理/宇宙学 Theoretical Physics/Cosmology

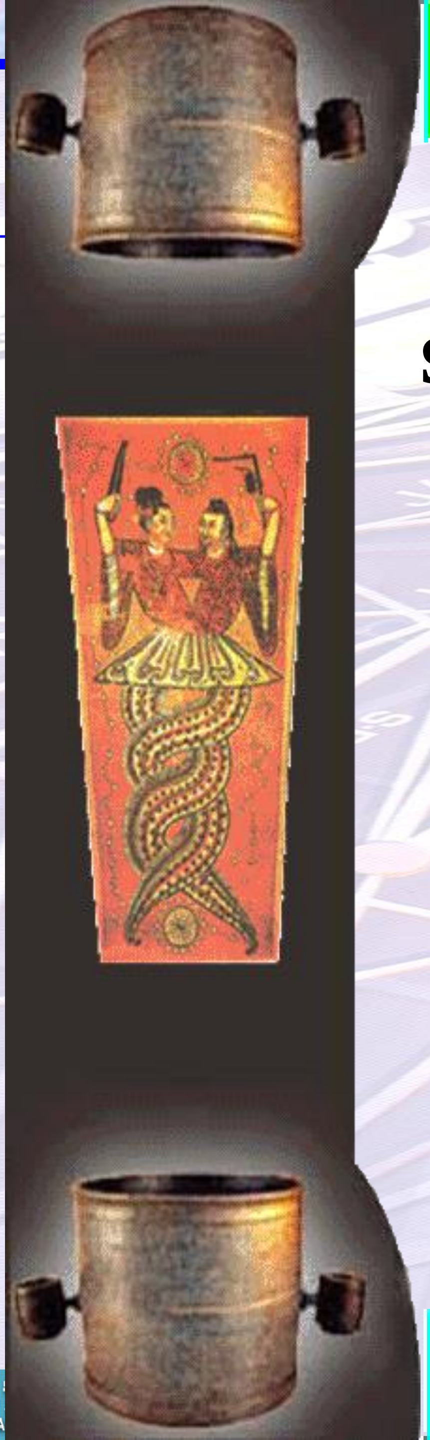

Activity of reinstalling X-pendulum and building a suspended prototype Fabry-Perot cavity for student training before going to KAGRA

Sheau-shi Pan and Sheng-Jui Chen

Center for Measurement Standards, Industrial Technology Research Institute R.O.C.

Dr. Sheau-shi Pan E-mail: Sheau.shi.Pan@itri.org.tw
Dr. Sheng-Jui Chen E-mail: SJ.Chen@itri.org.tw

國家度量衡標準實驗室
NATIONAL MEASUREMENT LABORATORY

Re-install X-pendulum

Re-install X-pendulum →

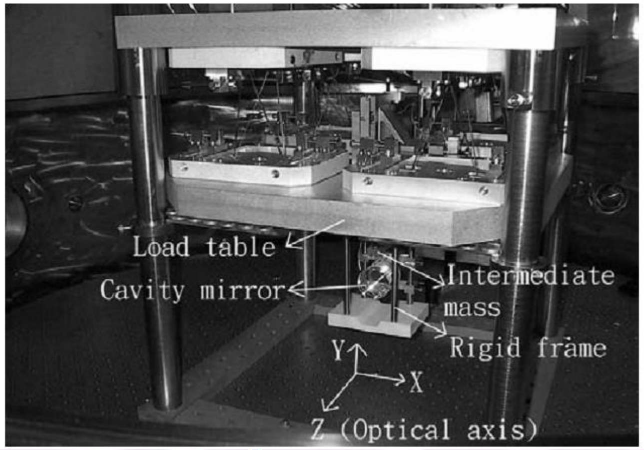

[2]

	CM_1鏡面參數	CM_2鏡面參數
基材 (Substrate)	Fused Silica	Fused Silica
尺寸 (Dimention)	ϕ50 mm×50 mm	ϕ50 mm×50 mm
懸吊線槽 (V-groove)	0.5 mm×2	0.5 mm×2
線槽間距 (V-groove separation)	20 mm	20 mm
鏡面曲率半徑 (Radius of curvature)	5 m	∞(flat)
反射面鍍膜 (Coating of inner surface)	High-Reflection	High-Reflection
反射面光強反射率 (Reflectivity of inner surface)	$R \simeq 99.99\%$	$R \simeq 99.99\%$
透射面鍍膜 (Coating of outter surface)	Anti-Reflection	Anti-Reflection
透射面光強反射率 (Reflectivity of outter surface)	$R \leq 0.25\%$	$R \leq 0.25\%$
透射率 (Transmittivity)	$\geq 0.85 \times (1-R)$	$\geq 0.85 \times (1-R)$

	Fabry-Perot 干涉儀參數
精細度 (Finesse) F	30,000±1,673
腔長 (Cavity Length) L(m)	3.45
光腰尺寸 (Beam waist size) w_0(mm)	0.088
縱模頻距 (Free Spectral Range) FSR(MHz)	43.478
縱模線寬 (Cavity Line-width) $\Delta\nu$(Hz)	1449

***Parameters*[1]**

KAGRA

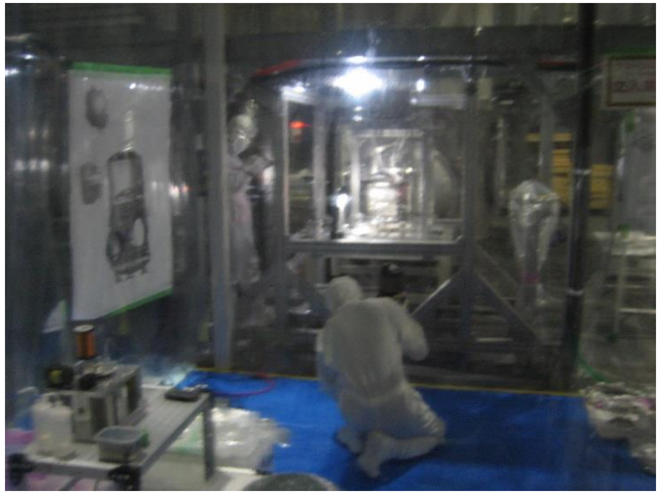

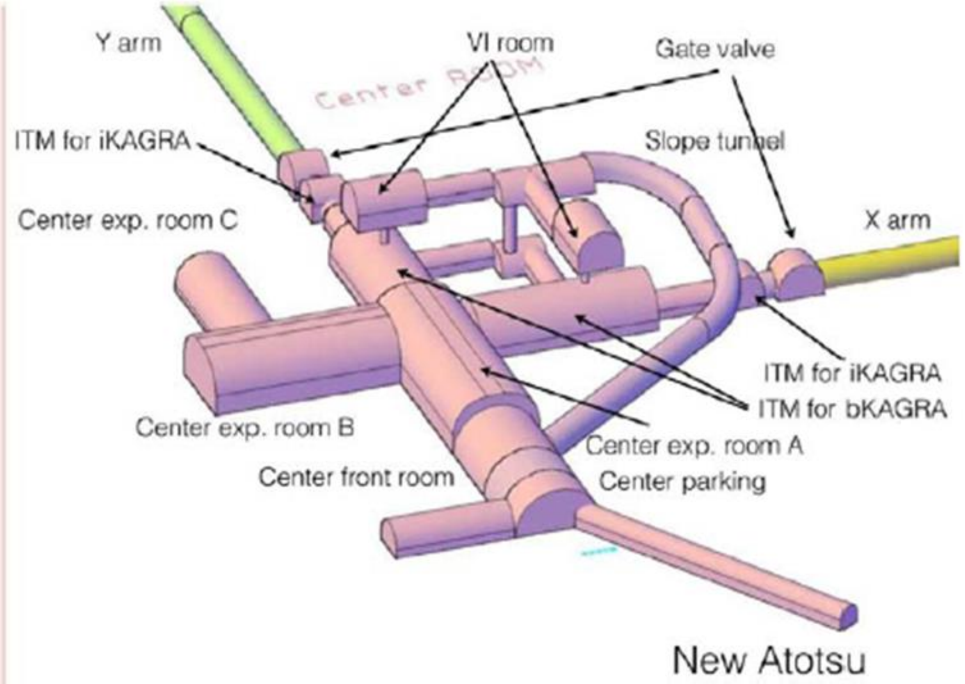
Y arm
VI room
Gate valve
Center ROOM
ITM for iKAGRA
Slope tunnel
Center exp. room C
X arm
ITM for iKAGRA
ITM for bKAGRA
Center exp. room B
Center exp. room A
Center front room
Center parking
New Atotsu


2016/12/30

Related Activities

(i)To reconstruct the X-pendulum (the X-pendulum is already installed), to do the wiring and alignment for control the position of the double-pendulum-suspended mirror, to take it apart and to re-install it.

(ii)To prepare a 30 cm-1 m Fabry-Perot interferometer with finesse about 1000 with a suspended mirror and a fixed mirror, and to train the students how to use it and how to assemble it initially.

(iii)To implement the Pound-Drever-Hall method for locking laser to the cavity using 1064 nm laser. In the meantime, prepare a single mode Nd:YAG laser for use at CMS

(iv)To learn how to measure the properties of the X-pendulum using laser metrology.

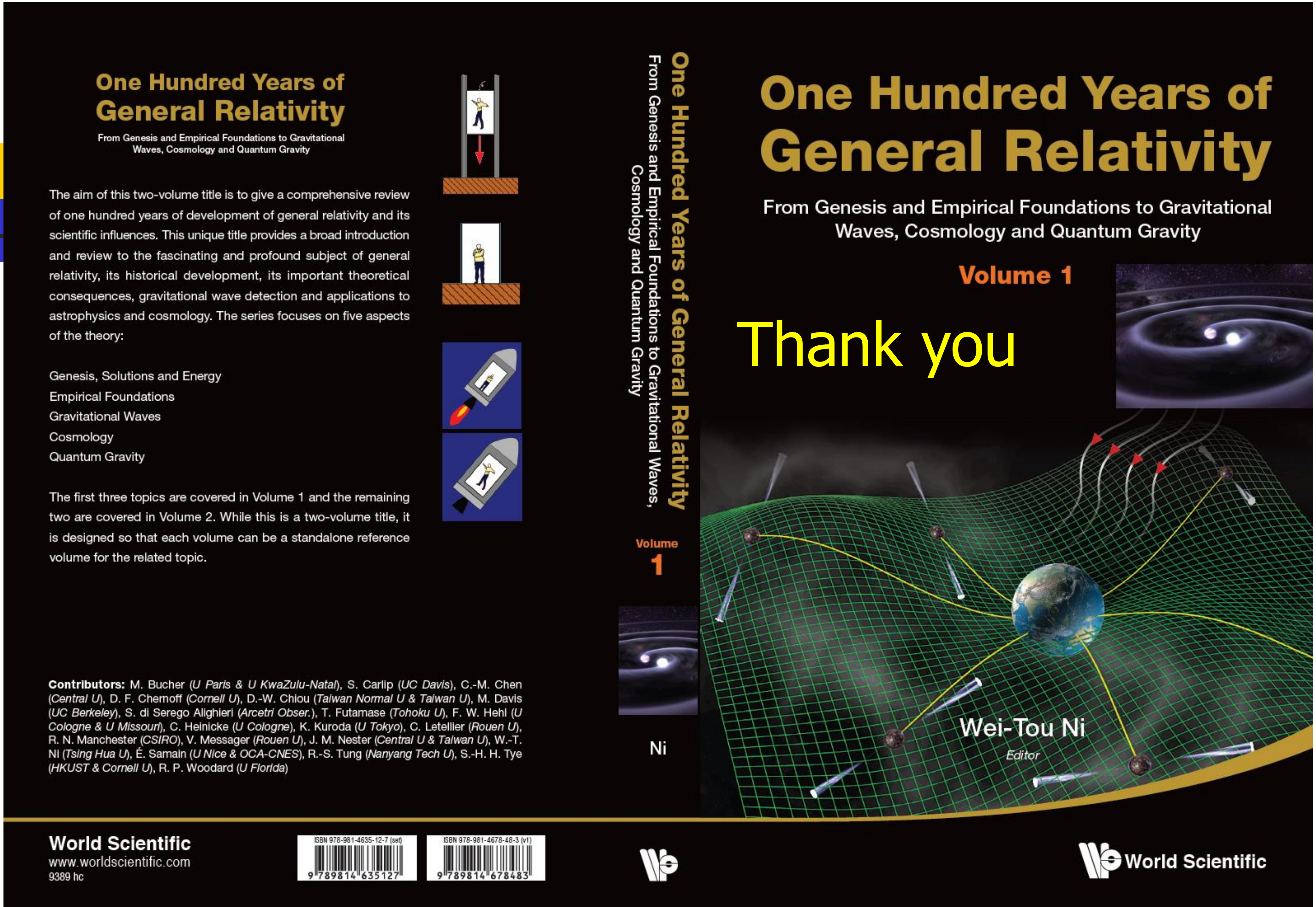
One Hundred Years of General Relativity
From Genesis and Empirical Foundations to Gravitational Waves, Cosmology and Quantum Gravity
The aim of this two-volume title is to give a comprehensive review of one hundred years of development of general relativity and its scientific influences. This unique title provides a broad introduction and review to the fascinating and profound subject of general relativity, its historical development, its important theoretical consequences, gravitational wave detection and applications to astrophysics and cosmology. The series focuses on five aspects of the theory:
Genesis, Solutions and Energy
Empirical Foundations
Gravitational Waves
Cosmology
Quantum Gravity
The first three topics are covered in Volume 1 and the remaining two are covered in Volume 2. While this is a two-volume title, it is designed so that each volume can be a standalone reference volume for the related topic.
Contributors: M. Bucher (U Paris & U KwaZulu-Natal), S. Carlip (UC Davis), C.-M. Chen (Central U), D. F. Chernoff (Cornell U), D.-W. Chiou (Taiwan Normal U & Taiwan U), M. Davis (UC Berkeley), S. di Serego Alighieri (Arcetri Obser.), T. Futamase (Tohoku U), F. W. Hehl (U Cologne & U Missouri), C. Heinicke (U Cologne), K. Kuroda (U Tokyo), C. Letellier (Rouen U), R. N. Manchester (CSIRO), V. Messager (Rouen U), J. M. Nester (Central U & Taiwan U), W.-T. Ni (Tsing Hua U), É. Samain (U Nice & OCA-CNES), R.-S. Tung (Nanyang Tech U), S.-H. H. Tye (HKUST & Cornell U), R. P. Woodard (U Florida)
World Scientific
www.worldscientific.com
9389 hc
ISBN 978-981-4635-12-7 (set)
ISBN 978-981-4678-48-3 (v1)
One Hundred Years of General Relativity
From Genesis and Empirical Foundations to Gravitational Waves, Cosmology and Quantum Gravity
Volume 1
Ni
One Hundred Years of General Relativity
From Genesis and Empirical Foundations to Gravitational Waves, Cosmology and Quantum Gravity
Volume 1
Wei-Tou Ni
Editor
World Scientific

Thank you

Thank you